DEVELOPMENT AND CHARACTERIZATION OF ULTRAHIGH MOLECULAR WEIGHT POLYETHYLENE (UHMWPE) NANOCOMPOSITES FOR BEARING APPLICATIONS UNDER WATER LUBRICATION

BY

ANNAS BIN ALI

A Thesis Presented to the
DEANSHIP OF GRADUATE STUDIES

KING FAHD UNIVERSITY OF PETROLEUM & MINERALS

DHAHRAN, SAUDI ARABIA

In Partial Fulfillment of the
Requirements for the Degree of

MASTER OF SCIENCE

In

MATERIAL SCIENCE AND ENGINEERING

APRIL 2016

KING FAHD UNIVERSITY OF PETROLEUM & MINERALS

DHAHRAN- 31261, SAUDI ARABIA

DEANSHIP OF GRADUATE STUDIES

This thesis, written by **ANNAS BIN ALI** under the direction his thesis advisor and approved by his thesis committee, has been presented and accepted by the Dean of Graduate Studies, in partial fulfillment of the requirements for the degree of **MASTER OF SCIENCE IN MATERIALS SCIENCE AND ENGINEERING.**

Dr. Nesar Merah
(Advisor)

Dr. Zuhair M. A. Gasem
Department Chairman

Dr. Abdul Samad, Mohammed
(Member)

Dr. Salam A. Zummo
Dean of Graduate Studies

Dr. Amro Al-Qutub
(Member)

17/5/16
Date

Dedicated to those who fight till the very end

ACKNOWLEDGMENTS

All thanks to Almighty ALLAH for giving me the strength, knowledge and courage to undertake this research and for making things easy when they appeared difficult. I am grateful to my father for keeping me strong and my mother for her relentless prayers and a never ending faith in me.

I would like to thank my advisor Dr. Nesar Merah whose guidance, support and encouragement led to timely completion of this work. I would also like to thank Dr. Abdul Samad whose constant technical guidance was always there and helped in discussion. I would like to thank my other committee member, Dr. Amro Al-Qutub for his input and guidance in this research work.

I would like extend special thanks to my friends Junaid Ahmad, Irfan Somrow and Arif Ibrahim who supported me in all matters throughout my stay at KFUPM. Dr. Anwar Ul Hamid at Research Institute deserves a special mention for allowing me out using the hot pressing facility which otherwise would seem difficult.

Finally, I would like to acknowledge the support provided by Mr. Lateef and Mr. Sadaqat for various laboratory tasks and KFUPM as a whole for providing the facilities and means to carry out this research.

TABLE OF CONTENTS

LIST OF TABLES

LIST OF FIGURES

LIST OF ABBREVIATIONS

UHMWPE	:	Ultrahigh Molecular Weight Polyethylene
HDPE	:	High Density Polyethylene
CNT	:	Carbon Nanotube
COF	:	Coefficient of Friction
SEM	:	Scanning Electron Microscopy
XRD	:	X-ray Diffraction
FESEM	:	Field Emission-Scanning Electron Microscopy
TWC	:	Total Water Content
DI	:	De-ionized
WC	:	Water Content
WR	:	Wear Rate
GO	:	Graphene Oxide
HA	:	hydroxyapatite

ABSTRACT

Full Name : Annas Bin Ali

Thesis Title : **Development and characterization of Ultrahigh Molecular Weight Polyethylene (UHMWPE) Nanocomposites for Bearing applications under water lubrication**

Major Field : [Materials Science and Engineering]

Date of Degree : April, 2016

Ultrahigh Molecular weight Polyethylene (UHMWPE) has amazing tribological properties that has paved ways in applications where high wear resistance is required. It is employed in variety of applications such as gears, pump housings, impellers, biomedical transplants and almost in every industrial sector both in the form of coatings and bulk. The addition of nano fillers like carbon nanotubes and nanoclay contribute significantly in improving the mechanical and wear resistance properties of UHMWPE. Even though lot of work has been done on UHMWPE composites in terms of their mechanical and tribological characterization, its potential to be used under water lubrication has not been tapped completely.

Hence, the objective of the present study is to explore the feasibility of using ***UHMWPE hybrid nanocomposites*** under water lubrication using nano clay and carbon nanotubes as reinforcements. The unique idea to use nanoclay along with CNTs in the development of hybrid nanocomposites stems from the fact that nano clay is widely used in reducing the water uptake of polymers and enhancing the mechanical properties. In the first part of the present work, 1.5 wt% of three different organo-modified clays I.30E, I.28E and C-15A were used as reinforcements in UHMWPE. XRD, micro-hardness tests, water uptake tests

and most importantly tribological tests have been conducted to evaluate the structural, mechanical and tribological properties of the developed nanoclay reinforced composites. It was observed from the water uptake tests that the addition of all the three types of nanoclays to UHMWPE resulted in reducing the water absorption. However, the addition of C15A and I30E nanoclays to UHMWPE also resulted in improving the tribological properties in terms of lowering the coefficient of friction and increasing the wear resistance. In the second stage, the C15A content was optimized based on its tribological performance using three different clay loadings (0.5, 1.5 and 3wt %). In the last part hybrid nanocomposite were developed with fixed clay content of 1.5 wt% while varying CNTs loading from 0.5 wt% to 3 wt %. Structural and morphological characterization using FESEM, XRD and Raman Spectroscopy for hybrid nanocomposites was done along with tribological testing. Optimized hybrid nanocomposite was tested under water lubricated condition along with pristine UHMWPE, C15A/UHMWPE and CNTs/UHMWPE. Hybrid nanocomposites showed highest reduction in wear rate by reducing wear rate by 63% as compared to pristine UHMWPE. Finally hybrid UHMWPE nanocomposites were tested under accelerated life testing (ALT) conditions under water lubrication with pristine UHMWPE and a reduction of about 45% was observed in specific wear rate with slightly increased coefficient of friction due to superior mechanical properties of CNTs.

ملخص الرسالة

الإسم الكامل : أنس بن علي

عنوان الرسالة : تطوير وتحسين حشوات UHMWPE لمركبة التطبيقات المحامل الواقعة تحت تزييت الماء.

التخصـــــص : علم وهندسة المواد

تاريخ الدرجة العلمية : ديسمبر 2015 م.

البولي إيثيلين شديد الثقل الجزيئي UHMWPE يحمل العديد من الخصائص الجيدة المتعلقة بالاحتكاك وقد شق طريقه في التطبيقات التي تتطلب تحملًا عاليًا للإهتراء مثل المسننات ,المضخات, الأغلفة, الدوافع , زراعة الأعضاء بالإضافة إلى كل الأقسام الصناعية تقريبا , سواءٌ أكان للتغليف أم التسجيم , على كل حال , فإن إضافة المعبئات مثل أنابيب النانو الكربونية CNTs والنانوطين (طين بوحدة قياس النانو) قد ساعد بشكل كبير في تطوير الخصائص الاحتكاكية والميكانيكية لحشوات UHMWPE. على الرغم من أن الكثير من الأبحاث والتجارب قامت بتطوير خصائص حشوات UHMWPE الإحتكاكية والميكانيكية إلا أن إمكانية إستخدامه في التطبيقات الواقعة تحت تزييت الماء بسبب مقاومته الممتازة للماء، لم يتم الإستفادة منها بشكل كامل بعد .

من هنا , فإن تركيز الدراسة الحالية هو دراسة جدوى إستخدام حشوات UHMWPE المركبة تحت تزييت الماء مع إستخدام النانوطين وأنابيب النانو الكربونية كدعامات. إن الفكرة الفريدة في إستخدام النانوطين مع أنابيب النانو الكربونية CNTs في تطوير قضبان الحشوات المركبة مبني على أن النانوطين مستخدم بشكل واسع لتقليل امتصاص المياه في البوليمرات. في الجزء الأول, تم استخدام 1.5% من 3 أنوع مختلفة من الطين المعدل عضويًا E1.30 ، E1.28 ، و C-15A لتدعيم UHMWPE .

تم تطبيق إختبارات أشعة إكس، صلابة المادة في مستوى المايكرو، مقياس إمتصاص الماء والأكثر أهمية هو اختبار قياس الإحتكاك على الحشوات المدعومة بالنانوطين لقياس الخصائص البنائية، والمكانيكية، والإحتكاكية .

عندما تم اختبار شدة امتصاص العينة للماء , لوحظ أن إضافة أنواع النانوطين الثلاثة إلى UHMWPE أدى إلى تقليل إمتصاص العينة للماء. على كل حال , فإن إضافة نوعي C-15A و E1.30 من النانوطين إلى UHMWPE قد أسفر عن تحسين الخصائص الإحتكاكية عن طريق تقليل معامل الإحتكاك وزيادة مقاومة الإهتراء في المرحلة الثانية, تم تحسين محتوى C-15A إعتمادًا على أدائه الإحتكاكي باستخدام ثلاث نسب مختلفة (0.5, 1.5, 3% من وزن الجسم) .

في الجزء الأخير تم تطوير حشوة مركبة بإضافة الطين المحسن بمحتوى ثابت ثم إضافة أنابيب النانو الكربوني CNTs بثلاثة كميات مختلفة (0.5, 1.5, 3% من وزن الجسم) .

تم تحديد الخصائص البنائية والشكلية باستخدام حقل انبعاث المسح الإلكتروني المجهري , أشعة إكس و طيف رامان للحشوة المركبة بالإضافة إلى إختبارات قياس الإحتكاك. تم إختبار نسخة محسنة من الحشوة المركبة تحت تزييت الماء مع عينات أخرى من UHMWPE نقي ، C15A/UHMWPE ، و CNTs/UHMWPE . أظهرت الحشوات المركبة أعلى مقاومة للإهتراء بمعدل 63% مقارنة بـ UHMWPE غير المعدل.

في النهاية ، تم إختبار حشوات UHMWP المركبة تحت ظروف حياة مسرعة تحت تزييت الماء مع UHMWPE نقي ، حيث تمت ملاحظة تقليل مقاومة الإهتراء بنسبة 45% في حالة محددة من الإستخدام مع زيادة جزئية في معامل الإحتكاك ناتجة عن الخصائص الميكانيكية العالية لأنابيب النانو الكربونية CNTs .

CHAPTER 1

INTRODUCTION

1.1 Background

Polymers and their composites have been used extensively in mechanical and tribological applications. Polymers are one such class of materials which have found their way in many mechanical sliding applications because of their ease of fabrication, low cost, low coefficient of friction and light weight. However, limitations such as low strength and low thermal stability have hindered the use of these materials to their full potential [1]. With the advent of materials such as carbon nanotubes (CNTs), graphene, carbon fibers etc. which can be used as reinforcements, a new class of materials called the polymer nanocomposites are being developed with enhanced mechanical, thermal and tribological properties. Hence, polymer composites are being extensively used in numerous applications such as bearings, cams, valves, vacuum pumps, seals and most significantly in the medical applications as implants and prosthesis [2, 3].

Polymer based composites incorporated with different fillers such as carbonaceous filler, metal oxides and as well as nanofillers have demonstrated a substantial improvement in not only in mechanical properties but also in tribological properties in terms of friction and wear. Polymers and their composites have demonstrated excellent properties under dry sliding conditions. Especially high wear resistant polymers such as UHMWPE, PEEK, PVDF and Polyimides and their composites have shown even drastic improvement in the

tribological properties even under dry and lubricated sliding conditions. However, for effective improvement in the tribological properties especially under water lubricated conditions where polymers are used as bearing material in bulk or coating there is much room to use different combination of nanofillers for enhancing the tribological properties. It should be mentioned that long exposures of polymers to water results in deterioration of mechanical or tribological properties and hence failure for intended applications [4, 5].

1.2 Nanocomposites

Nanocomposite materials are a novel class of materials encompassing different materials such as (ceramics, polymers, and metals) to produce a material with entirely new and desired properties. These engineering materials are paving ways for inter-connection between different classes of materials. The term ‘nanocomposite’ is used for the composites in which any one of the constituent materials has at least one of the dimensions less than 100 nm. Polymer nanocomposites have the advantage of exhibiting superior properties due to the very high surface to volume ratio and very high aspect ratio but their uniform dispersion is an issue which remains to date. Due to this high aspect ratio, the interfacial area between the matrix and reinforcement is many times greater in nanocomposites than in conventional composites which means that the matrix properties are substantially affected in areas in close vicinity of the reinforcement. Another implication of nano-size is that only a minute amount of nano reinforcement is enough to have a noticeable effect on the final composite [4, 5].

There are a wide variety of reinforcements available which can be added to these matrices to get desired properties. The current work deals with UHMWPE polymer matrix composites reinforced with nanoclay and carbon nanotubes (CNTs) for load bearing

applications. The expressions ‘hybrid composite’ and ‘hybrid nanocomposite’ will be used to describe the materials throughout this thesis, when two different nanofillers are used as reinforcements.

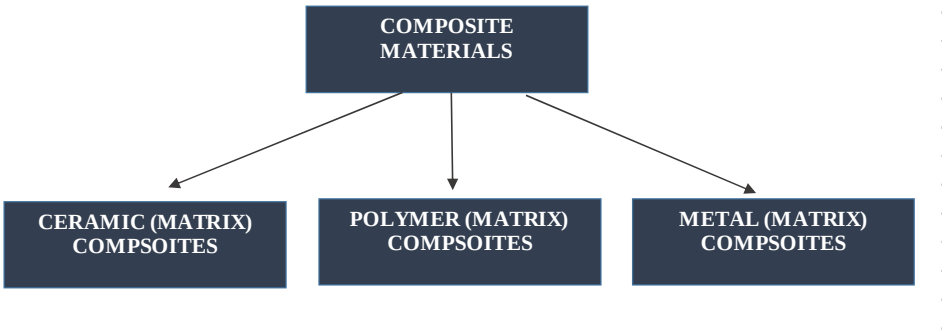

Figure 1.1 General classes of composites and nanocomposites

Ultrahigh Molecular Weight Polyethylene (UHWMPE) is often used to improve the tribological properties under contact loading applications. Carbon nanotubes are the potential nanofillers that are used for improvement of mechanical, tribological, thermal and other related physical properties in most of the polymer matrices including UHMWPE [6-8]. Carbon nanotubes have been shown to improve tribological properties of UHMWPE matrix in both dry sliding and lubricated conditions [9]. However, for more pronounced improvement in water lubrication nanoclay can be added to reduce the water uptake. Nanoclay has shown not only better tribological properties in different matrices [10] [11, 12], but its inherent advantage is in its barrier properties reducing the water absorption [13-15] hence resisting the plasticization of polymer surfaces and eventually avoiding deterioration of mechanical properties for polymers.

1.3 Objectives

The main objective of the present work is to develop and characterize UHMWPE Based Nano composites for mechanical bearing applications under water lubrication. The aim is to explore the concept of using UHMWPE as base material for water lubricated load bearing by further enhancing its tribological properties. The unique idea to use nano clay with CNTs as reinforcement in UHMWPE mainly to reduce water absorption as well as to improve tribological properties, if any. CNTs have been extensively studied with different polymer matrices for enhancing mechanical properties while nanoclay along with improvement in mechanical properties has also been shown to reduce the water uptake. The specific objectives of the proposed work are:

1- Development of UHMWPE clay nanocomposites with tribological (dry sliding and water lubricated) and structural characterization.

2- Determination of the effect of clay on the water uptake property of UHMWPE at low and high temperatures.

3- Development of CNTs UHMWPE nanocomposites with tribological and structural characterization.

4- Development and Tribological characterization of hybrid UHMWPE, nanocomposites under dry and water lubricated sliding under different loads and speed.

1.4 Research Phases (Experimental)

The overall project has been divided into three main phases covering three different composite systems, UHMWPE/Nanoclay composites; Selection of best clay and

optimization of clay content (Phase 1), Water uptake testing for best selected clay composites (Phase 2) and UHMWPE/CNTs and UHMWPE/Hybrid nanocomposites development, and tribological characterization (Phase 3).

1.4.1 Phase-1 is focused on selection of best clay in terms of tribological properties among C15A, I.28E and I.30E by developing their UHWMPE nanocomposites and perform structural characterization. The second step of this phase is to optimize the clay loading for the selected clay based on tribological properties.

1.4.2 Phase-2 deals with water uptake experiment for UHMWEPE and clay composites with different loadings. Water uptake is performed at both low and high temperatures.

1.4.3 Phase-3 includes development of UHMWPE/CNTs nanocomposites and UHMWPE/hybrid nanocomposites. Tribological characterization was done for optimization of CNTs content under dry sliding for both composites systems. Structural characterization was also done using FESEM, XRD and Raman Spectroscopy. Tribological characterization under water lubricated conditions was done for all optimized composites. Finally optimized hybrid nanocomposite was tested with pristine UHMWPE under extreme conditions i-e at higher load and higher speed in water lubrication for overall performance evaluation.

1.5 Motivation and Justification

There is constant need to develop materials light weight with excellent mechanical properties for load bearing applications. Number of applications are specific in a sense, where bearing materials are used either submerged in water or they are constant aqueous

media contact such as motors and pipelines. Moreover the working temperatures in such applications doesn't exceed beyond 80°C. Polymers acquire prominence in such cases, as they are easy to fabricate, light weight, have no corrosion related problems and are cheaper than the conventionally used metallic and ceramic bearing. Hence there is constant need to use polymer with high load bearing ability and wear resistance to perform efficiently under constant loadings. UHMWPE has been mostly used for applications demanding high wear resistance because of its higher abrasion resistance and impact strength.

To make use of UHMWPE up to its full potential in the indicated applications there is a need to make bulk modifications to UHMWPE by incorporating different reinforcements. CNTs are the most widely used reinforcements in polymer matrices for the purpose of increasing mechanical and tribological properties. Along with CNTs, clay is added to account mainly for reducing the water uptake for polymers constantly working under water and aqueous lubricated contacts. Moreover, nanoclay itself is a pronounced filler for improving tribological and mechanical properties. The motivation behind the objective is to use the dual advantage of nanoclay and CNTs to develop load bearing material that will enhance the tribological properties of UHMWPE under dry sliding and water lubrication conditions.

1.6 Research Methodology

The previously stated objectives will be achieved by performing following the tasks. (1) Synthesis of nano and hybrid nanocomposite (2) Morphology and structural characterization of developed nanocomposites (3) Testing for mechanical properties and water uptake (5) Tribological characterization of pristine UHMWPE and developed

nanocomposites under (dry sliding and water lubricated testing for hybrid nanocomposites).

1.7 Organization of thesis

In this work chapter 2 deals with relevant literature review. Studies done using UHMWPE polymer and related composites is reported and reviewed in context of current work. Chapter 3 deals with classification of materials used UHMWPE, CNTs and nanoclay. Description about the processes used to develop nanocomposites is delineated. Ball milling followed by hot pressing was used for preparation. In this chapters the details about the characterization techniques used to reveal structure/morphology and tribological testing parameters are also described. Chapter 4 presents all the experimental results with subheadings entitled to each nanocomposites morphology and Tribological testing results, nanoclay UHMWPE composites, CNTs UHMWPE composites and hybrid UHMWPE composites. Chapter 5 summarizes and concludes the discussion regarding comparison of performance of hybrid UHMWPE with its peers and bare UHMWPE. Finally conclusions and possible future research is proposed.

CHAPTER 2

LITERATURE REVIEW

2.1 Tribology

Tribology is termed as “Science of interacting surfaces that are in comparative motion”. Main tasks in the tribology is to reduce friction and wear so to lessen the energy consumption, eventually lessening the maintenance risks and increasing productivity of mechanical system. Bearing and Tribology have evolved from old times and they will remain important whenever surfaces come in contact in relative motion. The word “Tribology” is derived from Greek word “*tribous*” which means rubbing. Hence though it appears that, tribology is something new yet it actually finds its root deep in the past world also. Egyptians long ago (1880 BC) used sledges to transport big statues and lubricate them as well with the help of water, however in late fifteenth century Leonardo da Vinci (1452-1519) was first to state the coefficient of friction in terms of ratio of frictional force to normal force [16]. For century’s wood, iron and copper were being used as traditional bearing materials. With continued research in this area and with the development of new materials, Tool steels and alloys caught importance in early 1900s. AISI 52100 steel and its derivatives were much used in the roller bearing industry. Tribology has caught much importance with the development of high precision and accuracy machinery, as the need for improvement in bearing materials and lubricated environment has increased Now days plastics and composite bearing compounded with a variety of novice fillers are being widely used that are showing excellent properties in terms of friction and wear. [17, 18].

2.2 Polymers in Tribology

Polymers and polymers-based nano composites show good tribological performances because of their corrosion resistance properties and the capability of entrenching extrinsic matter such as wear particles. Polymer materials are increasingly used in dry sliding applications especially in machinery and in equipment requiring high precision and accuracy. Moreover their importance becomes more prominent in the areas where the fluids cannot be endured because of their contamination with the product like corrosive environments. Rapid increase in applications of polymers is mainly due to low cost of materials and manufacturing of large amount of components [10, 19, 20]. Tribology of Polymer materials is different from other materials like metals and ceramics as polymers mostly have low surface energy and properties like viscoelasticity changes the course of frictional force. The low processing costs and effectively low coefficient of friction makes polymers a competitive choice and need is there to need to further improve their coefficient of friction and wear [21]. Among polymers, the most used ones in tribological applications are Polyetheretherketone (PEEK), Polytetrafluoroethylene (PTFE) and Ultra high molecular weight polyethylene (UHMWPE). PEEK and UHMWPE have got excellent tribological properties, having high resistance to wear coupled with low coefficient of friction. Similarly PTFE is widely used in tribological related components, however one main drawback of this polymer is its low abrasion resistance that leads to failing of machinery parts for desired tribological applications, hence resulting in larger wear rate limiting its use as solid lubricant [22].

2.3 Ultrahigh Molecular Weight Polyethylene (UHMWPE)

UHMWPE is a linear photopolymer consisting of hydrogen and carbon. Monomer is ethylene that converts to polyethylene by polymerization of ethylene (C_2H_4) gas. It is represented in terms of chemical formula as (C_2H_4) n. The chemical structures for ethylene and polyethylene are shown in Fig. 2.1.

Figure 2.1 Structure of Polyethylene [24]

For ultra-high molecular weight polyethylene, a sole molecular chain can comprise millions of ethylene repeat entities with the molecular weight ranging also in millions. Some of the general properties of UHMWPE are illustrated in table 2.1.

Table 2.1 General Properties of UHMWPE in Bulk Form [24].

Property	**Value**
Elastic Modulus (GPa)	69
Poisson's Ratio	46
Yield Strength (MPa)	21.4-27.6
Tensile Strength (MPa)	38.6-43.8
Coefficient of Thermal Expansion 10^{-6} °C	234-360

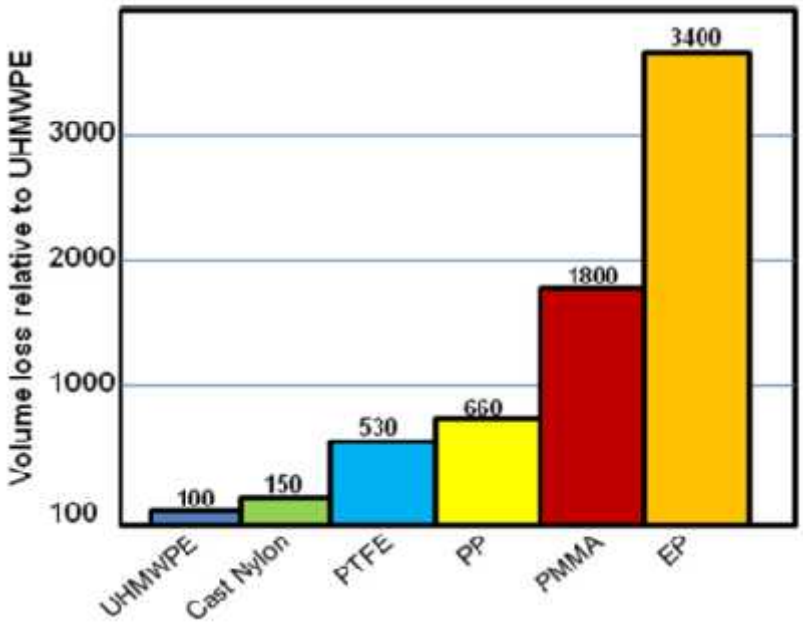

Figure 2.2 Wear rates of various Polymers [25]

Ultra-High Molecular Weight Polyethylene (UHMWPE) is an exceptional polymer which has special tribological properties. Among the known thermoplastics UHMWPE has the maximum abrasion resistance and notched impact strength. Figure 2.2 and figure 2.3, show respectively, the volume loss relative to UHMWPE and the impact strength among the various contemporary polymers. In comparison to UHMWPE, the most used polymers in such applications such as nylon and PTFE show high volume loss. Along with the excellent abrasion resistance, the property that outclasses this polymer even further is its impact strength. Till to the date, UHMWPE is reported to have highest impact strength for any known thermoplastic. Moreover it is abrasion resistant with self-lubricating non-stick surface as its coefficient of friction is much lower. As compared to other polymers in bulk form such as polyetheretherketone (PEEK), polyethylene (PE), polystyrene (PS),

UHMWPE is highly wear resistant. The normal working temperature range of UHMWPE is between -269^{o}C and 90^{o}C. UHMWPE can also perform at higher temperatures for short time period, its melting point is around 138◦C to 142◦C. This polymer material retain excellent dimensional stability u to 80^{o}C [23, 24].

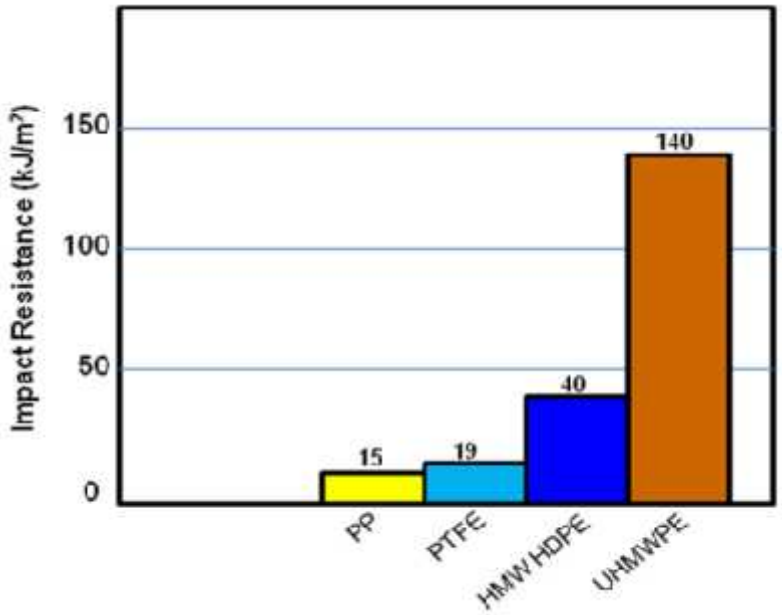

Figure 2.3 Impact resistance of various polymers [25]

2.4 Polymer Nanocomposites in tribological Applications

In polymer materials there are very limited materials having good tribological properties in terms of wear and friction as indicated above and among these very few of the polymeric materials are seen to because in pristine form simply to fulfill and optimize the application requirements. Therefore, there is in fact a continuous need to modify polymers using appropriate fillers that can help reduce wear rate and decrease or increase in coefficient of friction contingent on intended use. A lot of work has already been done using micron sized particles (conventional polymer composites) and are reported to enhance properties as well.

Polymer composites are famous for offering such physical properties that are manipulated to apply them in desired functional areas [18]. By using different classes and sizes of fillers enhanced tribological properties are gained.

Nanocomposites are gaining importance regarding their employment in tribological applications. Like polymers, their composite‘s tribology is very complex. The structure in terms of chain entanglements are one of most influential factor in tribological performance. Though previous studies have reported improvement in the tribological properties of polymer based composites (PBC) using hard micrometer size particles and fillers, there are some problems. One of them is that the hard micron sized particles abrade the counter face which leads to avert the formation of protective transfer film which leads to increase COF. Polymer based Nano-composites offers solution to such problems that as they have particles of characteristic size less than 100nm resulting in the reduced abrasion. Nanoparticles are of same size as of the counter face material asperities and sometime this lead to polishing the highest asperities eventually aiding in formation of promising transfer film. Therefore the transfer film safeguards composite surface of direct asperity interaction and damage [2, 8]. Moreover polymer nanocomposites (PNCs) have shown much increased mechanical and tribological properties. Polymer Nano-composites are especially being used where fluids and lubricants like grease miss the mark and superior tribological properties are necessary [25].

2.5 UHMWPE Nanocomposites

UHMWPE nanocomposites using nano sized fillers have shown excellent improvement in the tribological properties compared to bare UHMWPE. The choice of nanofillers can be based on the type of nanofillers in terms of dimension and structure. Nanowires, CNTs,

metal oxide nanoparticles such as zirconium dioxide, Aluminium oxide and Zinc oxide are among the most recent nanofillers with UHMWPE.

2.5.1 Carbon Nanotubes (CNTs) as Filler for Tribological applications

Carbon nanotubes are so far the most reliable nanofillers employed as reinforcement in polymer matrices. CNTs are excellent nanofillers with higher thermal conductivity, mechanical strength and modulus. CNTs are actually one of the allotropic form of carbon, one of most abundant element present on earth. They are in fact sheets of one atom thick layers of graphene being folded at different angles “Chirality”, giving them different properties metallic, nonmetallic and semiconductor [6]. Nanotube diameter is of the order of a few nanometers, with length range can be of the order of several millimeters. They are reported to be up to one hundred times as strong as steel [26].They are light, flexible, thermally stable and inert chemically [27].

The incorporation of carbon nanotubes in polymers for enhanced properties is very promising. Carbon nanotubes are among the most employed potential reinforcements for improving the tribological properties. Carbon nanotubes UHMWPE composites have enhanced tribological traits of UHMWPE pristine polymer [28-31]. Ajayan et al. [32] reported the pioneering polymer nanocomposite back in 1994 using carbon nanotube as filler. CNTs owe great flexibility and large aspect ratio (typically >1000), with enormously high tensile strength and moduli. Discrete single-walled carbon nanotubes (SWCNTs) are classified as metallic or semiconducting materials depending on chirality. Hence Carbon nanotubes have an excellent combination of electrical and properties with extra-ordinary thermal and mechanical properties [33].

Zoo et al. [34] studied the influence of CNT addition on the tribological properties of UHMWPE. From figure 2.4 and figure 2.5, it can be seen that with an increase in the CNT content from 0 to 5 wt. %, the wear loss decreased significantly from 35 mg to 025 mg and the friction coefficient increased from 07 to 12. The reduced wear loss of UHMWPE/CNTs composites is attributed to inherent excellent properties of CNTs. However the slight increase in coefficient of friction is due to increased hardness of UHMWPE as CNTs are added to it.

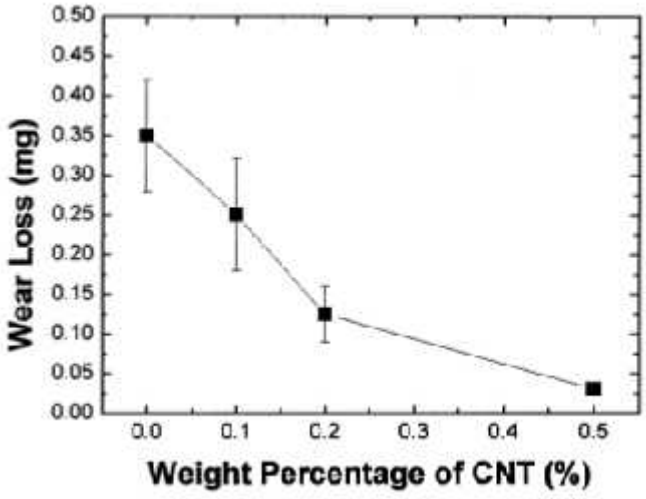

Figure 2.4 Effect of variation of CNTs on wear loss [33]

Ruan et al. [35], reported radically enhanced toughness in the ultrahigh molecular weight polyethylene (UHMWPE) films with 1 wt.% addition of multiwall carbon nanotubes (MWCNTs). Xue et al. [36]varied the concentration of CNTs from 2 to 2 wt.% in UHMWPE/HDPE blends and studied the tribological behavior of the composites using a pin-on-disk configuration. They found that decreased wear rate of the composites as CNT content was increased.

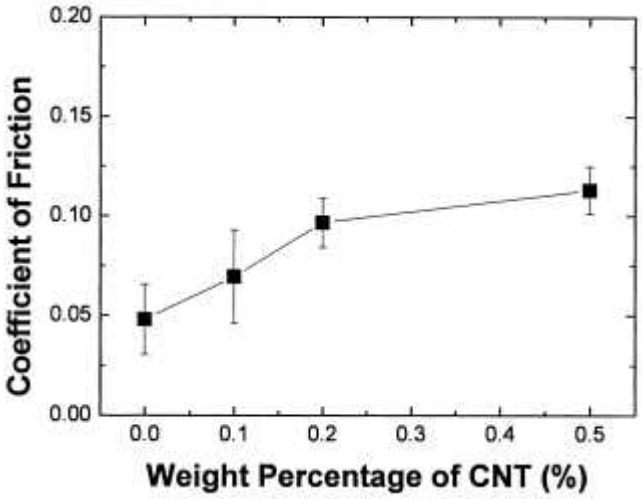

Figure 2.5 Coefficient of friction of UHMWPE with varied CNTs content

Johnson et al. [37] investigated the Tribological trend for the High density Polyethylene based Carbon nanotube Composites. From 2.6 illustrates the logarithmic wear rate of HDPE a polymer from same polyethylene family with addition of CNTs to it. By the incorporation of 5 % by weight the Stiffness increased by 8% and 13% increase in maximum to load to failure. Like other, the tribological properties were also greatly improved, up to 5 wt. % addition of CNTs resulted in almost 50% decline in the wear rate and 12 % in the coefficient of friction. The coefficient of friction decreased of UHMPWE decreased from 0.050 to 0.043.

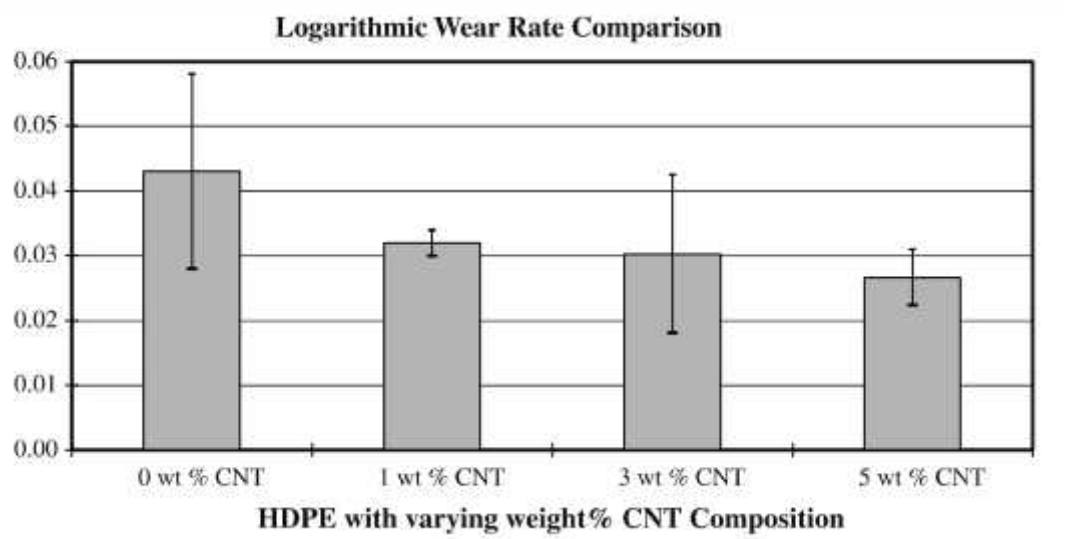

Figure 2.6 Wear rate with variation of CNTs [35]

From the above literature it is evident that CNTs improve the tribological properties of UHMWPE in terms of friction and wear. The wear rate reduction is significant for CNTs addition which most of the authors has attributed to excellent mechanical properties of CNTs. The behavior of COF is complex as compared to wear rate. It is seen that Zoo et al. [32] reported increase in COF with CNTs addition whereas studies done by Johnson et al. [35] reported decrease COF with addition of CNTs, however both studies show reduced wear rate. CNTs is expected to increase the COF slightly because of its hardness however decrease in COF is attributed to because of removal of CNTs from the surface of composite because of plastic deformation and these CNTs may have acted as lubricant just like solid graphite particles. Overall, CNTs/UHMWPE composites irrespective of the wear mechanism taking place have shown to improve the tribological properties.

2.5.2 Nanoclays as Filler in Tribological Properties

The montmorillonite clays are naturally occurring inorganic materials. They belong to the phyllosicilate category. Chemically they are composed of Aluminium silicate as a primary

constituent with addition of rare earth metals. The montmorillonite clays are naturally occurring inorganic materials. The chemical composition of 1/2 crystalline unit cell is [$Al_{1.67}$ Mg_{33} (Na $_{33}$)] Si_4O_{10} $(OH)_2$ [38]. Thickness of clay is around 1nm with other dimensions being between 100-1000 nm, giving the clay an aspect ratio in the range of 100-100 Smectic clays are composed of one layer of octahedral (AlO_6) sandwiched between two sheets of tetrahedral (SiO_4) forming 2:1, T-O-T (tetrahedral-octahedral-tetrahedral) [5], as shown in Figure 3.2. Gap of approximately 1nm is there present between each layer forming gallery where rare earth metal cations such as sodium, magnesium and calcium reside.

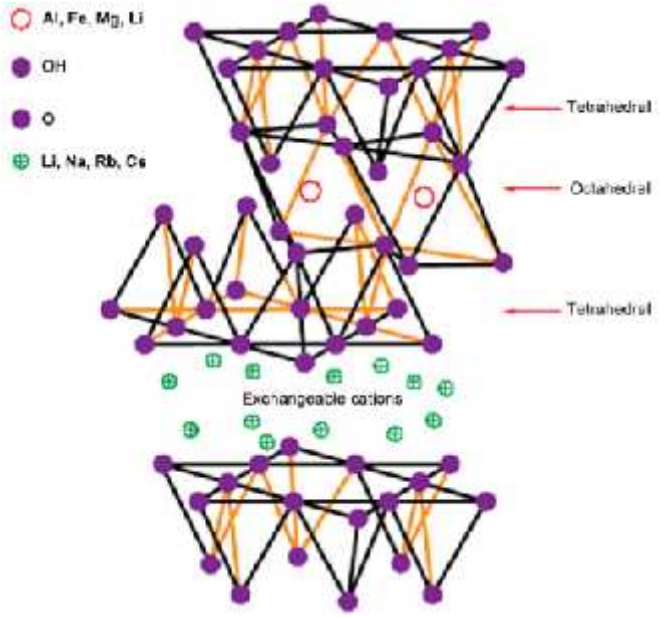

Figure 2.7 Structure of Smectic clay [39]

Modulus of an individual layer is in the range 170–180 GPa [38]. Based on composition, clay particles (ionic and polar in nature) it is hydrophilic, making the interaction of organic substance with clay problematic. However, the inorganic cations in the interlayer space are amenable to be exchanged by organic cationic molecules which change the clay from being

hydrophilic to organophilic. Classification of different commercial clays are based on different organic modifier that is replaced with the inorganic cations [40]. Three different types of structures can be formed depending on the degree of dispersion of clay platelets in the polymer matrix namely: phase separated, intercalated and exfoliated. Phase separated morphology is indicated by no change in the diffraction angle of the clay characteristic peak, pointing out the fact that polymer chains are unable to enter the gallery gap of the clay layers and d-spacing is unchanged. Intercalated and exfoliated morphology specifies good dispersion of clay platelets. XRD for intercalated structure is change in the clay peak position to lower diffraction angles hence increase in d-spacing of the clay. However the Exfoliated or disordered intercalation shows no peak for clay, meaning the d-spacing has increased much and amorphous structure is formed with clay individual platelets being randomly dispersed with a d-spacing greater than 8nm [5, 14].

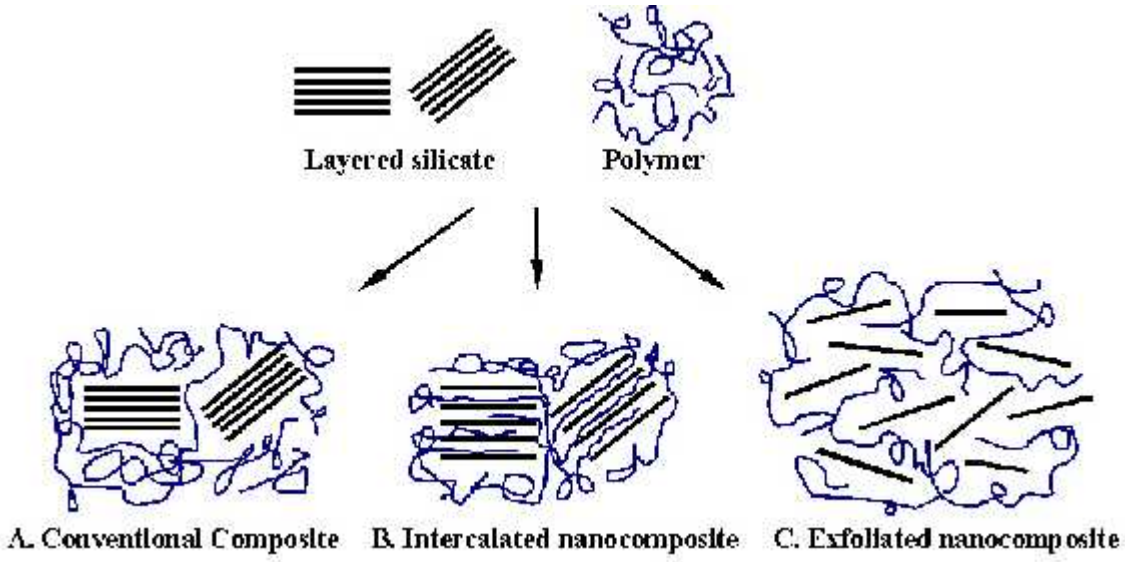

Figure 2.8 Schematics of possible morphologies for Clay composites, A) phase separated micro composite, B) intercalated nanocomposite and C) exfoliated nanocomposite

Polymeric materials reinforced with clay minerals and silicate layers are getting great attention due to their exclusive properties, such as enhanced thermal stability, improved gas and moisture barrier characteristics as well as reduction in flammability. The improvement of mechanical properties depend on the dispersion and compatibility of clay nano-filler with the polymer matrix. Kaloshkin et al. [41] studied the mechanically and Tribological properties of Clay reinforced (UHMWPE) composite. They found that the modulus of elasticity of nanocomposites increased as the clay percentage is increased, while the Percentage ductility showed decrease. Owing to tribological properties, the Coefficient of friction decreased from 19 to 16 as the percentage of Clay is increased from 0 to 30wt%. The wear rate also declined from $120*10^{-6}$ mm^3/Nm to $70*10^{-6}$ $mm^3/N.m$ as the Clay addition increased from 0 to 30wt %.

Peng et al. [42] reported consequence of Clay filler on the wear properties of Poly vinylidene fluoride (PVDF). The Clay was added up to 1, 2 and 5 wt. %. During the initial stages of sliding up to about 20 minutes the Coefficient of Friction increased at same rate for the Pure PVDF and the composite samples, but as the Distance/Time increased the Coefficient of Friction decreased for all the three percentages (1, 2 and 5 wt. %) as related to pristine PVDF. From figure 2.6, it can be seen that for each different loads 100N, 150N and 200N, lowest wear rate was observed at 1wt%, however as the clay loading is increased in PVDF matrix the wear rate increases with almost same wear rate as seen for PVDF. Clay particles reduced the large scale material removal hence reduces the wear rate however the COF was reported to stabilize rather increase. This was ascribed to the transfer layer that is formed on counterface and its good adhesive strength with the counter-face material because of the clay addition.

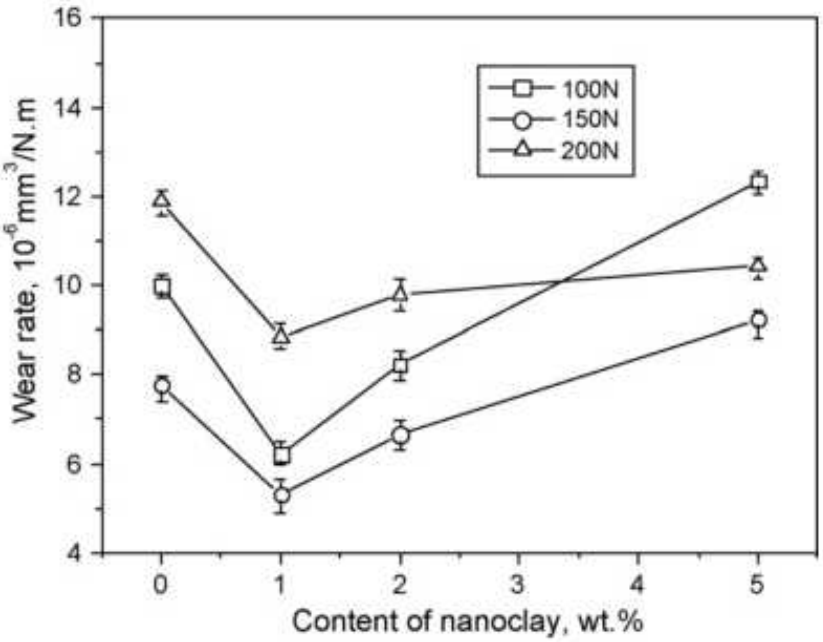

Figure 2.9 Effect of load on wear rates of PVDF composites with different clay content [43]

One of the studies done using polypropylene (PP) based nanoclay composites for tribological properties also showed reduced wear rate for PP as organoclay was added. 2wt% of clay showed least specific wear rate while the 5wt% showed a slight increased wear rate owing possible agglomeration of clay platelets. Along with the reduced specific wear rate, improve hardness and compressive strength with clay addition has also been reported. Figure 2.7 shows that 2wt% clay showed 85% reduction in wear. Uniformly dispersed clay platelets prevent large scale deformation and material removal, hence reducing wear rate [43]

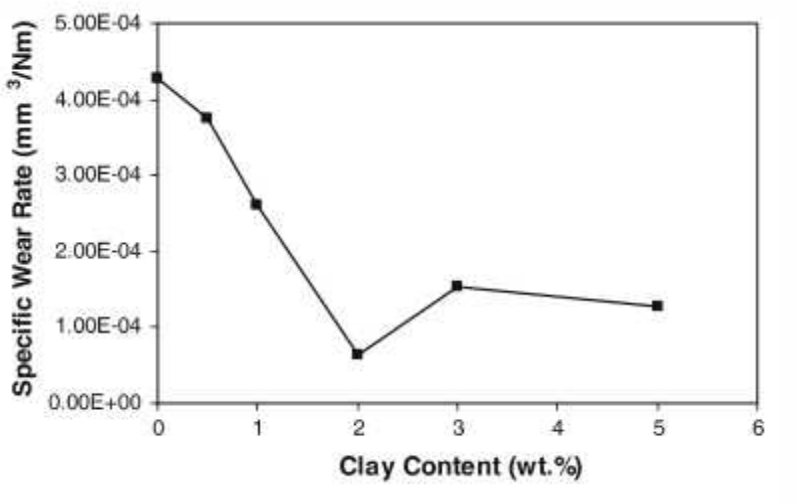

Figure 2.10 Specific wear rate of PP and clay composites [43]

2.6 UHMWPE composites tribology under lubricated sliding conditions

Recently Yingfei et al. [44] studied the influence of Graphene oxide (GO) on the tribological behavior of UHMWPE under the lubrication of deionized water and normal saline solution. The composite were prepared by ultra-sonication of GO with UHMWPE followed by ball milling of mixture and subsequent hot pressing. Figure 2.7 shows specific wear rate with graphene oxide addition in UHMWPE for both lubricated mediums. It can be seen that as the Graphene oxide content was increased the Wear rate was decreased though there was also some increased observed in coefficient of friction in both lubrication mediums. GO particles uniformly dispersed in UHMWPE matrix, resulted in efficient transfer of stress. Micro-hardness Vickers also showed improved hardness by the addition of graphene oxide in UHMWPE. Along with the wear results the scratch test results showed shallow depths for the case GO is added to UHMWPE. For 1wt% GO addition, the scratch depth was reduced to 22.93% and 23.77% for deionized water and normal saline solution,

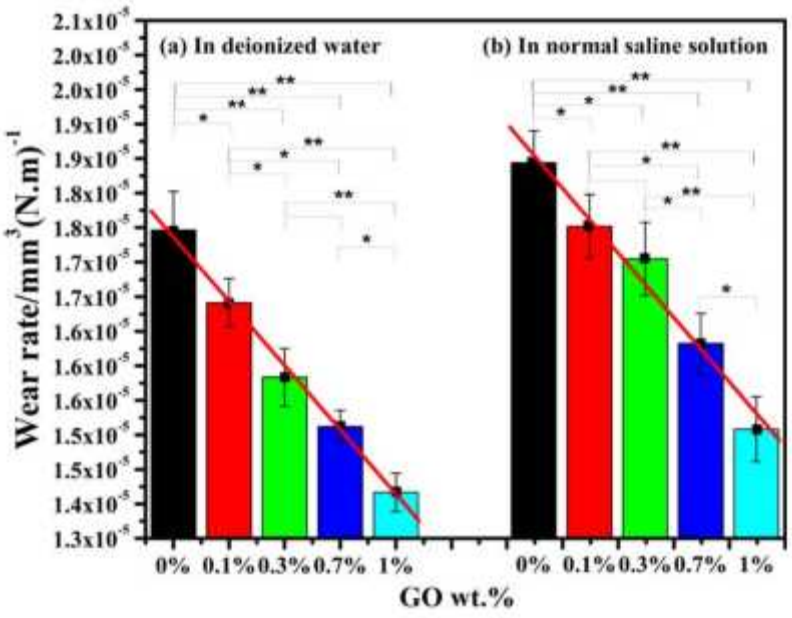

Figure 2.11 Specific wear rate of UHMWPE and GO/UHMWPE composites [44]

Xoing D et al. [45] studies showed that with Carbon Fiber amount increase, wear volume loss of the composites under both dry and distilled water lubricating conditions. However compared to dry sliding the wear rates were less in case of water lubrication. In figure 2.8, it can be seen that COF showed increased value with addition of carbon fiber under dry sliding as compared to pristine UHMWPE. Generally, COF is high under dry sliding as compared to water lubricated conditions. Under distilled water lubrication conditions composites showed very much lower friction coefficients than pure UHMWPE. The increased COF under dry sliding is attributed to increased area of contact with sliding distance. The frictional heat generated during the process results in softening of UHMWPE, and the adhesion aspect of friction resulted in high wear rates under dry sliding as shown in figure 2.8. For water lubricated conditions, water film present acts as gap and avoids the direct contact of UHMPWE block with steel ring. Hence decreased values under

water lubricated sliding are obtained. In one of the work by same author he stated that for pure UHMWPE underwater lubrication, water absorption affects frictional properties [46].

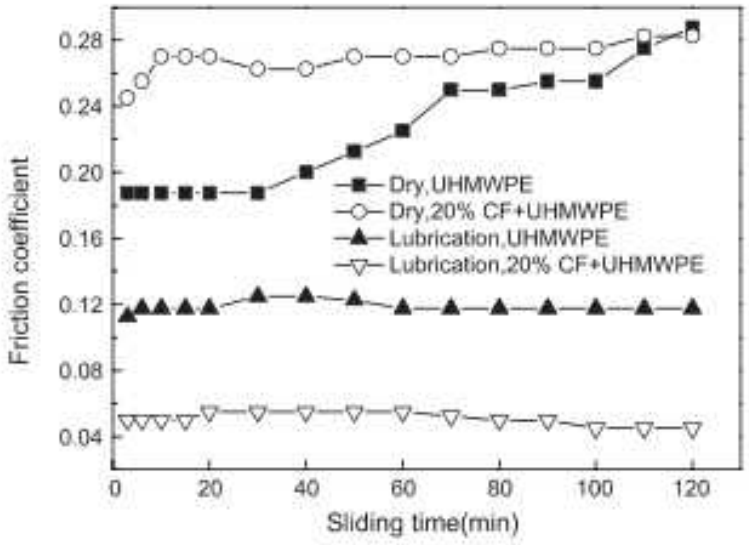

Figure 2.12 Variation of COF with sliding distance [9]

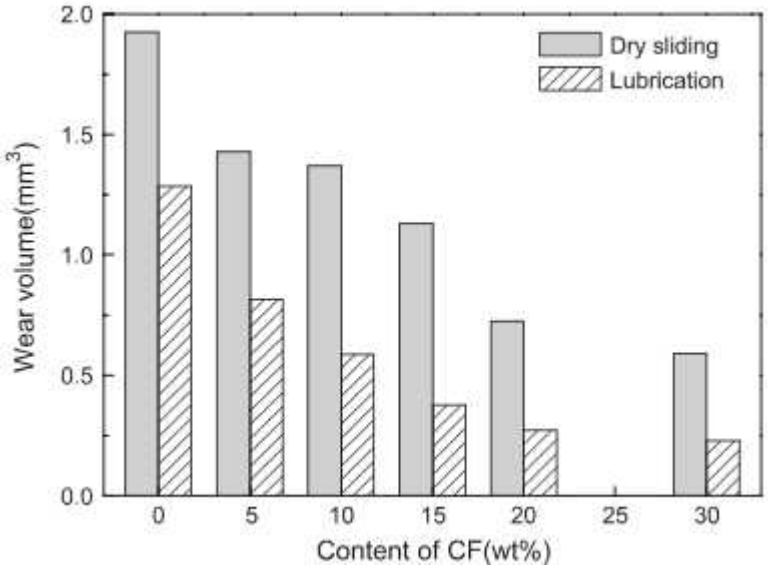

Figure 2.13 Wear volume as function of Carbon fiber loading under dry and lubrication sliding [9]

Polyamide UHMWPE blend was developed by melt mixing and then characterized under dry and lubricated sliding conditions, lower wear rates were found for lubricated sliding

attributed to elastohydrodynamic lubrication while higher wear rates were evaluated for dry caused by fatigue due to crack propagation and tearing [47].

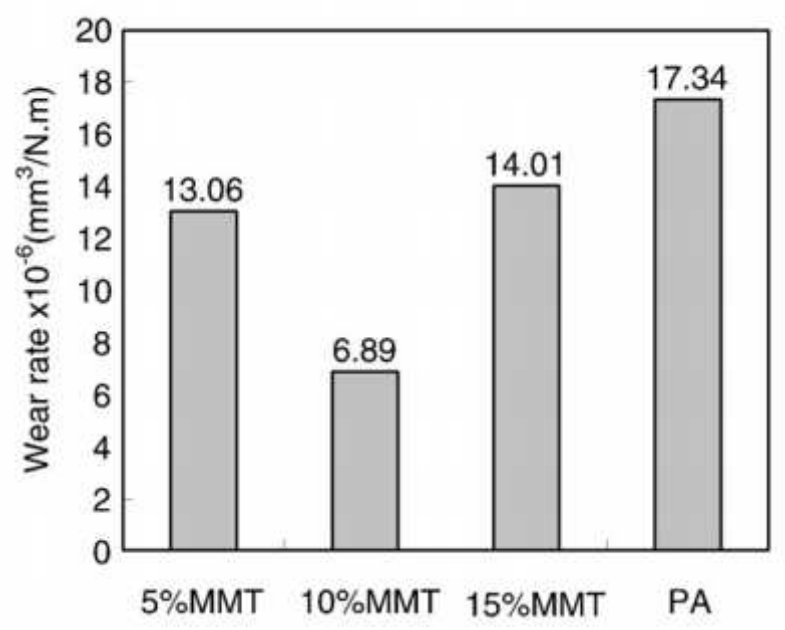

Figure 2.14 Wear rates for PA and UHMWPE/MMT composites [47]

.Similarly Wen et al. [48] us modified Nano-Montmorillonite (Clay Mineral) as filler in the ultrahigh Molecular Weight Polyethylene and was tested against J55 steel counter face using reciprocating tribometer under oilfield sewage conditions. The application of using UHMWPE was based on petroleum pumping system, where there was need to reduce the COF and wear between the sucker rod and pipeline. Polyamide was fixed on sucker rod and was used as stabilizer material. UHMWPE reinforced with nanoclay were prepared and tested for this application. Three percentages 5wt%, 10 and 15 wt.% MMT was used all the composites showed reduced COF and wear rate. 10wt % MMT composite showed maximum reduction in wear rate. The presence of abrasive sand particles in oilfield sewage resulted in deep ploughing of PA samples while for UHMWPE/MMT samples the wear

surface appeared smother. The presence of nano MMT prevented the large scale fragmentation of UHMWPE and showed reduced wear rate. Polyamide specimen showed increased wear rate, which was also attributed to poor water absorption of PA as compared to UHMWPE, which resulted in softening the surface and increasing real area of contact thereby enhancing wear rate.

From the above mentioned literature, it can be concluded that addition of nanofillers even in lubricated conditions adds to the performance of UHMWPE. The specific wear rate and COF values differ from lubricated medium to dry sliding. For polymers having low water uptake property such as UHMWPE, the water lubrication mostly results in reducing the severity of contact and frictional heating, thereby improving the wear resistance. However the performance under specific lubrication medium is strongly dependent on the properties of lubricant itself. E.g. Literature review for tribological properties under lubricated sliding showed softening of Polyamide surface due to poor water absorption. In short UHMWPE reinforced nanofillers is a promising choice for tribological applications in lubricated contacts as well. Literature review done for lubricated and as well as dry sliding conditions showed that fair amount work has been done in this direction using different nanofillers with UHMWPE as matrix. However it has been concluded that negligible amount of work has been done using two different nanofillers. One of the work for hybrid composites was done by using HDPE as matrix reinforced with HA (hydroxyapatite) and alumina particles [49]. The tribological testing was done under dry sliding and Stimulated body fluid conditions. Different volume percentages of Alumina and HA were used and it was concluded that reinforcement lead to improved load bearing capacity as well as wear resistance as compared to pristine HDPE with HDPE-20 vol % HA-20 vol % showing the

least wear. However, reinforcement used in both cases in micron scale rather than nanoscale. No work has been done using different nanofillers as reinforcement in UHMWPE. The idea presented in chapter 1, motivates to use CNTs and Nanoclay as reinforcement in UHMWPE. Hybrid nanocomposites of UHMWPE will be a unique concept in a sense to utilize the inherent traits of both nanoclay and CNTs for reducing the water absorption and improving the wear resistance under water as well as dry sliding conditions.

CHAPTER 3

MATERIALS AND METHOD

This chapter presents properties of materials used in experimental program as well as the experimental procedures followed during synthesis and characterization of nanocomposites. The chapter also covers the mechanical and tribological testing of the nanocomposites under different lubricated conditions.

3.1 Ultrahigh Molecular Weight polyethylene (UHMWPE)

The description and characteristics of UHMWPE polymer has already been delineated in chapter 2. UHMWPE powder was in the form of solid granules of characteristic appearance of white color. The average particle size ranged from 80-120 µm with flash point of about 341°C and melting point of 140°C. The powder was provided by Good Fellow Corporation USA. Figure 3.1 below shows the SEM image of UHMWPE powder confirming it to be approximately 80-120 µm.

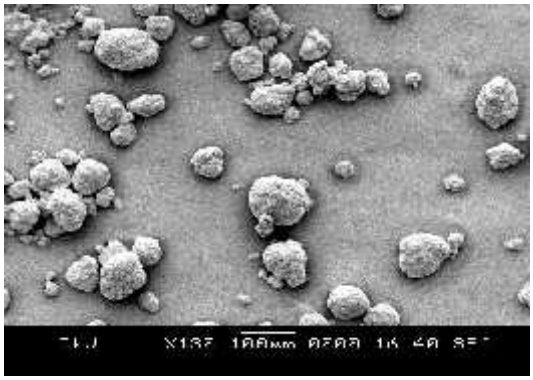

Figure 3.1 SEM image of UHMWPE powder

3.2 Nanoclay

Smectic clays were used as nanofiller material named organically modified montmorillonite clays. In the present work, three types of organically modified montmorillonite clays were used; namely: Nanomer I.30E, Nanomer I.28E, Cloisite and Cloisite 15A. The type and chemical structures of organic modifier for these nanoclays are listed in Table 3.1. The Nanomer I.30E and I.28E were acquired from Nanocor Inc, USA while the Cloisite 15A was supplied by Southern Clay Product, USA. The physical states of all nanoclays are powder having white to gray colors and their specific gravities are between 1.7 and 1.9 [14, 38].

Table 3.1 Types and chemical structure of Organic modifier clays with MMT

Organoclay	Type of Organic modifier	Structure of organic modifier
Nanomer I.30E	Primary octadecyl ammonium	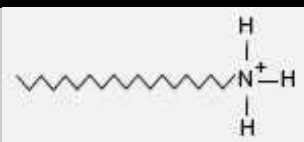
Nanomer I.28E	Quaternary octadecyl ammonium	
Closite C15A	Quaternary dimethyl dihydrogenated tallow ammonium	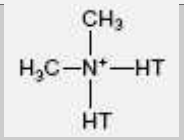

3.3 Carbon Nanotubes (CNTs)

CNTs will be used as potential reinforcement to enhance tribological properties mainly along with the organoclay. The CNTs to be used are multiwalled being functionalized with Carboxylic Acid (COOH). The CNTs were developed in Chemical Engineering laboratory

at King Fahd University of Petroleum and Minerals (KFUPM). The diameter of the mentioned CNTs is around 25-26 nm as depicted in the SEM image below.

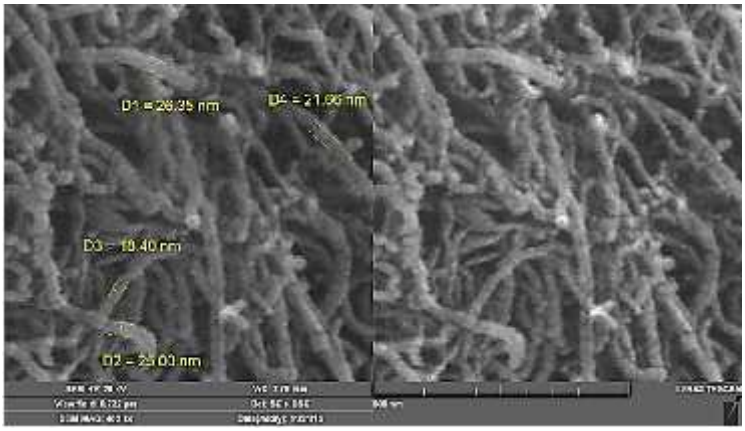

Figure 3.2 SEM Image of CNTs showing average diameter

3.4 Experimental Methodology

There are different methods that are used for preparation of polymer nanocomposites: (1) solution mixing with casting suspension of CNTs dissolved in polymer, (2) In situ polymerization of mixture of CNTS-polymer monomer, (3) Melt mixing by mechanical means using twin screw extruder, (4) dry mixing using roller or ball milling followed by Hot pressing [9, 50]. For the current work dry mixing process was used to prepare nanofiller-UHMWPE mixture followed by subsequent hot pressing. Dry mixing is reported to be an easy and effective fabrication process as compared to solution and melt mixing to disperse nanofiller in polymer and develop nanocomposite samples. UHMWPE is composed of long and heavy units of polyethylene, due to which its viscosity is very high. Dry mixing of family polymers of polyethylene (HDPE, UHMWPE) with nanofillers avoids the problem of viscosity as no solvents are added and blending /mixing of nanofillers with polymer takes place in powdered form. Final consolidation was done using

hot press. Hot press has advantage over injection molding as UHMWPE has high viscosity and melt flow index[50]. The overall process for development of nanocomposites can be divided into two parts, ball milling for dispersion followed by hot pressing to consolidate and make solid samples.

3.4.1 Mechanical Dry Mixing using Planetary Ball Mill

UHMWPE powder with the required quantity of nanofillers (nanoclay/CNTs) were ball milled using a ball to powder ratio of 10:1 i-e 10g balls for each 1g of powder, via a planetary ball mill PM-10 Planetary ball mill is one of the most used techniques to homogenize and prepare blend of powders. It consists of vials that are fixed on supports that rotate around axis same as the planetary motion of stars around sun. A milling cycle of 5 min with breaks of 10 minutes is repeated 8 times resulting in a total milling time of 1.5 hours at a speed of 250 rpm. After ball milling, mixed powders are taken out from stainless steel vials using spatula.

3.4.2 Hot Pressing Mold

The milled powders of UHMWPE and nanofiller (CNTs/nanoclay) were then hot pressed. The mixture was initially compacted in the molder using a pressure of 6 MPa at room temperature. Then the temperature was raised to 170°C and a pressure of 25 MPa was applied for 15 minutes. After that the mold was cooled to 50°C and the pressure was released. The final samples were of a cylindrical geometry with a diameter of 30 mm and a thickness of 6 mm. The measured average surface roughness (R_a) value was 0.928 ± 0.05 µm. Different weight percentages of nanoclay with UHMWPE, CNTs with UHMWPE and hybrid (CNTs/Clay with UHMWPE) were used to fabricate nanocomposite samples for characterization and testing. Table 3.2 illustrates the type and number of prepared samples.

Table 3. 2 Sample matrix with description

SAMPLE	DESCRIPTION		
Classification	**Category-type**		**Total number of samples**
UHMWPE	• Pristine		• 15 samples
UHMWPE Nanoclay composites	• 1.5% I30E/UHMWPE • 1.5% I28E/UHMWPE • 1.5% C15A/UHMWPE	• 0.5% C15A • 1.5% C15A • 3% C15A	• 6 for each different clay type composites (I28E, I30E and C15A) • 20 samples for UHMWPE/C15A nanoclay composites
UHMWPE CNTs composites	• 0.5% CNTs/UHMWPE • 1.5% CNTs/UHMWPE • 3% CNTs/UHMWPE		• 12 samples for UHMWPE/CNTs composites. • 3 additional samples for 1.5wt% CNTs/UHMWPE for water lubricated testing
UHMWPE Hybrid Nano composite	• 0.5%CNTs/1.5%C15A/UHMWPE • 1.5% CNTs1.5% C15A/UHMWPE • 3% CNTs1.5% C15A/UHMWPE		• 12 samples for UHMWPE hybrid nanocomposites • 6 additional samples for 1.5wt% hybrid nanocomposites for water lubricated testing and Accelerated life testing

3.5 Characterization of Nanocomposites

Characterization of UHMWPE nanocomposites and hybrid nanocomposites was performed to determine the basic morphology and structure. This section covers the structural or morphological characterization of nanocomposite using XRD, FESEM, and Raman Spectroscopy. Shore hardness testing and tribological characterization are also performed on the produced samples and the procedures are represented here.

3.5.1 X-Ray Diffraction (XRD)

Bruker D8 Advance is used for XRD analysis. It is equipped with auto-positioning of 9 specimen holders. The current was set at 30mA and Cu Kα was used as radiation source

having a wavelength of 1.5406Å. All samples are scanned between 2 and 70° using a step of 0.02º. The X-ray diffraction was conducted on the pure nanoclay, pristine CNTs, their respective nanocomposites and hybrid nanocomposites. Hot pressed samples were directly mounted in the stub and the diffraction data was recorded. X-ray diffraction is used to define the interplanar spacing (d-spacing) between clay platelets using Bragg's law.

3.5.2 Field Emission-Scanning Electron Microscopy (FE-SEM)

TESCAN field emission electron microscope was employed specifically to analyze the dispersion of carbon nanotubes in CNTs/UHMWPE nanocomposites and hybrid (CNTs/Clay/UHMWPE) nanocomposites. FE-SEM uses field emission gun to generate electron beam rather than thermionic gun which generates very narrow electron beam. FE-SEM micrographs have a large depth of field yielding a characteristic three-dimensional appearance useful for understanding the surface structure of a sample [51]. Lyra® imaging software was used to scan the surface. Accelerating voltage of 20KV was used for all the samples. Samples were coated with gold prior to imaging to make them electrically conductive using Quorum TechK 550X sputtering. Magnifications ranging from 10 to more than 100,000 times are possible using the FE-SEM. Images were recorded at two different magnifications, 40,000x and 60,000x. Low magnification was used for overall dispersion analysis and higher magnification for visualizing CNTs bundles and disentanglement.

3.5.3 Raman Spectroscopy

Raman Spectroscopy was performed for CNTs/UHMWPE composites and hybrid nanocomposites to analyze the interaction of carbon nanotubes with UHMWPE polymer. Raman spectroscopy is a powerful technique that can give information about the structure

of individual CNTs and their interaction with polymer chains. Its phenomenon is based on the Raman scattering of electromagnetic radiation. In this technique the sample to be analyzed is exposed to electromagnetic radiation of single wavelength, depending upon sample interaction with electromagnetic radiation, there is inelastic and elastic scattering, the electromagnetic radiation scattered inelastically is termed as “Raman Scattering”, which means that light scattered off the samples is of different frequency from radiation source. The intensity of absorbed radiation is plotted against wave number to depict the Raman spectrum [52]. The difference in the intensity of scattered and incident beam carries the information about vibration and stretching of molecules and bonds, which is used to characterize the interfacial interaction by observing the Raman shift in the band. The shifting of specific band from one wave number to another is based on vibrational, stretching and conformational modes of the bonds in interaction [51].

3.5.4 Water Uptake Testing

Two different experiments were performed to determine the amount of water uptake of UHMWPE and its nanocomposites. Frist experiment was performed at room temperature which was 23°C. Three samples for each different clay weight percentages (0.5%, 1.5% and 3%) along with pristine UHMWPE were placed, for 7 days, in a beaker of deionized (DI) water as shown in figure 3.7 (a). Samples were cleaned with acetone and dried before weighing. After weighing the samples (initial weight) samples were immersed in DI water. The water absorption was estimated using an analytical microbalance which is capable of reading 0.0001 g. Weights were recorded after 24hrs (1day), and likewise percentage water content after each day (%WC) and percentage total water content (%TWC) after 7 days

were recorded and evaluated using the equation (1). The average values were reported and compared with literature.

The second experiment of water absorption test was performed under (ALT) accelerated life test conditions, i-e at elevated temperate. Three samples of each different weight percentages (0.5%, 1.5% and 3wt.%) of UHMWPE/C15A along with pristine UHMWPE were immersed in a beaker of deionized water (DI) for a total duration of 48 hours. The temperature was maintained at 70°C during all the immersion time as shown in figure 3.7 (b). The temperature 70°C was selected below the maximum value where UHMWPE maintains its dimensional stability due to the fact that its outstanding characteristics are maintained from -269°C to 90°C [28]. A separate beaker of deionized water was also placed in the oven to account for the decrease in the water level of the testing beaker. Similar process was followed for weighing samples before and after water uptake. Weight of both UHMWPE/C15A nanocomposite sample and pristine UHMWPE were recorded after every 8hrs with a total of six readings. Average value of percentage water content (%WC) after every 8hrs and total percentage water content (%TWC) after 48 hours was evaluated using equation (1).

$$Wt(\%) = \frac{Wi - Wo}{Wo} \times 100 \qquad (1)$$

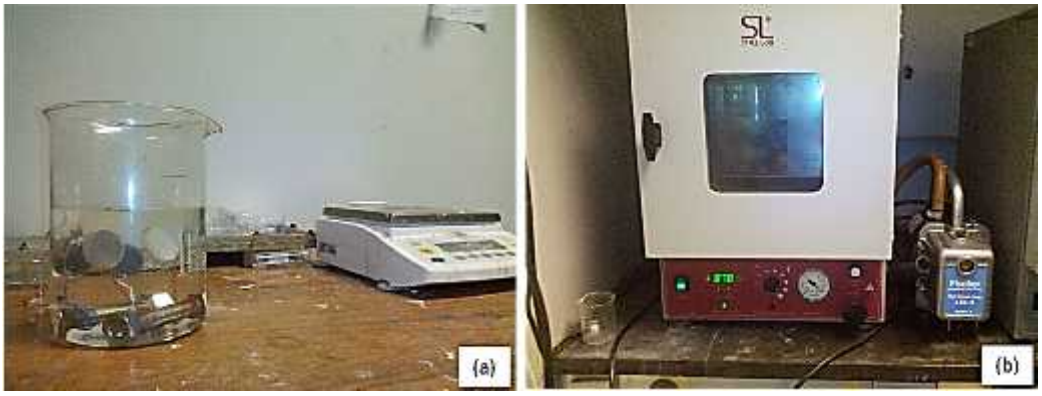

Figure 3.3 Water uptake testing (a) Room Temperature testing, b) Elevated Temperature testing (70°C)

3.5.5 Shore D Hardness

Shore D hardness of the samples was measured, as per ASTM D 2240 using Digi-Test Shoro Durometer at room temperature and a relative humidity of 30 % [53]. Shore D hardness was measured on the pristine UHMWPE, Clay/UHMWPE, CNTs/UHMWPE samples and the hybrid nanocomposite samples. For the clay composites (Clay/UHMWPE), separate shore D hardness was recorded for samples before and after water uptake to observe the effect of water absorption on the samples. Measurements were carried out on three samples of each type and nine readings at different locations were noted and the average value is reported.

3.5.6 Tribological Testing

Tribological testing was conducted using Bruker UMT-3 Tribometer. Ball on Disc configuration was used to simulate the contact conditions in tribological applications such as bearings as shown in figure 3.8. A stainless steel ball of hardness RC 38 (having a diameter of 6.3 mm was used as a counterface. Initially, all the wear tests were performed with a normal load of 30 N, corresponding to a Hertzian contact pressure of 115 MPa, and a sliding speed of 6.82 cm/sec (300 rpm), for a sliding distance of 68.2 m (5000 cycles) on

all the nanocomposite samples (nanoclay composites, CNTs composites and hybrid nanocomposites). Wear tests were also conducted at different loads (30N, 60N and 90N) for UHMWPE clay composite samples as well. Same speed and loads were used in the water lubrication tests, finally the best UHMWPE nanocomposite composition was tested under accelerated life test conditions using 50N, 800Rpm, for 25000 cycles and its performance was compared with pristine UHMWPE. Table 3.3 illustrates the complete experimental matrix for tribological testing. Tribological testing was done under dry sliding and water lubricated conditions. Table 3.3 shows complete details for tribological testing conditions and respective samples for which the testing was performed. Figures 3.9 and 3.10 show the tribometer setup and lubricant cup assembly used in current study. For each set of different samples three wear tests were conducted for each sample type and the average value of the coefficient of friction (COF) and the specific wear rates are reported. All the wear tests were carried out at a room temperature of 25±2 °C and a relative humidity of 30±5%.

Table 3.3 Detailed Experimental Matrix for Tribological Characterization

SAMPLE	APPLIED LOAD (N)	SPEED (m/s)	CYCLES	CONDITIONS
UHMWPE Pristine	30 , 60, 90	0.06	5000	Dry
UHMWPE Pristine	30	0.06	5000	Water lubricated
UHMWPE-Nanoclay composites **(Three different Clays, I28E, I30E and C15A)** • 1.5% I.30E • 1.5% I.28E • 1.5% C15A	30	0.06	5000	Dry
UHMWPE- Nanoclay composites • 0.5% C15A • 1.5% C15A • 3% C15A	30	0.06	5000	Dry
UHMWPE- Nanoclay composites • 1.5% C15A • 1.5% C15A • 1.5% C15A	30	0.06	5000	Water lubricated
UHMWPE-CNTs composites • 5% CNTs/UHMWPE • 1.5% CNTs/UHMWPE • 3% CNTs/UHMWPE	30	0.06	5000	Dry
UHMWPE- Hybrid nanocomposites • 5% CNTs/1.5% C15A/UHMWPE • 1.5% CNTs1.5% C15A/UHMWPE • 3% CNTs1.5% C15A/UHMWPE	30	0.06	5000	Dry
All optimized Nanocomposites • 1.5% CNTs/UHMWPE • 1.5% CNTs1.5% C15A/UHMWPE • 1.5% C15A/UHMWPE	30	0.06	5000	Water lubricated
Accelerated life testing (ALT) for performance evaluation • UHMWPE Pristine • 1.5% Hybrid nanocomposites	50	0.5	25,000	Water lubricated (ALT)

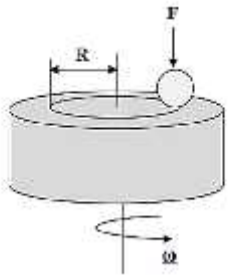

Figure 3.4 Schematic illustrating Ball on disc configuration

Figure 3.5 Tribometer setup used in current study

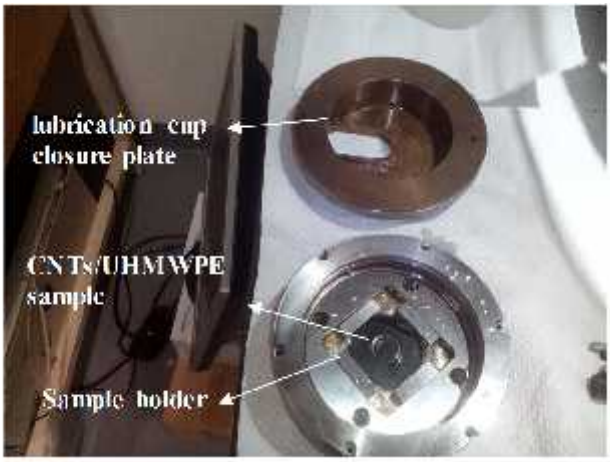

Figure 3.6 Lubricant holder cup assembly

3.5.7 Wear Morphology and Counterface Surface Analysis

Jeol JSM-6460LV Scanning electron microscopy (SEM) was used to study the wear morphology and the type of wear mechanisms. The samples were coated with gold prior to SEM Imaging. The transfer film formed on the surface of the counterface ball running against the sample was analyzed using Leica CTR-6000 optical microscope, no sample preparation was needed for this case. The ball holder itself was placed under the microscope and the ball face which was in contact with the sample during the wear test was observed and the images recorded. Both wear morphology and optical imaging of counterface was done for each sample being tested for tribological properties.

3.5.8 Profilometry

GTK-A, 3D optical profiler from Bruker Co. was used to characterize the wear track profiles after the wear tests. 3D images, 2D profiles and contour plots were recorded to understand the various wear mechanisms involved and to calculate the wear volume loss. Optical lens of magnification 5x was used for viewing the wear track area. Dominant wear mechanisms in polymers are plastic deformation, polymer pull-out resulting in the formation of the transfer film on the counterface and polymer displacement along the wear track [54]. In the present work, the wear volume loss is measured by taking into consideration all the above mechanisms. The wear volume was calculated by measuring the area under the 2D profile using the software Vision 64 of the 3D optical profiler and then multiplying it by the wear track length. No sample preparation was needed for this analysis, samples were placed directly under the lens of optical profilometer.

CHAPTER 4

RESULTS AND DISCUSSIONS

4.1 Introduction

In UHMWPE nanocomposites, the mechanical and tribological properties are strongly dependent of the structure of the nanocomposite formed. As the reinforcements used in this study are of nanometer scale so the dispersion of these nanofillers in the respective polymer matrix is very important. The level of dispersion of the nanofillers CNTs and nanoclays will determine the improvement and degradation in tribological properties. Hence, this chapter starts with the discussion on the results of dispersion and structure after which the mechanical and tribological properties are delineated for each set of UHMWPE nanocomposites as shown in sample matrix figure 3.2 (section 3.4.2). Dry sliding results are discussed initially for UHMWPE nanocomposites and then finally water lubricated results are elaborated on.

4.2 Morphology and Dispersion of UHMWPE Nanocomposites

Dispersion and morphological examination of nanofillers in UHMWPE were done using different characterization techniques such as XRD, FESEM and Raman spectroscopy for all three sets of composite systems: UHMWPE-Nanoclay composites, UHMWPE-CNTs composites and UHMWPE hybrid composites.

4.2.1 UHWMPE Nanoclay composites

Initially three different nanoclays namely I.30E, I.28E and C15A were selected and 1.5wt% of each nanoclay was used as nanofiller in UHMWPE matrix. The choice of these clays was based on previous results reported by Al-Qadhi et. al [14], where these three organoclays showed better performance with 1.5wt% of I30E depicting improved properties in terms of mechanical strength and modulus of epoxy. XRD of pristine UHMWPE is shown in figure 4.1, UHMWPE has semi-crystalline structure with two intense sharp peaks in the pattern corresponding to ortho-rhombic phase, (110) at 21.66° and (200) at 24.16° [55]. An amorphous hump can be seen along with sharp crystalline peaks indicating that UHMWPE is semi-crystalline polymer. XRD graphs are shown for three different clays and their respective 1.5wt% nanocomposites in figure 4.2 and 4.3. Figure 4.2 shows characteristic peaks of three clays (I.28E, I.30E and C15A). Organoclay C15A shows a peak at 2.52°, I.28E at 3.48° and I.30E at 4.06° corresponding respectively, to intergallery distance of 35.03 Å, 25.36 Å and 21.74 Å. The table 4.1 shows the diffraction angles and d-spacing of nanoclay composites.

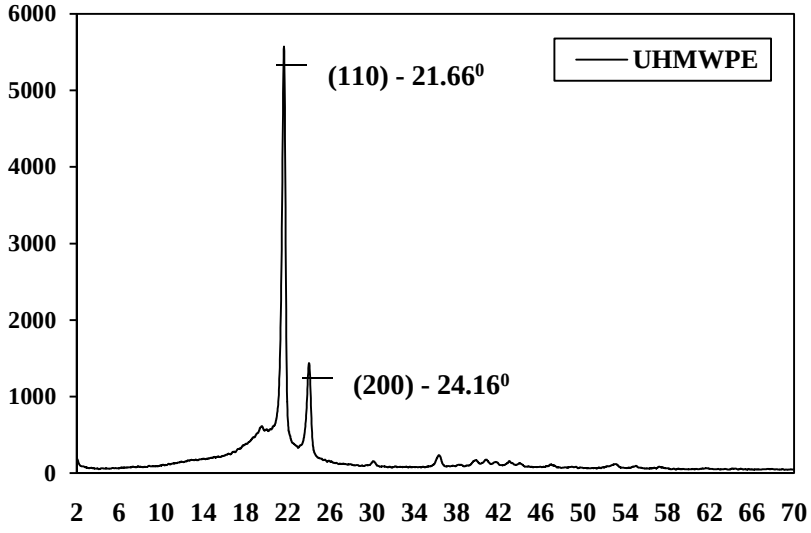

Figure 4. 1 XRD pattern for pristine UHMWPE

From XRD curve of relative intensity (R.I) vs. angle 2Θ (figure 4.3), it can be seen that the characteristic clay peak is absent from C15A/UHMWPE nanocomposite while I28E/UHMWPE and I30E/UHMWPE show peaks at 2.88° and 3.82° respectively. Hence a shift has taken place in diffraction peak form 3.48° to 2.88° and from 4.06 to 3.82° resulting in the increased intergallery (d-spacing) from 25.36 Å to 31.52 Å for I28E/UHMWPE, whereas 21.74 Å to 23.11 Å for I30E/UHMWPE has taken place. This indicates that for these nanocomposites intercalation has taken place. For C15A/UHMWPE the absence of clay peak indicates either exfoliated or disordered intercalation. The exfoliated morphology is referred to dispersion of clay platelets breaking their layer order forming amorphous structure [5].

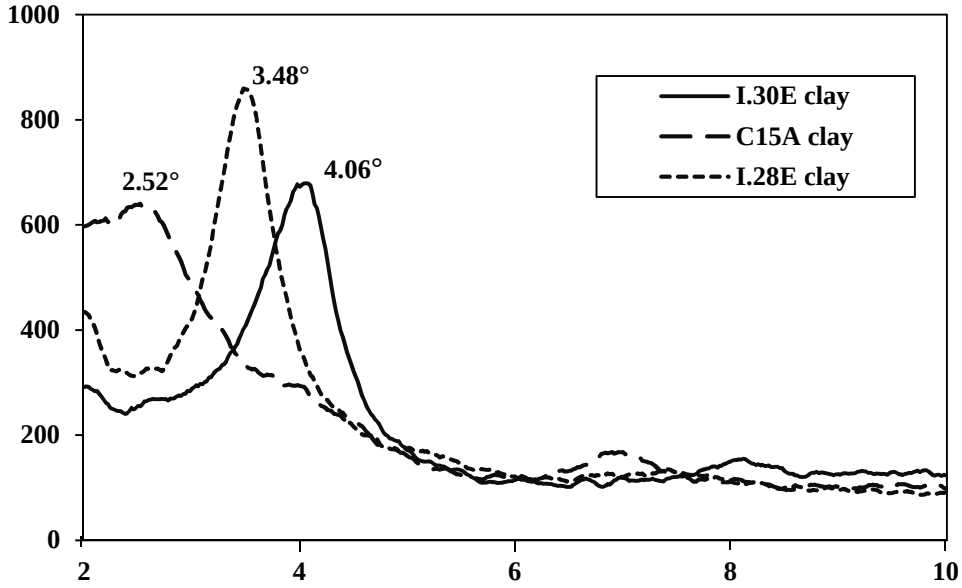

Figure 4.2 XRD showing characteristic peaks positions for I28E, I30E and C15A organoclays

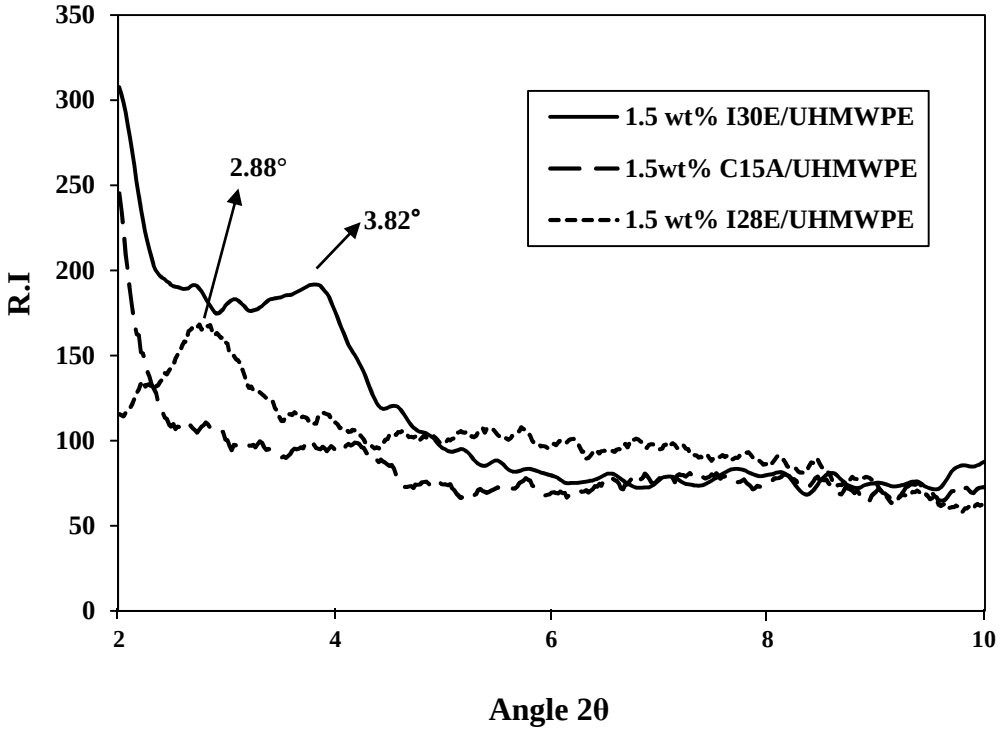

Figure 4.3 XRD for I.28E, I.30E and C15A organoclay UHMWPE nanocomposites

Table 4.1 Diffraction angles and d-spacings for clays and their respective nanocomposites

Sample	Diffraction Angle	d-Spacing A^0
I30E Organo-Clay	4.06	21.74
C15A Organo-Clay	2.52	35.03
I28E Organo-Clay	3.48	25.36
1.5wt% I30E Clay/UHWMPE	3.82	23.11
1.5wt% I28E Clay/UHMWPE	2.88	31.52
1.5wt% C15A Clay/UHMWPE	----------	----------

The level of dispersion and interaction of the clay with the polymer matrix is believed to be different due to the difference in the type of the organic modifier for each of the clays. It can be seen from table 4.1 that C15A organoclay has highest d spacing among I30E and I28E organoclay since it has been modified by larger organic modifier, quaternary dimethyl dihydrogenated tallow ammonium ion while I30E is modified with primary octadecyl ammonium ion and I28E with quaternary octadecyl ammonium ion. Attraction Energy (U) between any two clay platelets of equal thickness is defined as shown in equation (1), where A is Hamarker constant, h is the separation distance between clay platelets and δ is the platelet thickness. It can be seen that attraction energy between clay platelets is inversely proportional to the square of separation distance. Hence the clay modified with larger

molecule having increased interlayer distance is most likely to show delamination of clay platelets resulting in an exfoliated morphology as in the case of C15A composite [38]

$$U = -\frac{A_{11}}{12®}\left[\frac{1}{h^2} + \frac{1}{(h+2¢)^2} - \frac{2}{(h+¢^2)}\right] \qquad (1)$$

4.2.2 Dispersion and Morphology of UHMWPE/C15A clay composites

C15A among other clays resulted in possible exfoliated morphology showing no signature peak of clay. However, as initially 1.5wt% of C15A clay was used, hence to optimize the clay loading three different weight percentages of C15A clay 0.5wt%, 1.5 wt% and 3wt% were prepared and analyzed by XRD**.** The XRD of the respective clay composites showed no distinct peaks at 2.52◦ in the diffraction patterns are seen for 0.5wt% and 1.5wt% nanoclay composites, indicating possible exfoliation or disordered intercalation. The absence of peak can be ascribed to either exfoliated morphology or disordered intercalation with average interlayer distance higher than 7nm [56]. It has also been reported that to achieve an exfoliated morphology. During high energy ball milling process which has been used in this study, shearing takes place because of high rotational speeds and continuous impingement of the balls with the powder particles. This shearing action results in the infusion of polymer chains in the intergallery spacing of clay resulting in either exfoliated or intercalated morphology [56, 57].

The XRD spectra for 3wt% C15A composites indicates a characteristic clay peak at 2.46◦ corresponding to a d-spacing of 35.88 Å, with a slight shift to the left of the signature peak for C15A. This very slight shift to lower angle from (2.52° to 2.46°) results in interplanar

distance to slightly increase from 35.03 Å to 35.88 Å, indicating negligible amount of intercalation due to possible agglomeration at higher clay contents.

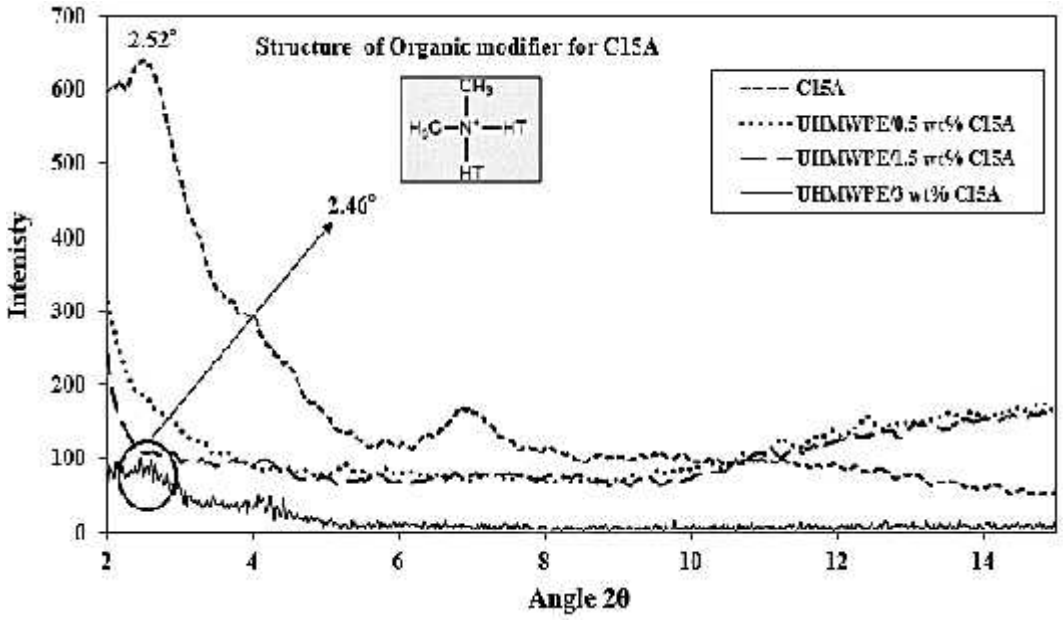

Figure 4.4 XRD graph of UHMWPE and its C15A nanocomposites

4.2.3 UHMWPE/CNT composites

The second set of nanocomposite was based on UHMWPE reinforced with CNTs. Three different percentages of CNTs 0.5wt%, 1.5wt% and 3wt% were used as reinforcements to develop nanocomposites. CNT reinforced UHMWPE composites were prepared and XRD, FE-SEM and Raman spectroscopy were employed to study the structure, dispersion and interaction of CNTs with UHWMPE polymer.

XRD results for CNT/UHMWPE composites are depicted in figure 4.5. Graph shows characteristic peaks of CNTs, UHMWPE and their respective nanocomposites. CNTs show characteristic peaks at 25.58° which corresponds to (002) ordered arrangements of concentric cylinders of the graphitic carbon atom [58, 59], while peaks at 43.12◦ refer to

(100) graphitic planes. The characteristic peaks for pristine UHMWPE can be seen at 21.66◦ and 24.16◦. XRD for CNT/UHMWPE for all the three different weight percentage composites illustrates no characteristic CNT peak. The absence of CNT peaks for these composites is due to the effective mixing of CNTs in polymer matrix. Moreover, it was also observed that intensity of UHMWPE characteristic peaks show reduction as CNTs are added, which hints altered crystalline and amorphous phases.

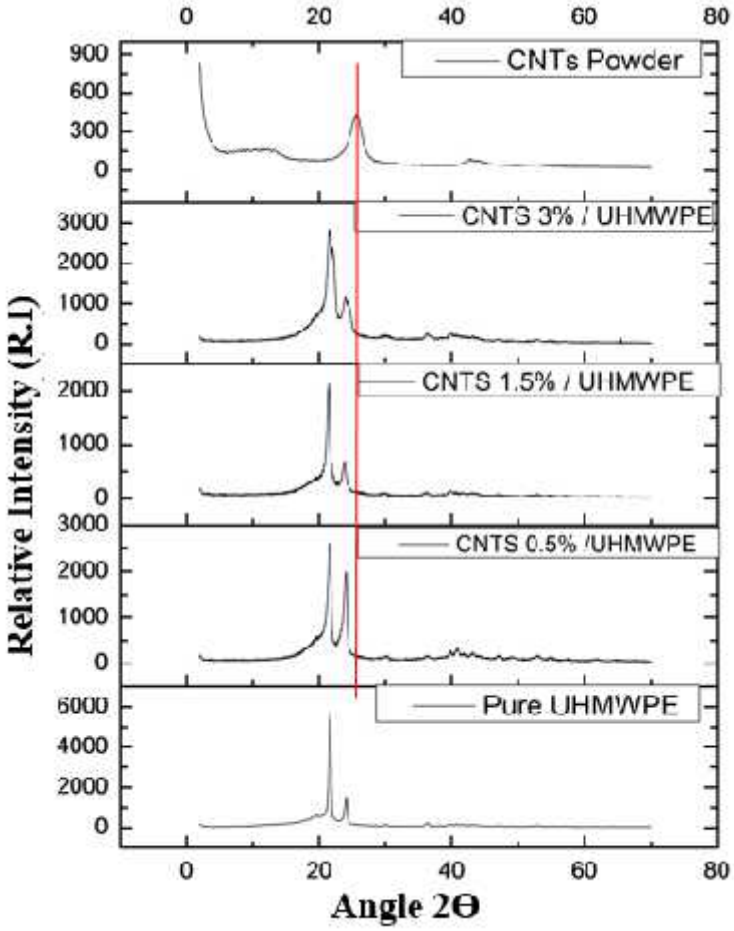

Figure 4.5 XRD graph of UHMWPE and its CNTs/UHMWPE composites

FESEM results for the CNTs alone and CNTs/UHMWPE composites are shown in figure 4.6. It can be seen that CNTs are well dispersed in 0.5wt% CNTs/UHMWPE and 1.5 w%

CNTs/UHMWPE composites. Individual CNTs are present in different locations pointing out almost negligible agglomeration. Hence, the ball milling has resulted in effective dispersion of CNTs in UHMWPE matrix. Figure 4.6 [(a), (b) and (c)] are low magnification images at 40,000 while (d), (e) and (f) are images taken at 60,000 magnification. FESEM results for 3w% CNTs/UHMWPE showed signs of agglomeration. Agglomeration started to appear and become dominant as CNTs content is increased from 1.5wt% to 3wt% having jumbles and clustered areas of CNTs.

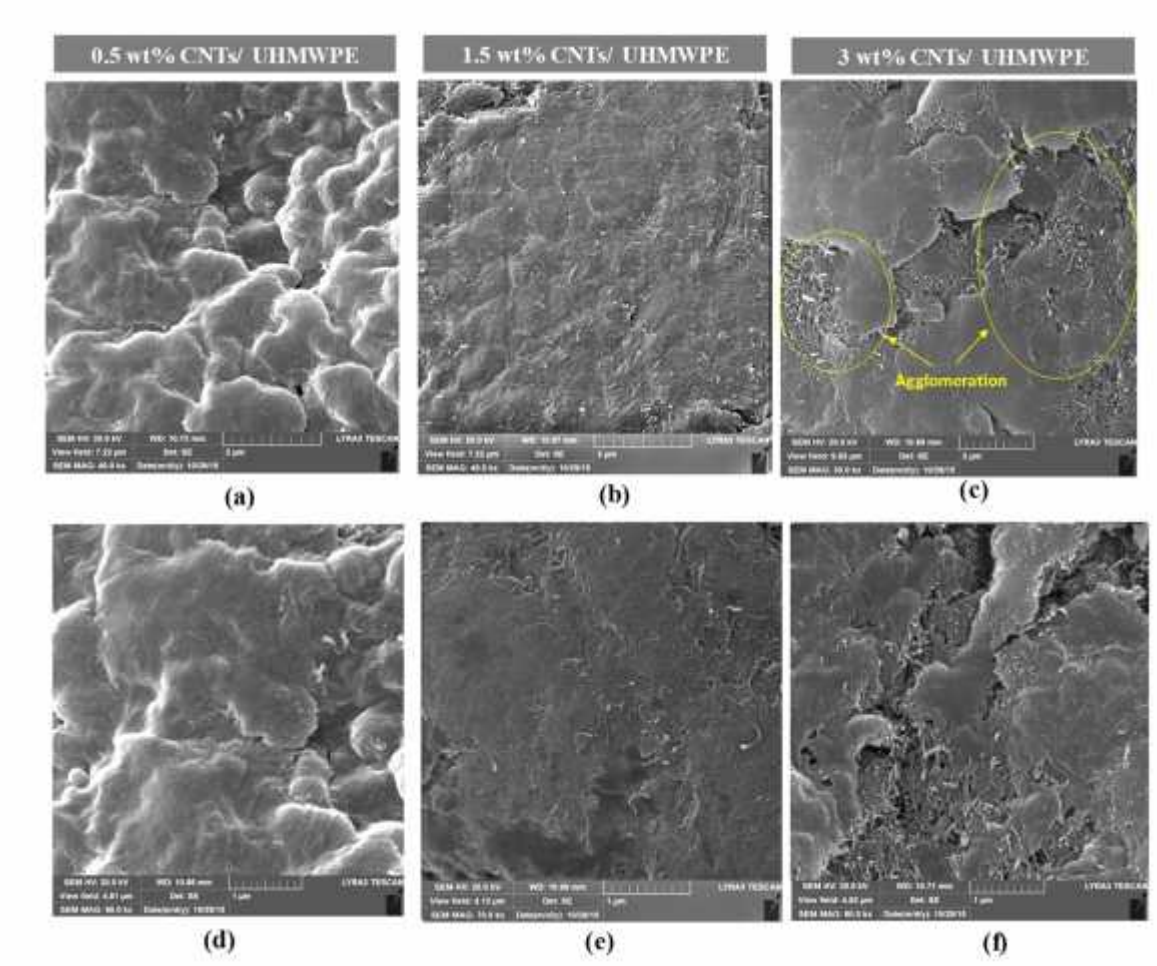

Figure 4.6 FESEM images of 0.5wt%, 1.5wt% and 3 wt% CNTs/UHMWPE composites, low magnification images (a), (b), (c) and high magnification (d), (e) and (f)

Raman spectroscopy was performed for analysis of interfacial interaction of CNTs with UHMWPE. Figure 4.7 shows Raman spectra for pristine UHMWPE, CNTs and CNTs/UHMWPE composites. Pristine UHMWPE main peaks are shown at 1439 cm^{-1}, 1295 cm^{-1}, 1129 cm^{-1} and 1062 cm^{-1}. These are high intensity peaks characteristic to UHMWPE. The peaks at 1062 cm^{-1} and 1129 cm^{-1} correspond to asymmetric and symmetric stretching modes of C-C bonds for polyethylene [60-62]. While bands 1295 cm^{-1} and 1439 cm^{-1} are related to twisting and bending modes of CH_2 [63]. The characteristic peaks for CNTs are at 1359 cm^{-1} and 1567 cm^{-1} corresponding to D and G bands. D band depicts disordered graphitic structures whereas G band occurs due to tangential C-C stretching [64, 65].

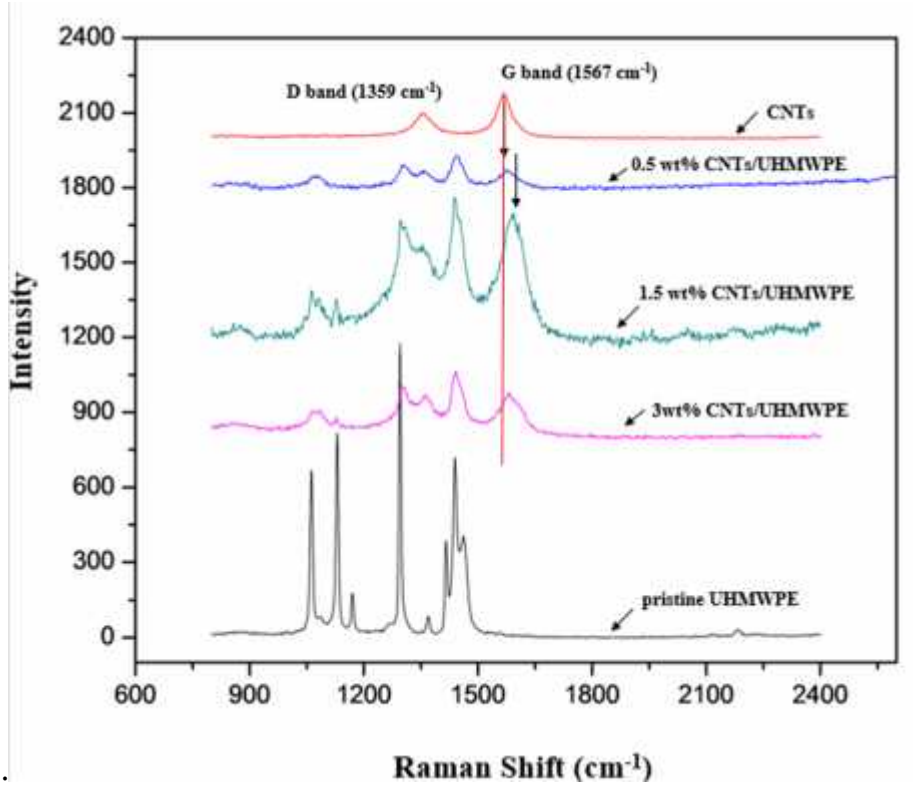

Figure 4.7 Raman Spectra for pristine UHMWPE, CNTs and their respective weight percentage composites

It can be seen that upon addition of CNTs to UHMWPE, a clear shift is observed in G band. For 1.5wt% CNTs/UHMWPE, the G band shifts from 1567 cm^{-1} to 1595 cm^{-1} with a shifting of 29 cm^{-1}, this large shifting of G band to higher frequencies is attributed to disentanglement of CNTs network and following dispersion of CNTs in polyethylene matrix. Similar shifting of G band peak has been reported in other studies owing to enhanced interaction of CNTs with polyethylene and other polymer matrices [66-68]. Similarly 0.5wt% and 3wt% show shifting in G peak to higher frequencies at 1578 cm^{-1}, owing to fair dispersion of CNTs in UHMWPE, however the shift is not as large as seen for 1.5wt% CNTs.

4.2.4 Hybrid UHMWPE nanocomposites

Fig 4.8 shows XRD results for hybrid nanocomposites. The graph shows characteristic peaks of CNTs, C15A nanoclay, UHMWPE and those of their respective hybrid nano composites. The characteristic peak of C15A is absent from all the nanocomposites, pointing towards possible exfoliation or disordered intercalation of clay platelets, which is same observed for 1.5 wt% C15A/UHMWPE nanocomposites (Section 4.1). With addition of CNTs to C15A/UHMWPE mixture, no peaks of CNTs were present indicating efficient mixing of CNTs in the composite. It can also be observed that pristine UHMWPE shows high intensity peak, however as CNTs content is increased in hybrid nanocomposites, the only change observed was a decrease in the intensity of characteristic UHMWPE peaks with 1.5 wt% CNTs and 3 wt% hybrid nanocomposites showing lower values. This indicates a reduction in crystallinity as the CNTs addition has brought some changes in crystalline and amorphous phases.

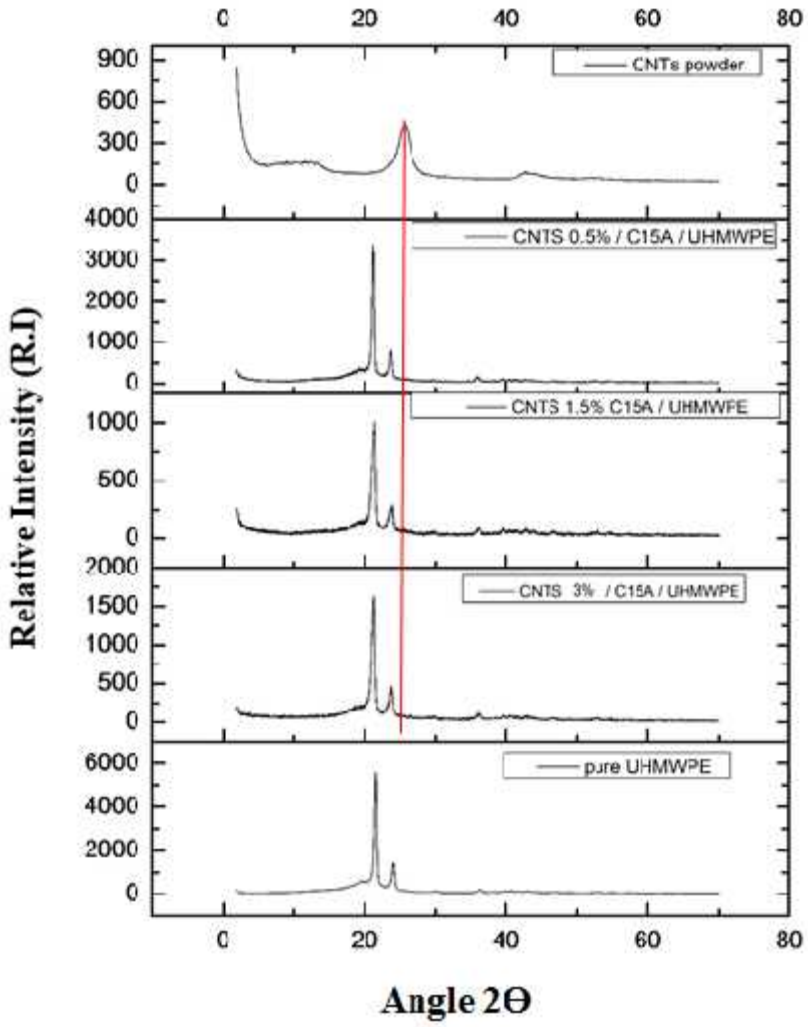

Figure 4.8 XRD graph of UHMWPE and its CNTs/C15A/ UHMWPE composites with varying CNTs content (5wt%, 1.5wt% and 3wt %)

FESEM micrograph for the CNTs/C15A/UHMWPE composites are presented in figure 4.9. The CNTs seems to be well dispersed in matrix for especially for 1.5 wt% and 0.5 wt% CNTs addition to clay/UHMWPE composites. Ball milling has effectively dispersed CNTs resulting in almost negligible agglomeration. High resolution images for 1.5 wt% of CNTs at (140,000 x) is shown, where single CNTs can be seen on UHMWPE particles, this shows excellent dispersion of CNTs in composite mixture. However, similar trend was seen when

increasing CNTs content from 1.5 wt% to 3 wt%, agglomeration sings for CNTs can be seen, CNTs have made jumbles and clustered at few places owing to increased amount.

Raman spectrum of UHMWPE, Hybrid CNTs/C15A/UHMWPE composites are shown in figure 4.10. Pristine UHMWPE, main peaks are shown at 1439 cm^{-1}, 1295 cm^{-1}, 1129 cm^{-1} and 1062 cm^{-1}. These are high intensity peaks characteristic to UHMWPE as discussed in previous section (section 4.2.3) also that, peaks at 1062 cm^{-1} and 1129 cm^{-1} correspond to asymmetric and symmetric stretching mode of C-C bonds for polyethylene [61, 69]. CNTs peaks for D and G band are also evident at 1359 cm^{-1} and 1467 cm^{-1}. With addition of CNTs in C15A/UHMWPE, the G band peak shows shifting to higher frequencies as observed in CNTs/UHMWPE composites. Here it was noticed that shifting of G band is same for all the nanocomposites, the G band shifts from 1467 cm^{-1} to 1483 cm^{1}. 0.5 wt%, 1.5 wt% and 3 wt% of hybrid UHMWPE composites showed same degree of shift. The shifting of characteristic G band is attributed to penetration of UHMWPE chains into CNTs bundles, hence creating disentanglements for CNTs bundle ensuring good interfacial interaction between CNTs and UHMWPE chains in hybrid nanocomposites.

Three different characterization techniques has been used to conclude about the dispersion and interfacial interaction of CNTs with UHMWPE polymer chains. Each characterization technique used in the study supports and adds to conclusion. The main points of concern, when adding nanofiller to polymer matrix, is basically; (1) structure/morphology of the nanocomposites giving notion about the signs of new phase and information about the amorphous and crystalline phases (2) agglomeration and dispersion of nanofiller in

polymer matrix and (3) interfacial interaction/compatibility of nanofiller with polymer matrix.

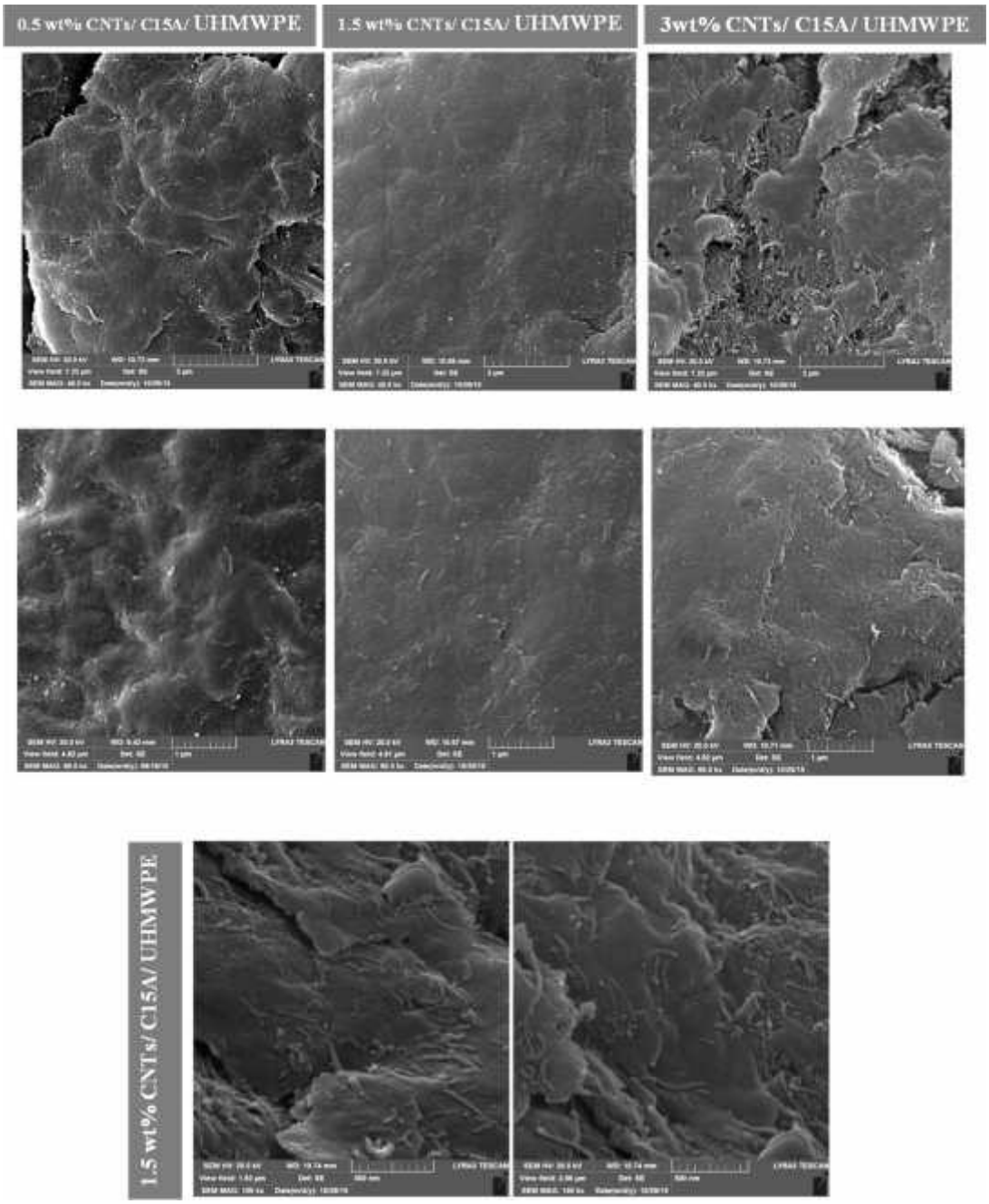

Figure 4.9 FESEM images of Hybrid Nanocomposites [(a), (b) and (c)] low resolution images and [(d), (e) and (f)] high resolution images. [(g) and (h)] images of 1.5 wt% hybrid nanocomposites at 140,000 and 150,000 magnification

XRD results for CNTs/UHMWPE nanocomposites and hybrid nanocomposites showed alteration of crystalline and amorphous phases on addition of CNTs. Raman spectroscopy results for CNTs/UHMWPE depicted shift in G band owing to disentanglement of CNTs network where greatest shift was observed for 1.5 wt% nanocomposites. Hybrid nanocomposites also showed shifting of G band pointing towards efficient mixing and good interfacial interaction between CNTs and UHMWPE polymer chains. Raman spectroscopy results were supported by FESEM results, where CNTs showed excellent dispersion for 0.5 wt% and 1.5 wt%, however slight agglomeration was seen for 3 wt% CNTs in both CNT/UHMWPE composites and hybrid UHMWPE nanocomposites. Hence, it was concluded from dispersion and morphological characterization that CNTs are effectively mixed in UHMWPE and hybrid UHMWPE nanocomposites with good interfacial interaction between each other. However, 3 wt% indicated agglomeration signs as suggested by FESEM.

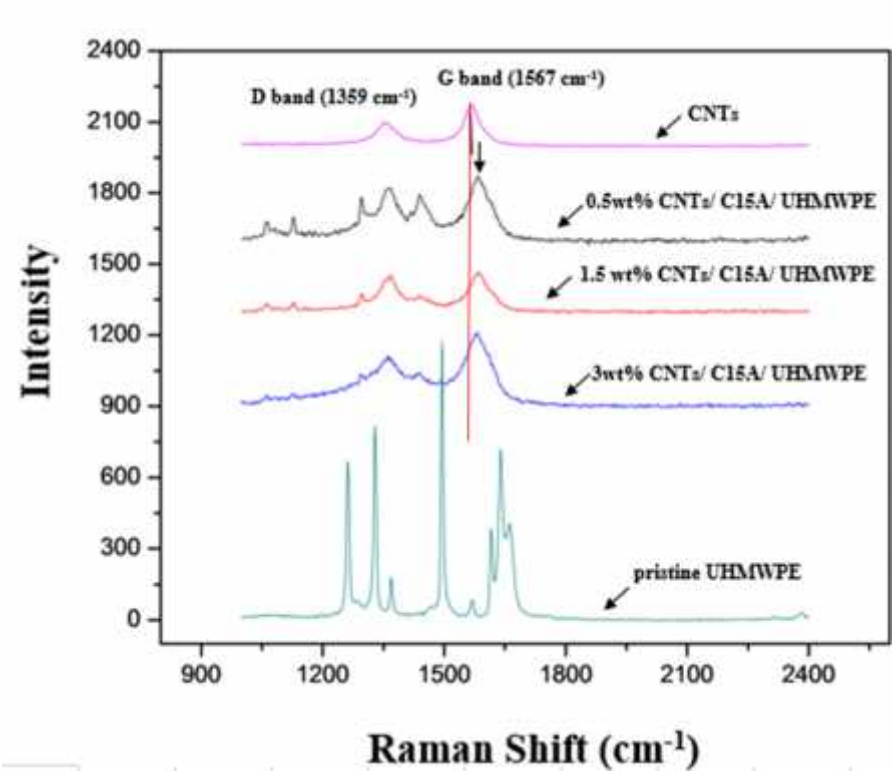

Figure 4.10 Raman Spectrum for pristine UHMWPE, CNTs and their respective hybrid nanocomposites

4.3 Effect of Clay loading on the water absorption of UHMWPE

Water uptake testing was performed for pristine UHMWPE and its clay composite samples. Water absorption tests both at room and elevated temperatures were done. Variation of the percentage of water absorption after 7 days of immersion at room temperature results is shown in figure 4.11 and figure 4.12. Figure 4.11 illustrates the water uptake recorded after each 24 hours 1 (day), while figure 4.12 indicates the total percentage water (%TWC) content after 7 days. All of the clay composites showed comparatively reduced water absorption with reference to UHMWPE. The average water uptake for pristine UHMWPE was evaluated to be ~ 0.01 % which is in agreement with literature [70, 71]. In general, all nanocomposites with different clay loadings showed reduced values in comparison to pristine UHMWPE. The variation of water absorption by the pristine UHMWPE and the

UHMWPE nanocomposites reinforced with different loadings of C15A nanoclay at a temperature of 70 °C is shown in figure 4.13 and figure 4.14. Figure 4.13, depicts the percentage water content (% WC) after every 8 hrs. It can be seen that there is change in the slope of % WC curve for all the samples after 24 hrs which is reduces further after 40 hrs. This indicates the saturation for water absorption by the samples with no room for further reduction. From figure 4.14, it can be observed that an increase in the nanoclay content resulted in a decrease in the water uptake of the samples with 1.5 wt% and 3 wt% of clay loading showing similar reduction with 0.173% and 0.169%.

The significant improvement in the resistance to water absorption with the addition of nanoclay is attributed to the ability of the nanoclay to increase the tortuous path of the water molecules in the polymer matrix as they diffuse into the nanocomposite. The presence of high aspect ratio layered silicates makes diffusion of water molecules into the composite difficult by making a tortuous track [72, 73]. In the present study, it is also observed that with an increase in the nanoclay content the resistance to water uptake also increased. For the case of water uptake results at 70°C, 10% reduction for 0.5 wt% of C15A, and a 23% reduction in water uptake for 1.5 wt% of C15A and 3 wt% of C15A as compared to pristine UHMWPE was observed. This is attributed to the fact that the presence of greater number of clay platelets in UHMWPE polymer, makes it more tortuous for the water molecules to diffuse into the nanocomposite, hence decreasing the water uptake [74, 75]. However it was also observed that further addition of clay from 1.5wt% to 3wt% doesn’t improve the water barrier. This can be attributed to possible agglomeration and low intercalation of clay in UHMWPE matrix as evident from XRD (Figure 4.4).

Figure 4.15 shows comparison between percentage total water content for water uptake testing done at room temperature and water uptake testing done at 70°C. It can be observed that an increase in temperature has resulted in more water absorption. The water absorption results at room temperature (23°C) shows reduced values for all samples comparing to samples tested at higher temperature (70°C) i-e, there is approximately 70% reduction in total water content (%TWC) for pristine UHMWPE samples tested at room temperature in comparison to samples tested at higher temperatures. This can be due to the softening of the polymer surface at elevated temperatures resulting in more water molecules penetrating through the surface due to high diffusion owing to higher temperature [76, 77]. However, in both the cases it can be clearly observed that the presence of the nanoclay platelets in the polymer matrix has significantly helped in increasing the resistance to water uptake.

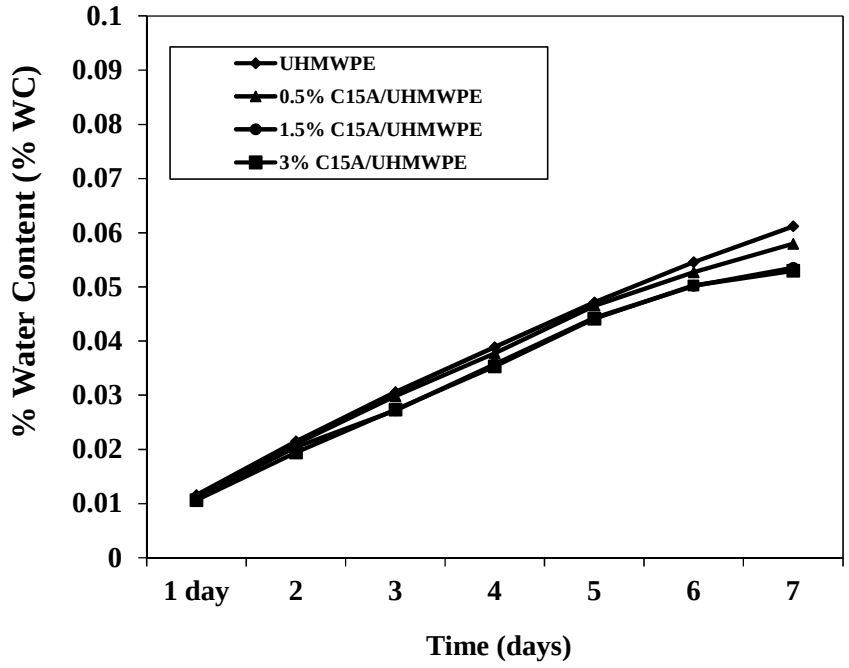

Figure 4.11 Variation of water uptake with immersion time at room temperature

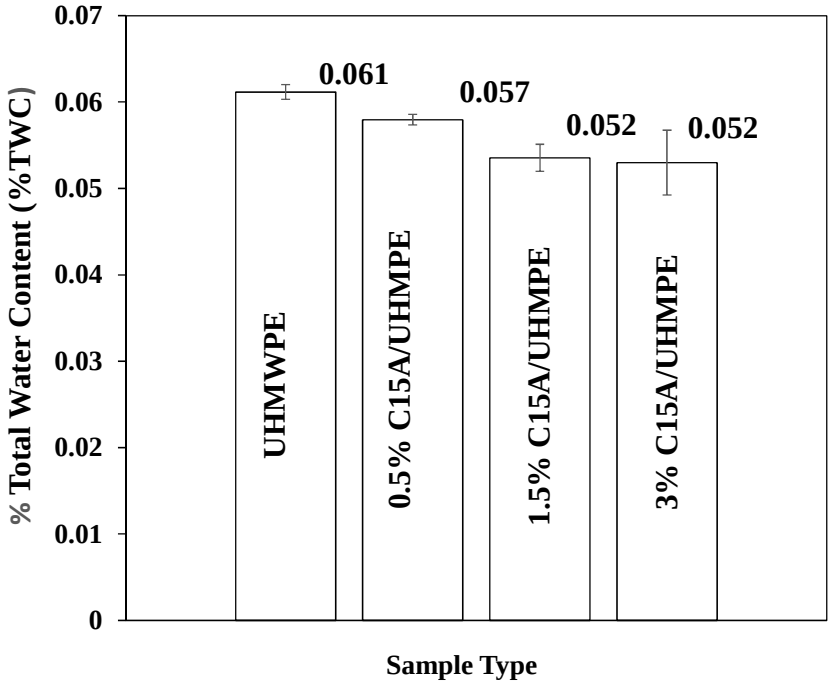

Figure 4.12 Total water uptake after 7 days of immersion in water at room temperature

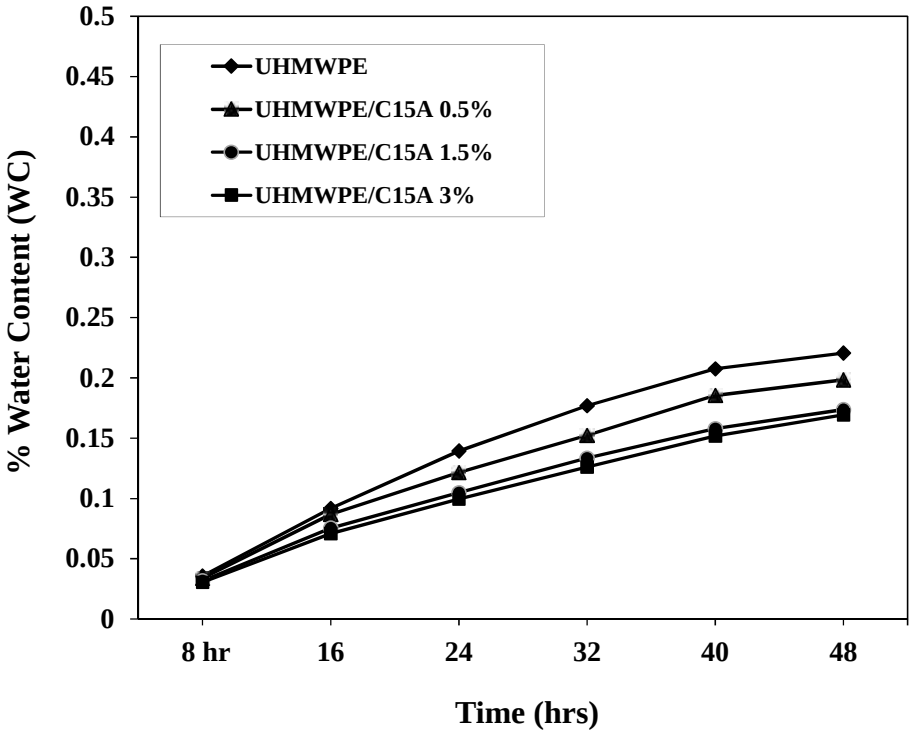

Figure 4.13 Variation of water uptake with immersion time at temperature of 70°C

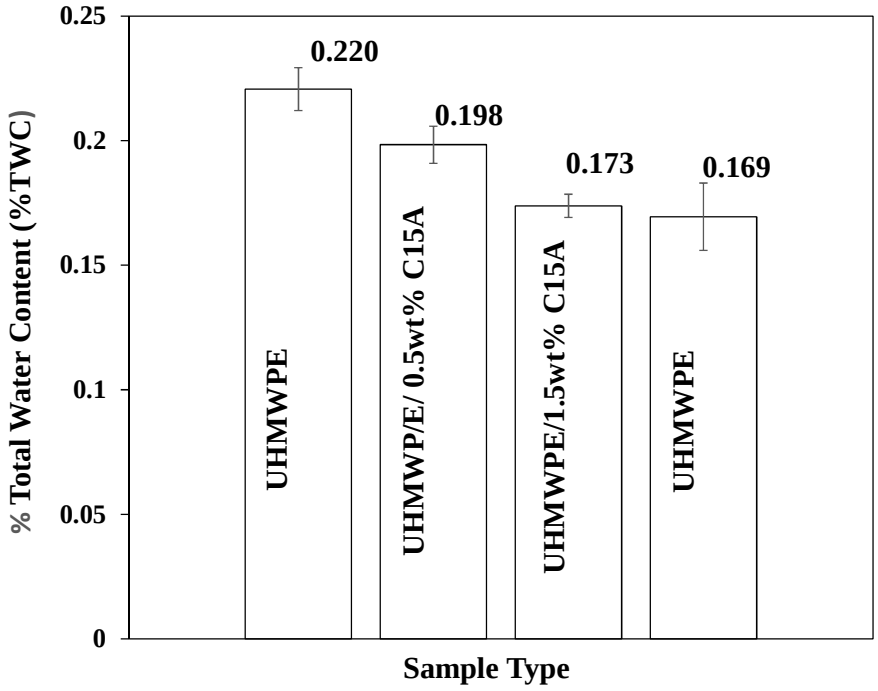

Figure 4.14 Total percentage water content (% TWC) after 48 hrs for samples tested at Room temperature water

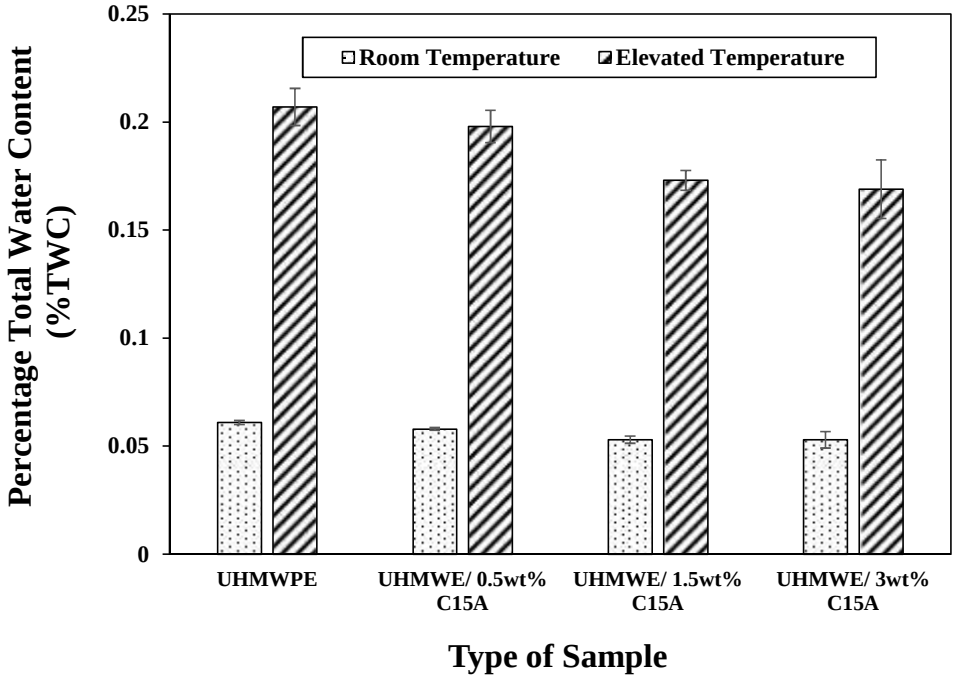

Figure 4.15 Graph showing comparison of total percentage water content at room and elevated temperature

4.4 Effect of nanofiller loading on hardness of UHMWPE

Evaluation of hardness of UHMWPE nanocomposites was done using Shore D hardness following ASTM D2240 Standard [53]. Hardness testing was performed on pristine UHMWPE and all three nanocomposites: UHMWPE-Nanoclay composites, UHMWPE-CNTs composites and UHMWPE hybrid composites.

4.4.1 Effect of nanoclay loading

Figure 4.16 shows that all of the clay composites resulted in improved average hardness by about 4% compared to pristine UHMWPE. The increased hardness of all three different 1.5wt% clay composites is due to higher hardness of clay platelets, increasing the resistance to indentation. C15A showed greater improvement in hardness possibly due to better dispersion of clay platelet and good wettability with polymer matrix.

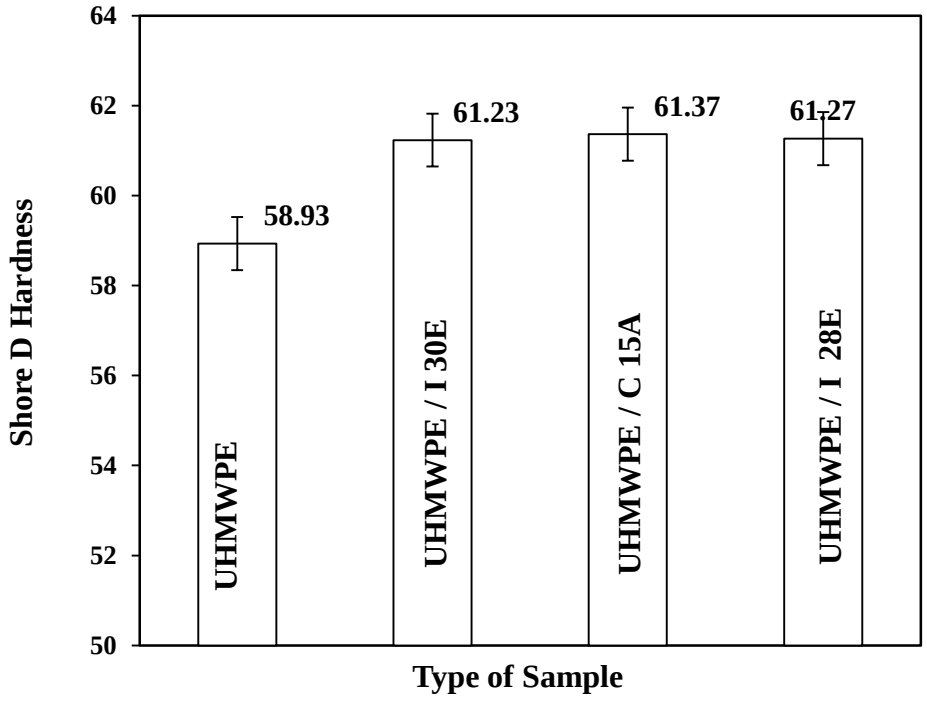

Figure 4.16 Shore D hardness values for three nanoclay composite

Shore D hardness testing was also conducted on the nanocomposite with three different C15A clay loadings (0.5 wt%, 1.5 wt% and 3 wt%). From figure 4.17. The results reveal that average value of shore D increases with increasing clay loading. Greater amount of hard clay platelets in softer matrix results in greater resistance to indentation. It has been observed in other studies as well, that clay platelets effectively add to increased hardness in polymer matrices [43, 78, 79]. However, it is observed that the increase in the hardness of the nanocomposites was not found to be very significant on varying the clay content from 1.5 wt% to 3 wt%.

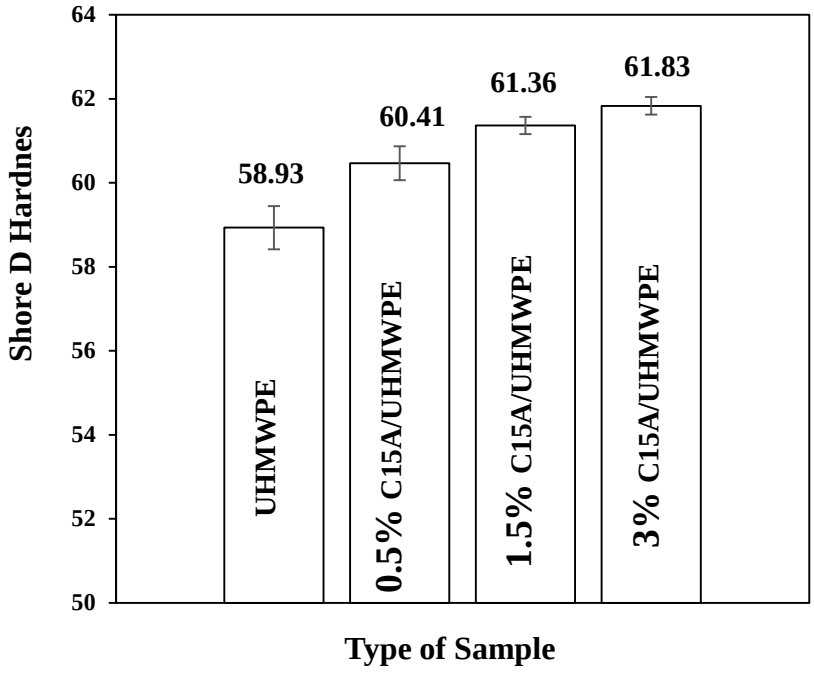

Figure 4.17 Shore D hardness of UHMWPE and C15A (5wt%, 1.5wt%, 3wt %) reinforced UHMWPE composites

4.4.2 Effect of CNTs loading

Figure 4.18 illustrates the variation of average value of shore D hardness with CNTs content. Similar to nanoclay loading, CNTs addition has shown to increase the hardness of

UHMWPE. This is expected knowing the fact that, CNTs have enhanced mechanical properties in terms of strength, modulus, hardness and stiffness [80] which results in increased hardness or increased resistance to indentation. Similarly for the results obtained from the shore D testing of hybrid nanocomposites (figure 4.19), it was noticed that the addition of CNTs to 1.5 wt% C15A/UHMWPE composites adds to further improvement in hardness, though it can be seen that the improvement is not very significant as compared to UHMWPE and CNTs composites. The maximum value for hardness for CNTs/UHMWPE is 63.4 while for the hybrid nanocomposites the maximum increase is found to be 64.5 on shore D scale with nearly about 10% improvement compared to pristine UHMWPE.

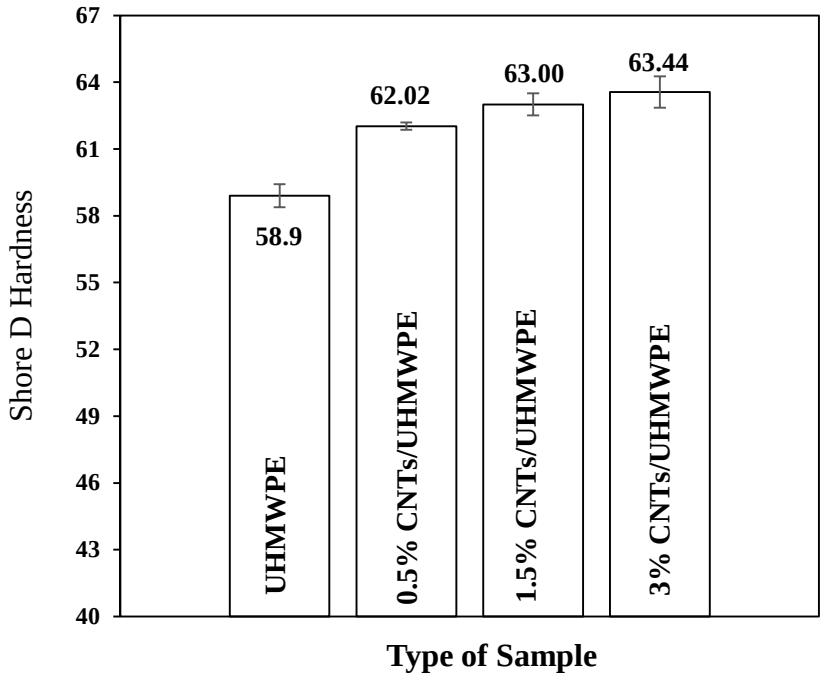

Figure 4.18 Shore D hardness for UHMWPE and its CNTs composites

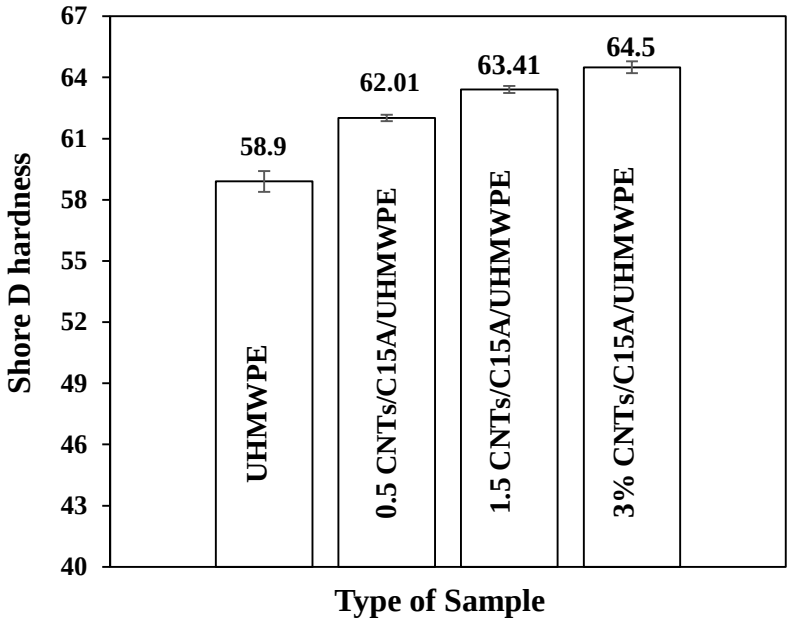

Figure 4.19 Shore D hardness for UHMWPE and its hybrid nanocomposites

4.5 Effect of water absorption on the hardness of nanoclay composites

The samples used for conducting the water absorption tests at elevated temperature were characterized for hardness and tribological properties after water uptake measurements. Shore D hardness values of pristine UHMWPE and UHMWPE/C15A nanoclay composites before and after water uptake are shown in Fig. 4.20 for comparison. The C15A/UHMWPE nanocomposites showed higher hardness than pristine UHMWPE even when tested after the water uptake, which can be attributed to the reduced water absorption by C15A/UHWMPE composites as compared to pristine UHMWPE. Increased water absorption leads to the softening of the polymer resulting in decreased hardness. Hence the nanocomposites performed better in terms of hardness when compared to pristine UHMWPE. Moreover it was seen in Section 4.3 that, increased percentages of C15A/UHMWPE showed less water absorption which has resulted in terms of better

hardness value as compared to pristine UHMPWE, therefore clay particles along with its characteristic of resisting the indentation also reduces the water absorption, which played vital role in better properties of organoclay composites.

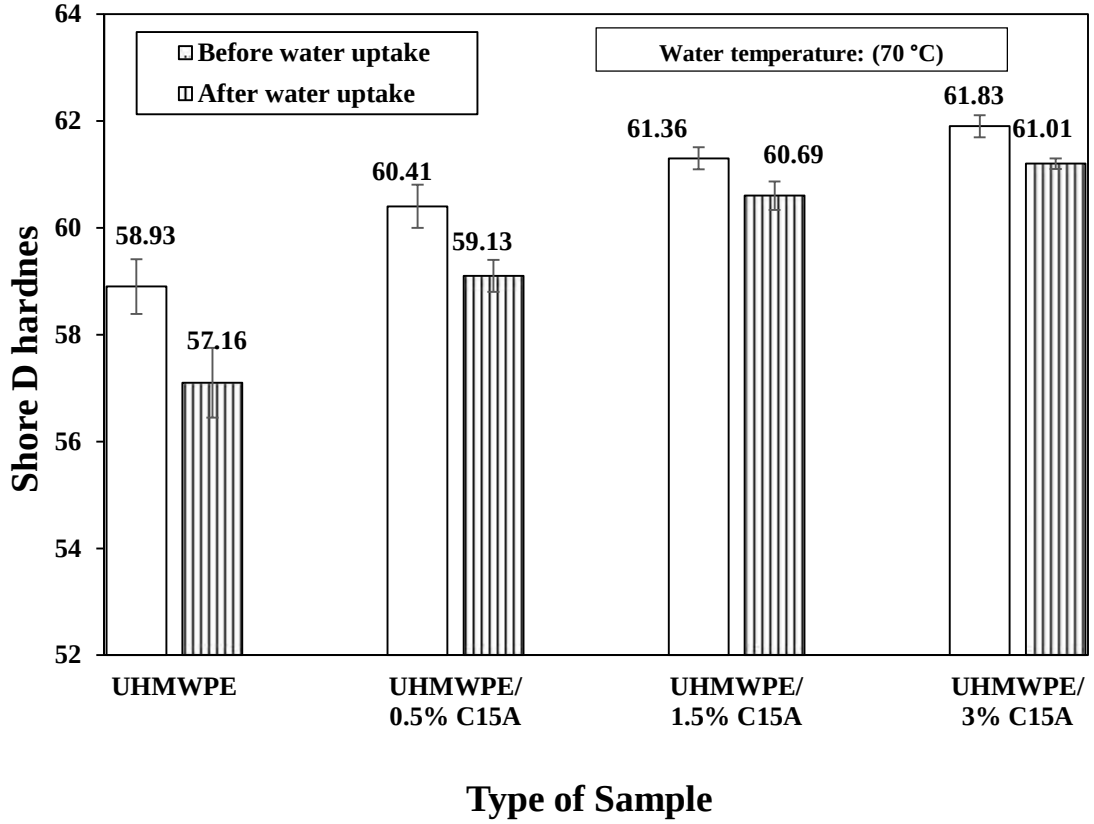

Figure 4.20 Shore D hardness for UHMWPE and C15A organoclay composites before and after water absorption

4.6 Dry sliding tribologial testing for UHMWPE Nanocomposites

Basically all the optimization of the nanofiller content both nanoclay and CNTs in UHMWPE matrix was performed under dry sliding. All three UHMWPE nanocomposite systems, namely UHMWPE-nanoclay composites, UHMWPE-CNTs composites and UHMWPE hybrid composites were tested. For all of three UHMWPE nanocomposites system, same weight percentage of nanofiller were used (0.5 wt%, 1.5 wt% and 3 wt %).

Parameters for tribological testing under dry sliding were unchanged (Load =30N, linear speed=06 m/s, Cycles =5000) for all nanocomposites system.

4.6.1 Effect of nanoclay type on the tribological properties of UHMWPE

Specific wear rate (WR) and coefficient of friction (COF) for 1.5wt% of three different nanoclays (I.28E, I.30E and C15A) is shown in figure 4.21 and figure 4.22. From both graphs, it is quite clear that all three different types of nanoclay have resulted in decreasing both the specific wear rate and COF. Nanoclay C15A has resulted in almost 41% reduction in specific wear rate and 37% reduction is observed for C15A composites in comparison to pristine UHMWPE. The decreased wear rate for Clay composites is believed to happen because of clay platelets holding the polymer chains just like anchors and avoiding the easy removal of material during testing [43]. This effect can be more clearly seen from the SEM images of the wear tracks (Fig. 4.23).

The dominant wear mechanism appears to be plastic deformation initiated by the ploughing action of the counter-face asperities of the hard 100Cr6 ball. Looking at the worn surfaces morphology, figure 4.23 [(e), (f), (g), (h)], it is clear that the nanoclay composites wear surface is smoother with much less grooves whereas pristine UHMWPE surface is heavily deformed with deep furrows. The nano level reinforcement actually bridges the polymer chains and avoids easy material removal which is evident after comparing the wear track images of organoclay composites and pristine UHMWPE. 3D and 2D optical images of wear tracks in figure 4.24 also delineates more furrowed surface with deep tunnels indicating high plastic deformation due to poor load bearing ability of UHMWPE which is evident from depth of wear tracks. However, the surface for organoclay composites is

smooth with less groove marks and maximum depth has decreasd for organoclay composites as well, with highest reduction for C15A organoclay composites.

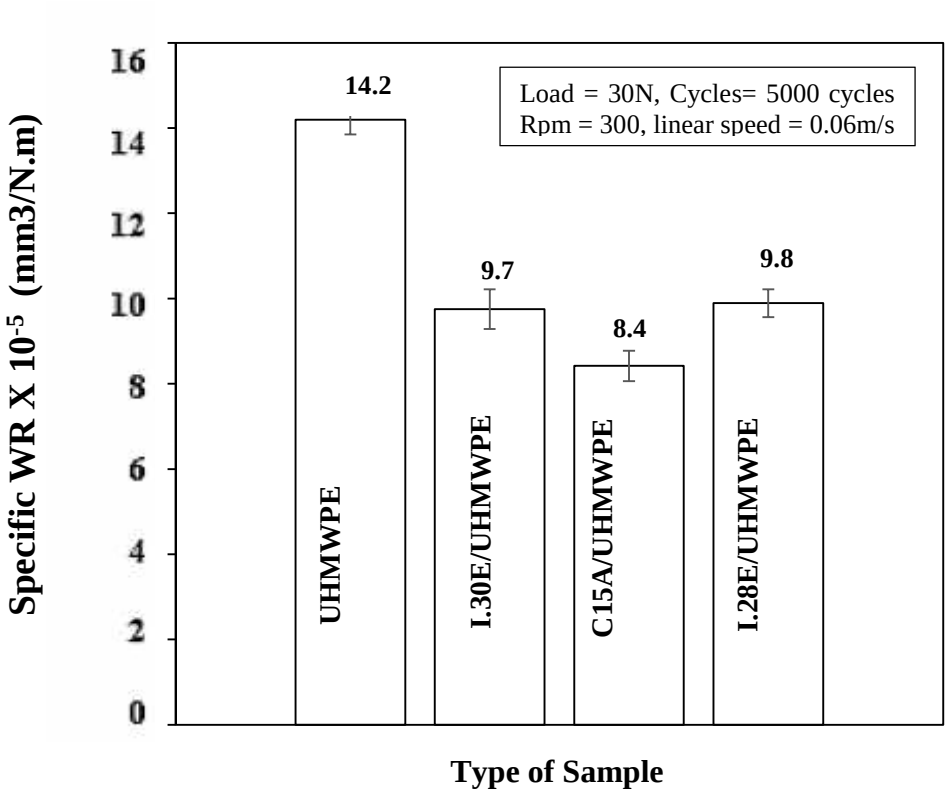

Figure 4.21 Specific wear rate of UHMWPE and three different UHMWPE clay composites

Among different clays, C15A showed most reduced specific wear rate while COF is almost the same for different organoclay nanocomposites. The improved performance of C15A clay composites could be attributed to enhanced dispersion of C15A clay platelets as compared to I.28E and I.30E. Intercalation results in possible formation of two phase structure, hard phase (intercalated structure) and soft phase (polymer matrix alone), making easy the removal of soft phase (polymer), hence increased wear rate for intercalated structure, as reported by Jawahar et al. [81].

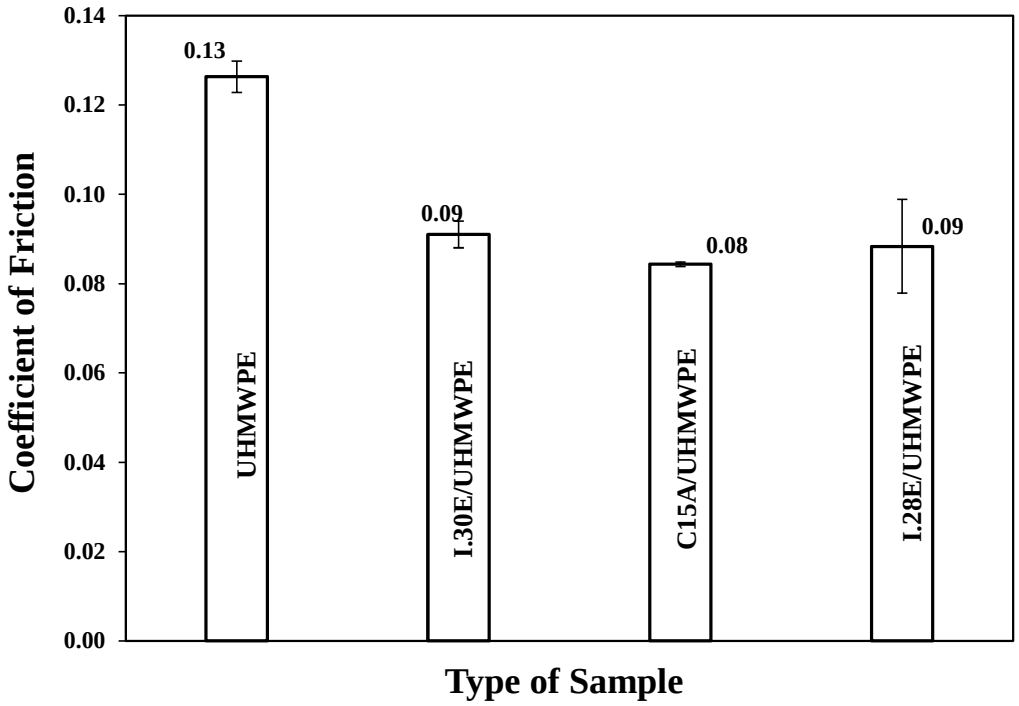

Figure 4.22 Variation of COF for UHMWPE and Three different Clay composites

From the optical images shown in figure 4.25, it can be seen that, the counterface shows formation of continuous transfer film whereas for pristine UHMWPE transfer film is patchy and discontinuous. The formation of smooth transfer film actually hinders the direct contact of steel counterface with the polymer surface, hence reduction is observed in all the organoclay composites. The formation of smooth transfer film is attributed to good adhesion of transfer film with the counterface. The researchers [42, 82] have reported that, the clay addition increases the adhesion of transfer film with the counterface with one of the work done using PVDF clay composites and Nylon 6 clay composites. Because of the nano level reinforcement having same size as of polymer chains, so the material exclusion of nanoparticle is trivial and supports formation of uniform persistent transfer film hence reducing WR and COF [8].

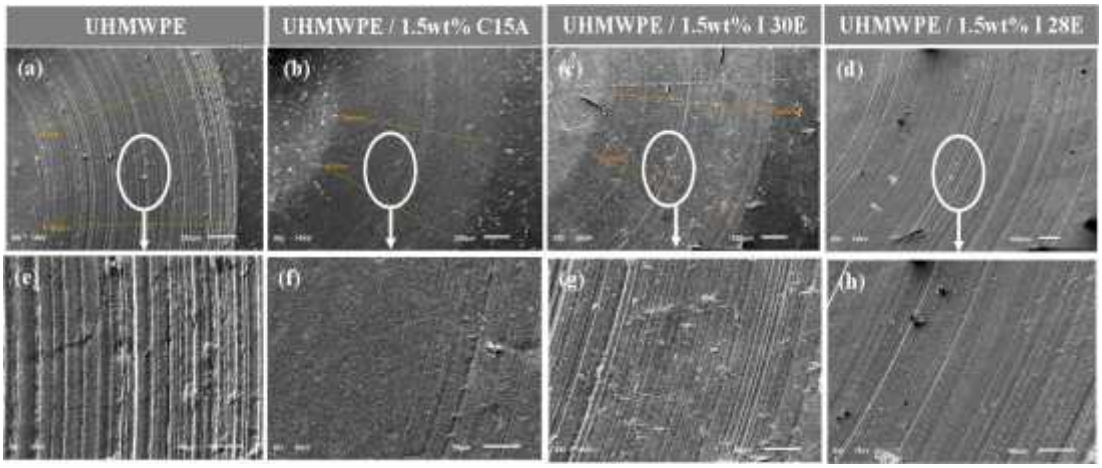

Figure 4.23 SEM images showing wear morphology of UHMWPE and clay composite samples

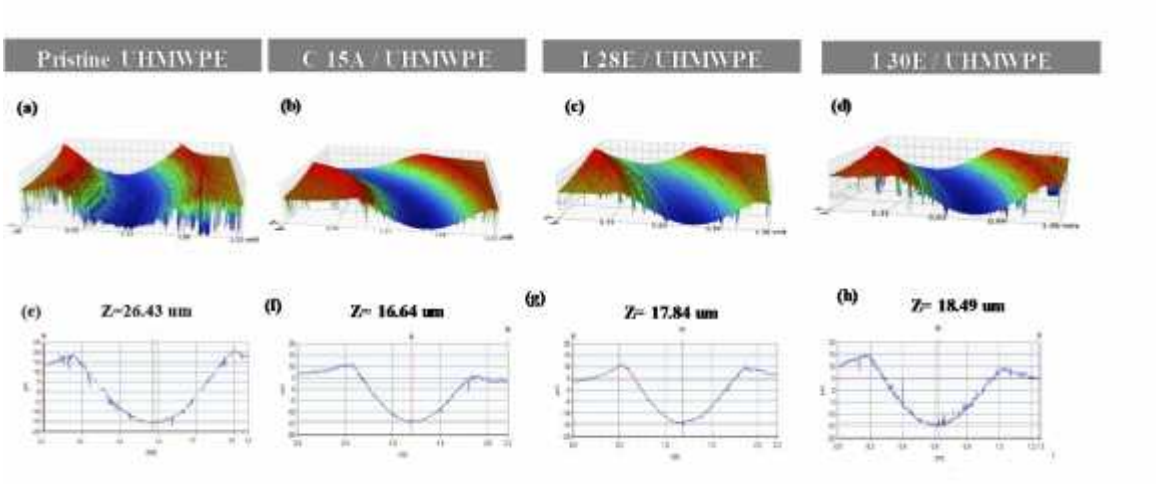

Figure 4.24 Optical 3D (a-d) and 2D (e-h) profiles of the wear track for pristine UHMWPE organoclay composites, I28E/UHMWPE, I30E/UHMWPE and C15A/UHMWPE

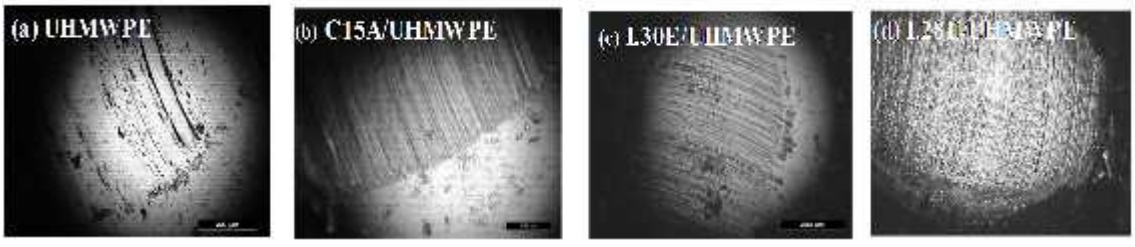

Figure 4.25 Optical images of counterface for different nanoclay composites

4.6.2 Effect of C15A Clay loading on the tribological properties

The variation of specific wear rate and the coefficient of friction (COF) for the pristine UHMWPE and UHMWPE composites reinforced with 0.5, 1.5 and 3.0 wt% of C15A clay is shown in figure 4.26. It can be seen that the COF and the specific wear rate of all the UHMWPE nanocomposites reinforced with different clay loadings of C15A are lower than that of pristine UHMWPE. Both COF and WR seems to vary in similar fashion, reaching am minimum for1.5 wt% of C15A loading. Higher clay loading (3 wt %) resulted in increase of both the tribological parameters. These results come to prove once more that the optimum amount value of C15A clay loading is 1.5 wt%.

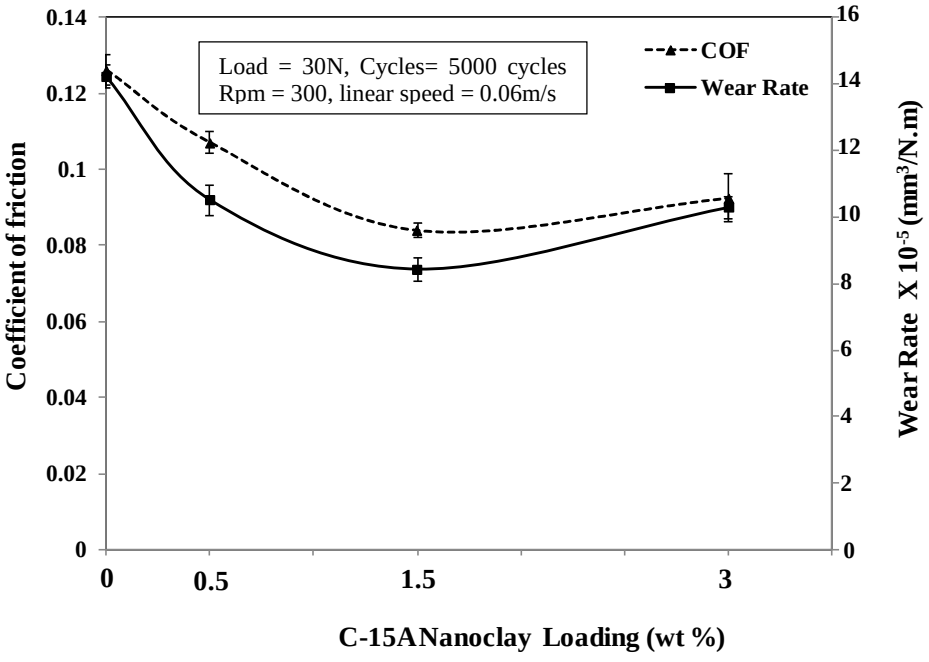

Figure 4.26 Variation of COF and specific wear rate with clay loadings in UHMWPE matrix

SEM images of the wear tracks is shown in figures 4.27 [(a) to (h)]. Generally, the dominant wear mechanism appears to be plastic deformation caused by the ploughing

action of the counterface asperities of the hard 100Cr6 ball sliding against the sample. From morphology of worn surfaces (figure 4.27), it is observed that that as amount of nanoclay is increased up to 1.5wt%, the worn surface becomes less grooved and appear more smooth. Further, it can also be seen from Fig. 4.28 [(a), (e) and (i)] that for the case of pristine UHMWPE the wear tack is wider (1.341 mm) and deeper with a lot of polymer build up around the wear track as compared to that of nanoclay composites showing least width for 1.5wt% C15A/UHMWPE about (1.112 mm). Though UHMWPE, is known to form thin transfer films [83], but the transfer film formed for the case of UHMWPE is more patchy and discontinuous as evident from figure 4.27 (i). This indicates poor adhesion of transfer film with the counterface. Contrary to this nanoclay composites show continuous films as it has been reported and also previously stated that the clay content actually increases the adhesion between the counterface ball and the transfer film [42, 82]. Nanoclay having metal/transition metal oxides that actually increase the van der waal bonding of transfer film to the counterface, hence a continuous transfer film is present for clay composites.

Among UHMWPE nanocomposites, 3 wt% demonstrated lower tribological properties. This is attributed to agglomeration of clay platelets at higher clay content (3 wt %). The characteristic peak for the C15A nanoclay is observed at 2.46° (figure 4.4), corresponding to interplanar distance of 35.88 Å suggesting almost no intercalation of polymer chains with possible agglomeration of the nanoclay platelets and formation of two phase structure hard phase (clay platelets) and soft phase (polymer matrix alone) as reported by Jawahar et al. [81]. So these agglomerated particles are not able to effectively protect the large scale deformation of the polymer matrix from ploughing, which is evident from the SEM image of the wear track as shown in Fig 4.27(h). Also it can be seen that counterface for 3 wt%

shows large material transfer in Fig 4.27(l). Moreover, for lower clay content the transfer film adhesion is believed to be poor as evident from the optical micrograph of Fig 4.27 (i). hence for the counterface sliding against the composite with 0.5 wt.% of C15A, the transfer film formed is being continuously peeled off so almost negligible or a discontinuous transfer film can be seen on the counterface ball leading to a higher COF and higher wear rate when compared to the other clay loaded composites.

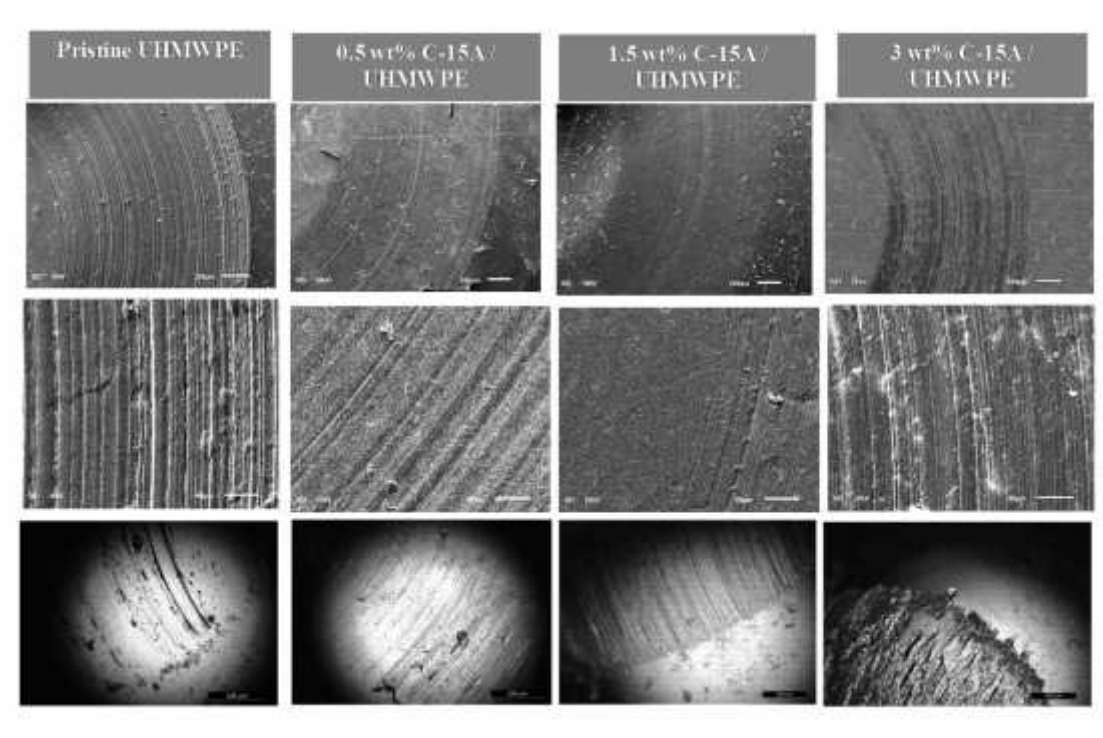

Figure 4.27 (a-d) SEM images of the wear tracks at lower magnification (e – h) higher magnification (I –l) Optical micrographs of the counterface balls after the wear tests for the pristine UHMWPE

The reduction in wear is attributed to two factors. Firstly, the uniform dispersion of nanoclay in the polymer matrix and secondly the formation of a smooth, tenacious and a continuous film on the counterface ball which prevents the direct contact of the ball asperities with the nanocomposite surface. In the studies of transfer film and their role in

tribology, Bahadur [84] concluded that wear occurs before the transfer film formation on the counter-face and secondly due to the loss of material because of peeling off the film from the counterface.

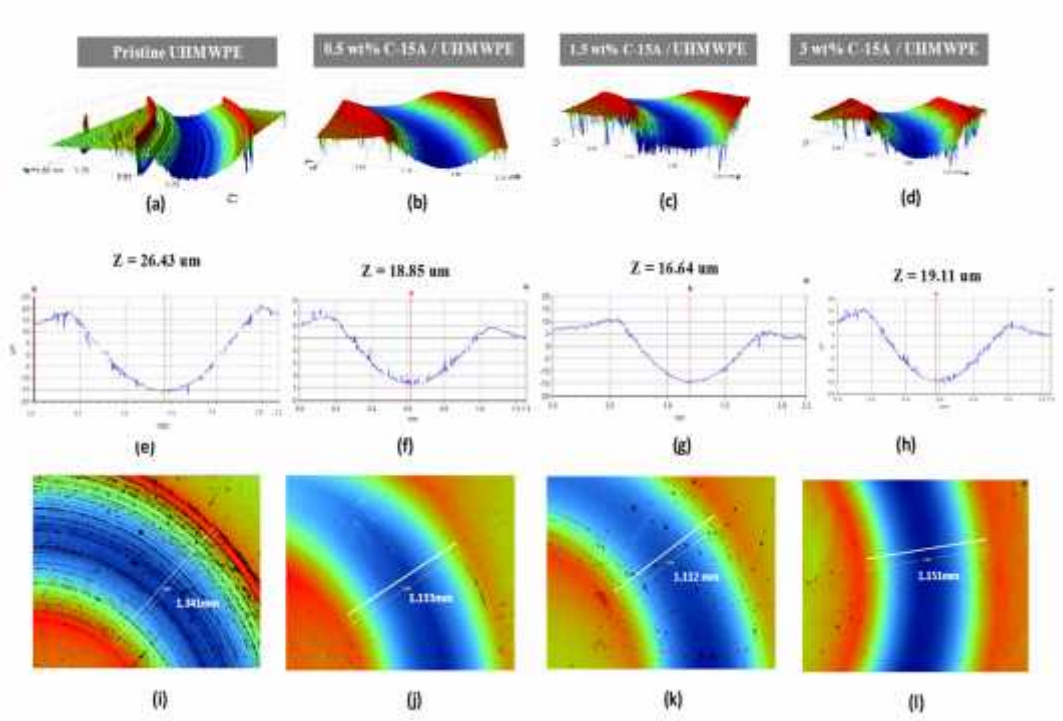

Figure 4.28 Optical 3D (a – d) and 2D (e – h) profiles of the wear tracks. Optical contour images of the wear tracks for the pristine UHMWPE and nanoclay composites (i-l)

Wear tests were also carried out on the 1.5wt% C15A/UHMWPE nanocomposites under different loads (30, 60 and 90 N). Figure 4.29 illustrates the effect of varying load on COF and specific wear rate of pristine UHMWPE and UHMWPE nanoclay composites. It can be seen that, specific wear rate increases with increasing normal load. Normal load of 30N with ball on disc contact type results in Hertzian contact pressure of almost 115 MPa with ball diameter of 6.3mm. With increased pressure, the plastic deformation is expected to be more effective hence as result of increased plastic deformation more tearing and fracturing

of material will take place leading to increased material removal. Moreover, COF also increases as result of increase in normal load from 30N to 90N which could have resulted in softening of surface because of frictional heating leading to easing of material pull out [45]. Nanocomposites exhibited lower COF when compared to the pristine UHMWPE for all test loads. For instance, at 90N load corresponding to max contact pressures of ~115 MPa, there is still reduction in specific wear rate by 20% and COF reduces by 32 % reduction for 1.5wt% C15A/UHMWPE. Hence, nanoclay reinforcement of polymer matrix helps to bear the load while effectively reducing the wear rate.

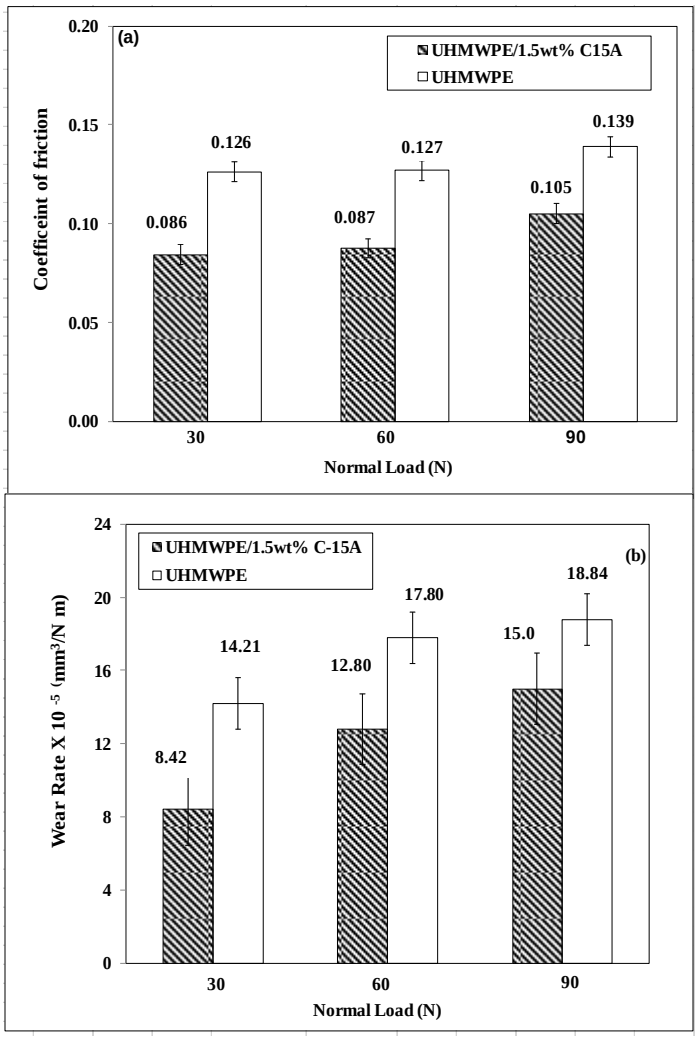

Figure 4.29 Effect of Load on UHMWPE and 1.5wt% C15A composites

4.6.3 Effect of water uptake on the tribological properties of UHMWPE nanocomposites

The effect of water absorption on the tribological properties of UHMWPE and its nanocomposites is evaluated. All of the samples are tested under applied load of 30N with sliding speed of 0.06 m/s for 5000 cycles and COF and specific wear rate are reported. Fig. 4.30 and figurer 4.31 shows the comparison of specific wear rate and coefficient of friction before and after water absorption. It can be seen that, generally specific wear rate has

increased after water absorption for pristine UHMWPE and nanoclay composites. However it is also clear that greater increase in specific wear rate has resulted for pristine UHMWPE before and after water uptake. For UHMWPE, there is 15% increase in specific wear rate after water uptake. While lesser increase in wear rate seen for clay composites after water uptake. This improvement can be attributed to the presence of the nanoclay platelets in the nanocomposites which make it difficult for the diffusion of the water molecule as they present a very torturous path as explained earlier leading to less water absorption.

The reduced water absorption leads to less plasticization and softening of the surface. Plasticization results in breaking of the bridging action of the nanoclay platelets with polymeric chains resulting in polymer swelling and softening due to which the resistance to wear reduces. Since clay nanocomposites showed reduced water uptake (Section 4.5), hence as compared to pristine UHMWPE, there is less plasticization of surface. Due to this, the surface of nanocomposites is able to withstand the normal and tangential shear stresses during sliding. It can also be analyzed that water absorption results (Section 4.5) showed least water uptake for that 3 wt% of C15A and 1.5 wt% of C15A composites, which is supported by greater wear resistance for these samples after water uptake. Quantitatively, for 0.5 wt% C15A and 1.5wt% C15A there is nearly 6% and 2% increase in specific wear rate after water absorption while for 3wt% C15A almost no change in specific wear rate was observed after water uptake. Mohan et al. [85] also reported better wear resistance for nanoclay added epoxy-sisal fiber matrix when tested after water absorption with nanoclay playing a role in fewer water absorption.

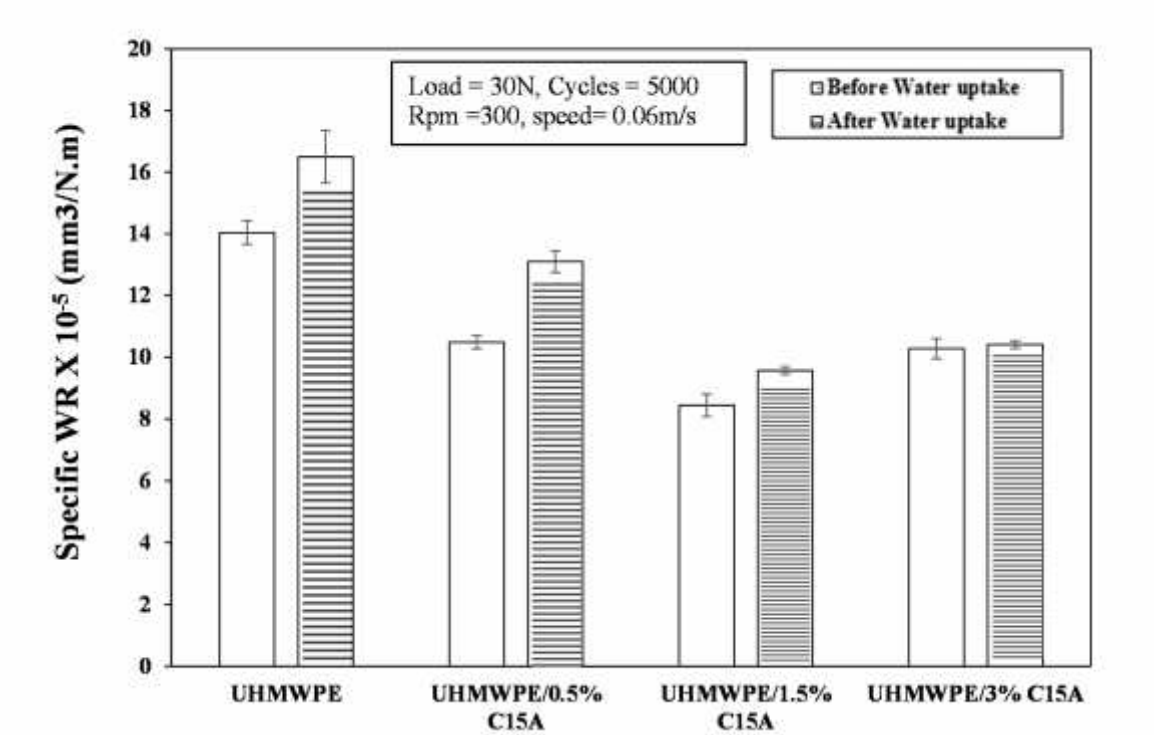

Figure 4.30 Effect of water absorption on (WR) of UHMWPE and its nanoclay composites

SEM images of wear morphology are shown in Fig. 4.32. It is difficult to observe some appreciable difference in worn morphology before and after water uptake. However it can be seen that even after water uptake the characteristic worn morphology trend remains same with pristine UHMWPE showing deeper furrows while nanoclay composites show smoother worn morphology. Comparing samples after water uptake testing, it can be seen that Worn surface of 1.5wt% C15A even after water uptake as can be seen before water uptake especially shows smooth and less furrowed surface. Moreover, from figure 4.31 it can be observed that the 0.5 wt% and 3 wt% of reinforcements showed slightly higher wear rate than 1.5 wt% of C15A reinforcement. The higher WR for the 0.5 wt% of C15A reinforcement can be attributed to more absorption of water because of lesser clay content. Even though, 3wt% reinforcement showed almost the same amount of water absorption as

that of 1.5 wt% of reinforcement, the 3 wt% of C15A reinforcement resulted in slightly higher WR as compared to 1.5wt% C15A, which may be attributed to the agglomeration as confirmed by the XRD spectrum and discussed earlier in section 4.6.2.

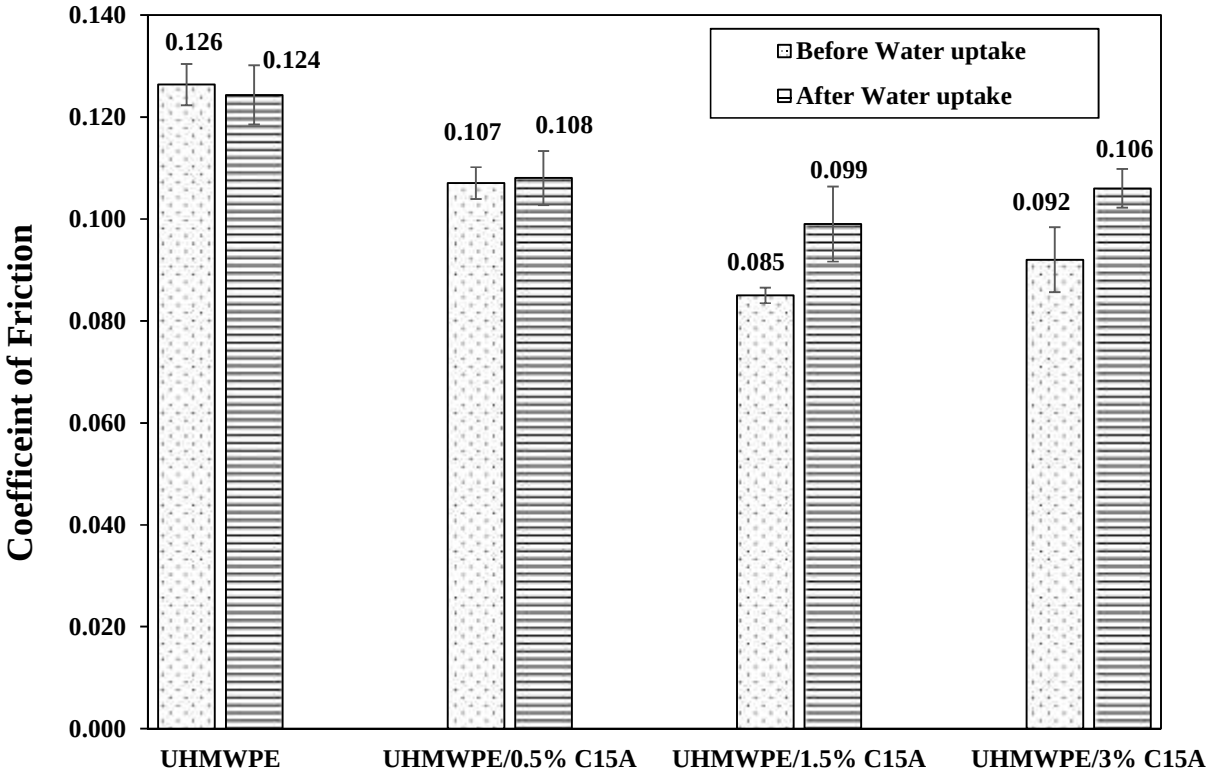

Figure 4.31 Effect of water absorption on (COF) for UHMWPE and its nanoclay composites

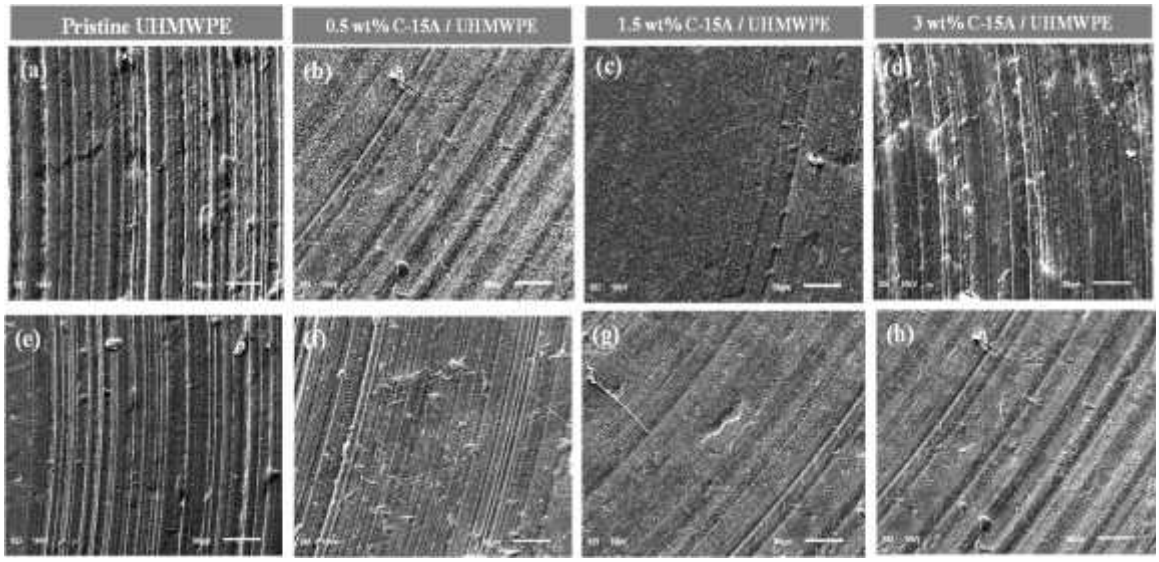

Figure 4.32 (a) – (d) SEM micrograph images of wear tracks before water absorption and (e) – (h) after water absorption

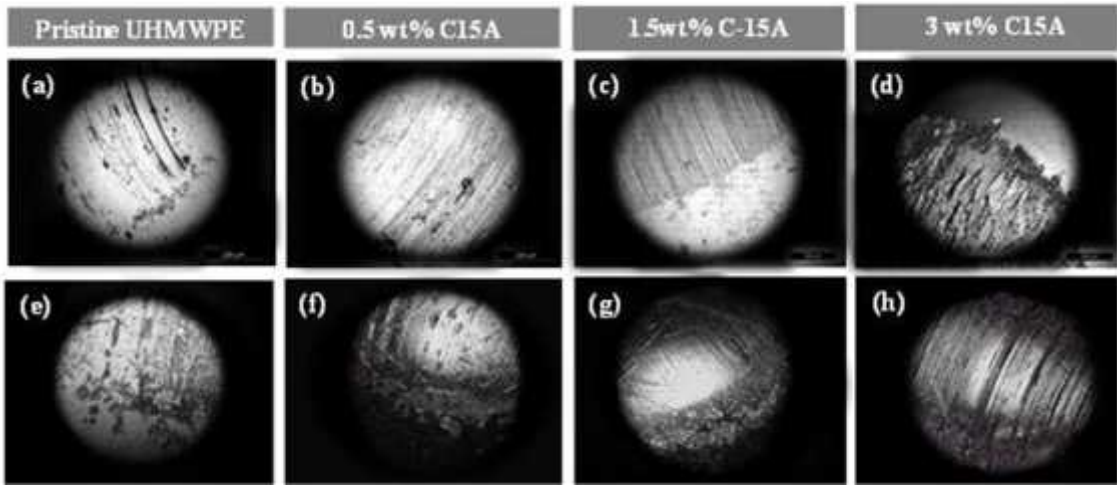

Figure 4.33 Counterface optical images for wear tested samples (a)-(d) before water uptake and (e)-(h) after water uptake

Effect of water uptake on COF doesn't seems to follow any specific trend just as the case observed for specific wear rate. Rather it followed different trend for pristine UHMWPE and UHMWPE nanocomposites. But within the after water uptake category, COF follows the same trend as observed before water uptake i-e, reduced COF for clay composites due

to presence of continuous and adhered transfer film is observed for clay composites while for pristine the film is patchy and discontinuous (figure 4.33). Water absorption has not lead any changes in transfer film formation to affect COF.

4.6.4 Tribological testing of UHMWPE/CNTs composites

Tribological testing was conducted on UHMWPE reinforced with different content of CNTs, 0.5 wt%, 1.5wt%, 3 wt% to obtain the optimum loading of CNTs that will result in improved wear resistance. Figure 4.34 and Figure 4.35 show specific wear rate and COF at same parameters as used previously for clay reinforced composites (load= 30N, speed=300Rpm, cycles=5000). In general, All CNTs composites showed much reduced wear rate as compared to pristine UHMWPE, reduction of almost 55 % is seen for 1.5wt% CNTs composites. Reduction in specific wear rate, is due to presence of CNTs as nanofiller being uniformly dispersed and effectively transferring load across the interface, which results in more uniform stress distribution and minimizing the stress concentration area [86]. Superior properties of CNTs allow load to be efficiently carried as comparable to pristine UHMWPE, the carbon nanotubes not only results in increasing the load bearing capacity but also are instrumental in anchoring the chains of UHMWPE, avoiding the material removal due to plastic deformation taking place as result of wear testing. SEM micrograph of pristine UHMWPE and CNTs reinforced UHMWPE are shown in figure 4.36. UHMWPE surface indicate severely grooved surface with deep furrows indicate of poor load bearing ability of material, it can be seen from image that even fractured and fatigue separated layers of UHMWPE are there, whereas CNTs/UHMWPE composites show smooth surfaces and very minor deformed surface.

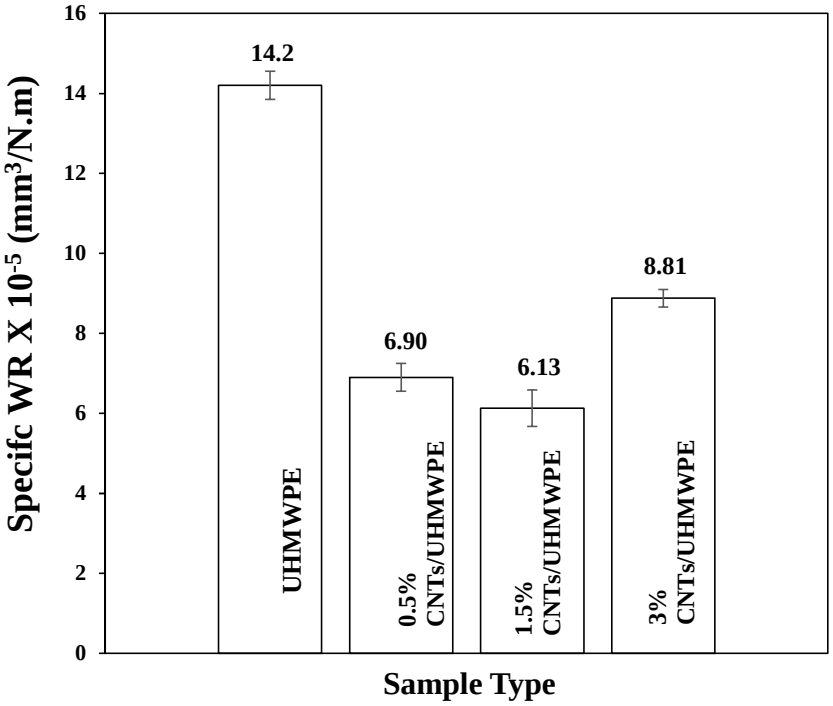

Figure 4.34 Specific wear rate for UHMWPE and UHMWPE/CNTs composites

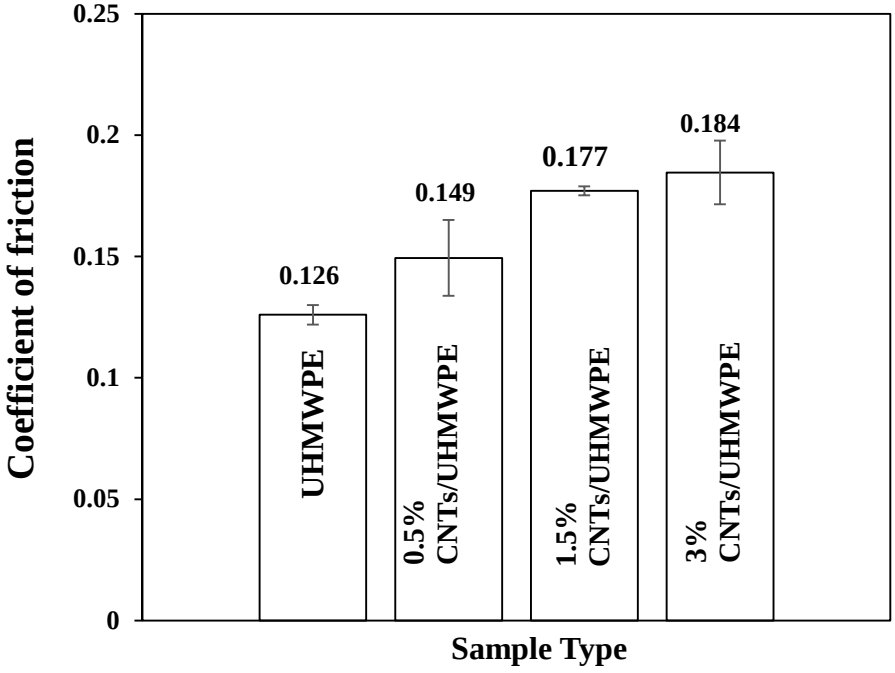

Figure 4-35 Average COF for UHWMPE and UHMWPE/CNTs composites

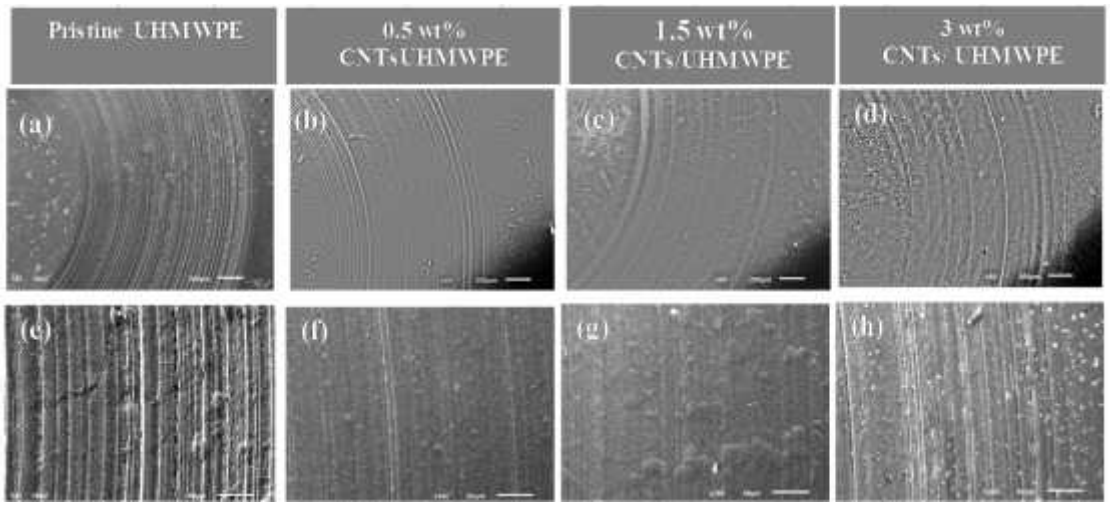

Figure 4.36 SEM images of the wear tracks for UHMWPE and its CNTs composites at lower magnification (a – h) higher magnification (I –l)

3D images and 2D profiles (figure 4.37) of wear track also illustrates high ploughing taking place for UHMWPE as compared to CNTs/UHWMPE composites, reduced maximum depth of wear track of indicative of improved load bearing capacity of CNTs reinforced UHMWPE. The least depth of wear track is seen for 1.5wt% CNTs/UHMWPE with 14.11 um, however for pristine UHMWPE shows much higher maximum wear track depth of 26.43 um. Slight increase in wear rate for 3%CNTs/UHMWPE was observed, which is in agreement with FE-SEM (Section 4.2.2) results pointing out agglomeration of CNTs that are not able to transfer load efficiently and resist deformation. Also, agglomeration of CNTs is unable to hold the polymer material by bridging action, hence material removal is easier. Uniform dispersion to the case of individual CNTs coated on particle of polymer is the key for improved mechanical and tribological properties. COF graph depicts increased COF as the CNTs amount is increased from 5wt% to 3wt%.Contrary to C15A/UHMWPE, the CNTs composites show high coefficient of friction as compared to pristine UHMWPE as evident from graph (figure 4.32). CNTs have been reported to increase COF slightly owing to its high hardness. The shore D value rises from 58. 9 for

pristine UHMWPE to 63.4 for maximum content of CNTs as seen from figure 4.18 [34], moreover it was also observed from the optical images of counterface shown in figure 4.35 (g-h) ,that almost no transfer film has been found as observed for C15A/UHMWPE composites, this may also have attributed to increase COF, making direct contact of counterface ball with the sample.

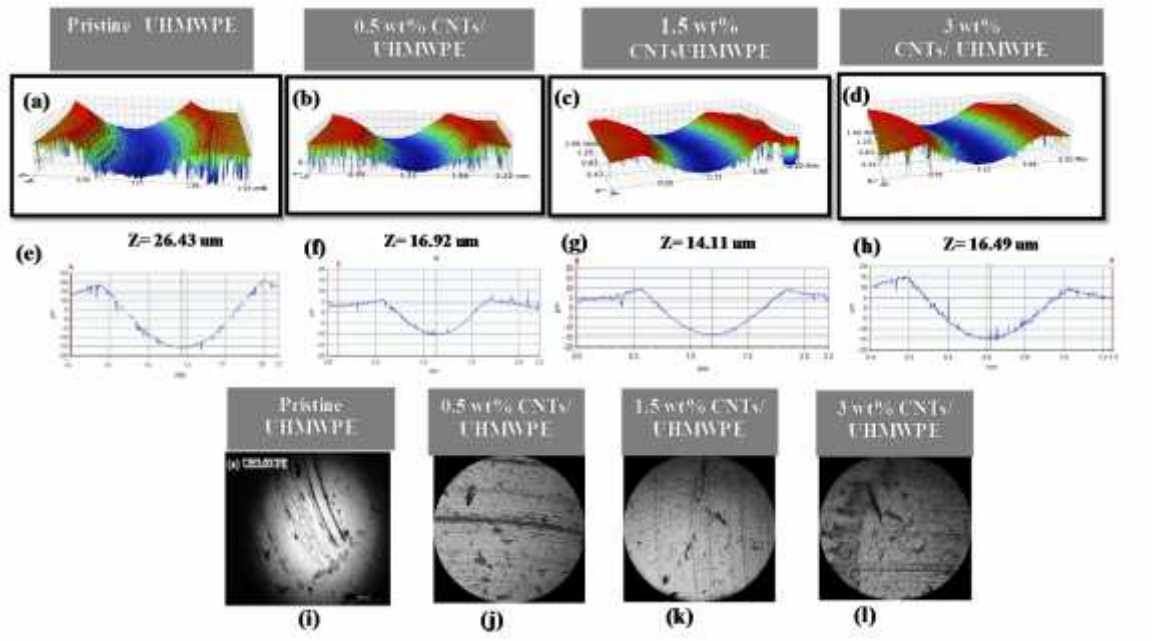

Figure 4.37 3D/2D Optical profile images of the wear tracks along with counterface for UHMWPE and its CNTs composite.

4.6.5 Tribological performance of UHMWPE hybrid nanocomposites

CNTs with three 5wt%, 1.5wt% and 3wt% were added in 1.5wt% C15A/UHMWPE composites and tribological testing is done to optimize the CNTs content. 1.5 wt% of C15A is selected due to the fact that results of tribological testing for C15A clay composites (section 4.6.2) proved 1.5wt% of C15A/UHMWPE to be optimized content. Figure 4.38 and Figure 4.39 shows specific WR and COF. Reduced value of specific wear rate is seen

for all the hybrid composites. It was also observed that reduction in specific wear rate was even lower as compared to CNTs/UHMWPE. Almost 10% further reduction has occurred for CNTs addition to C15A/UHMWPE, comparing 1.5wt% CNTs/C15A/UHMWPE and CNTs/UHMWPE.

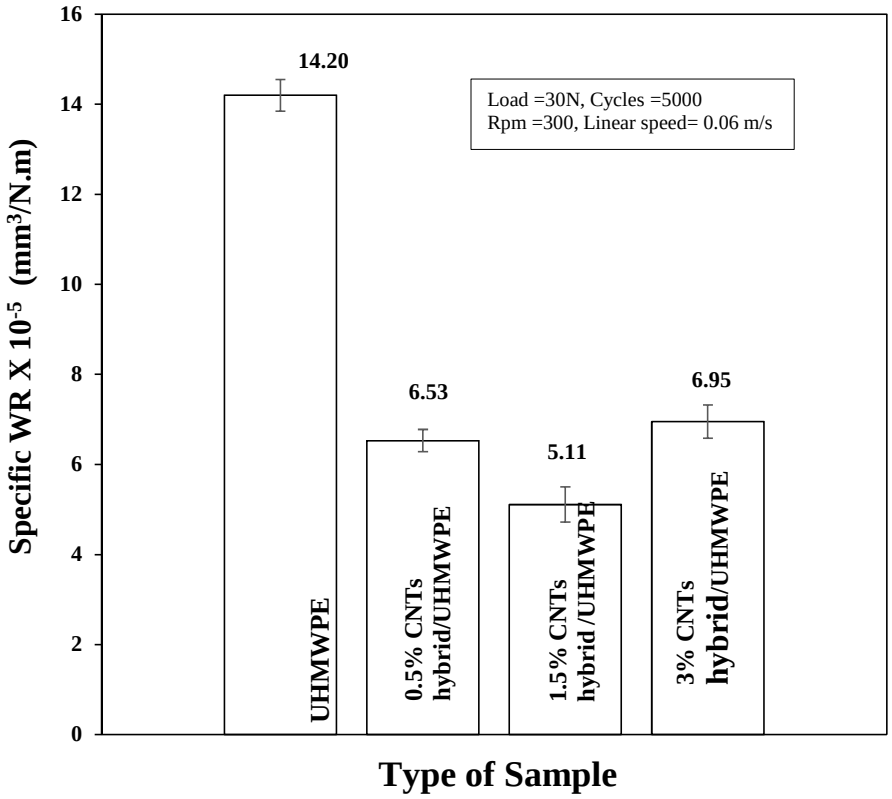

Figure 4.38 Specific wear rate of UHMWPE hybrid composites with varying CNTs content

SEM wear morphology images figure 4.40, showed nanocomposites showed smooth surface with negligible ploughing for all hybrid composites. SEM wear track image for 3wt% hybrid composites showed some signs of ploughing with shallow grooves seen on the surface, which can be attributed to agglomeration of CNTs as the content of CNTs is increased, the increased content of nanofillers such as CNTs, Clay or other lead to

agglomeration because of high surface energy and they form packs rather than uniform dispersion. This result in loss of load transferring ability of composites, they are unable to bear the load and chains of polymer are easy to be removed by ploughing action of hard counter face asperities.

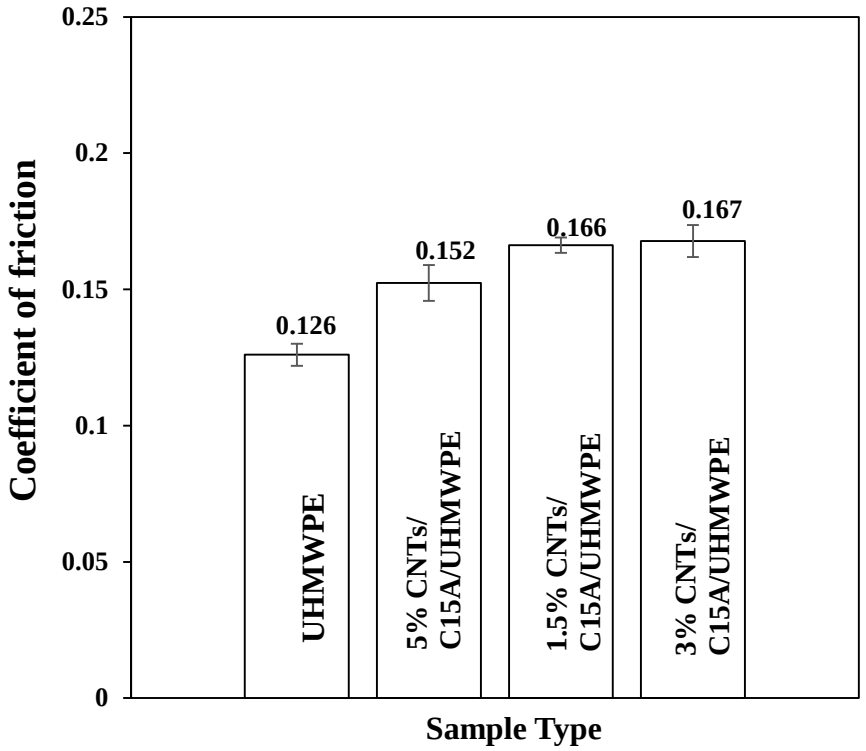

Figure 4.39 COF of UHMWPE hybrid nanocomposites with varying CNTs content

Optical profilometry also illustrates less ploughing, smoother surface and less maximum wear depth for hybrid nanocomposites (figure 4.41). CNTs and clay platelets reduces the increase the load bearing capacity of UHMWP. It is also observed from the hardness testing results (figure 4.20) that CNTs addition does increase the resistance to indentation which is reflected in less plastically deformed surface. Shore D value rises from 58.9 to 64.5 with addition of 3wt% CNTs in UHMWPE matric. This high hardness and less deep wear tracks indicate the fact that both applied stress during indentation and frictional stresses are

carried by CNTs and Clay particles effectively. The maximum depth of wear track is reduced for hybrid nanocomposites (Figure 4.42) as compared to that of UHMWPE/CNTs composites. The least depth is 12.14 um for 1.5wt% CNTs Hybrid UHMWPE composites whereas for UHMWPE/CNTs the least depth is 14.11 um. Hence both nanofillers are able to bear stresses more effectively in UHMWPE matrix.

COF graphs for hybrid nanocomposites show increased COF values as compared to pristine UHMWPE due to increased hardness by addition of CNTs. The COF rises from 0.126 to 0.167 with maximum of 3wt% CNTs addition to UHMWPE. Regarding transfer film, it was observed in the previous session (figure 4.28) that C15A increases adhesion of transfer film to counterface and nanoclay promotes the formation of smooth transfer film. Now comparing it with Figure 4.42, as CNTs are added along with C15A nanoclay, formation of transfer film is hindered. CNTs tends to hold polymer chains together and avoids material transfer as observed from figure 4.38. So for hybrid case it can be seen from figure 4.42, that small transfer film is there for 0.5wt% CNTs hybrid nanocomposites while as CNTs addition is increased in hybrid nanocomposites, especially for 1.5wt% CNTs hybrid nanocomposites there is no material transfer. For 3wt% hybrid nanocomposites, fewer material can be seen transferred which can be attributed to agglomeration of CNTs as seen in FESEM images (figure 4.9), resulting in minor reduction in holding UHMWPE chains.

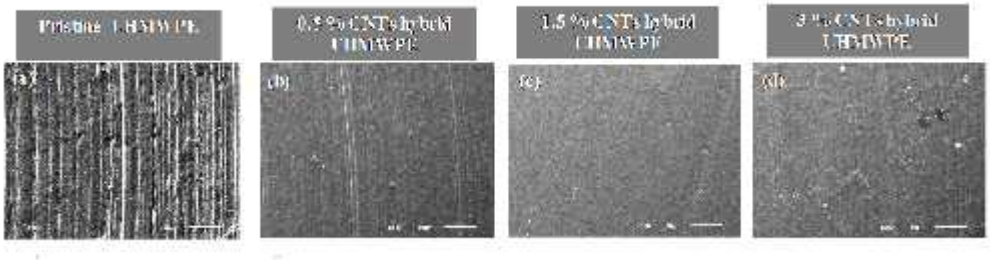

Figure 4.40 SEM morphology of wear tracks of UHMWPE and its hybrid composites.

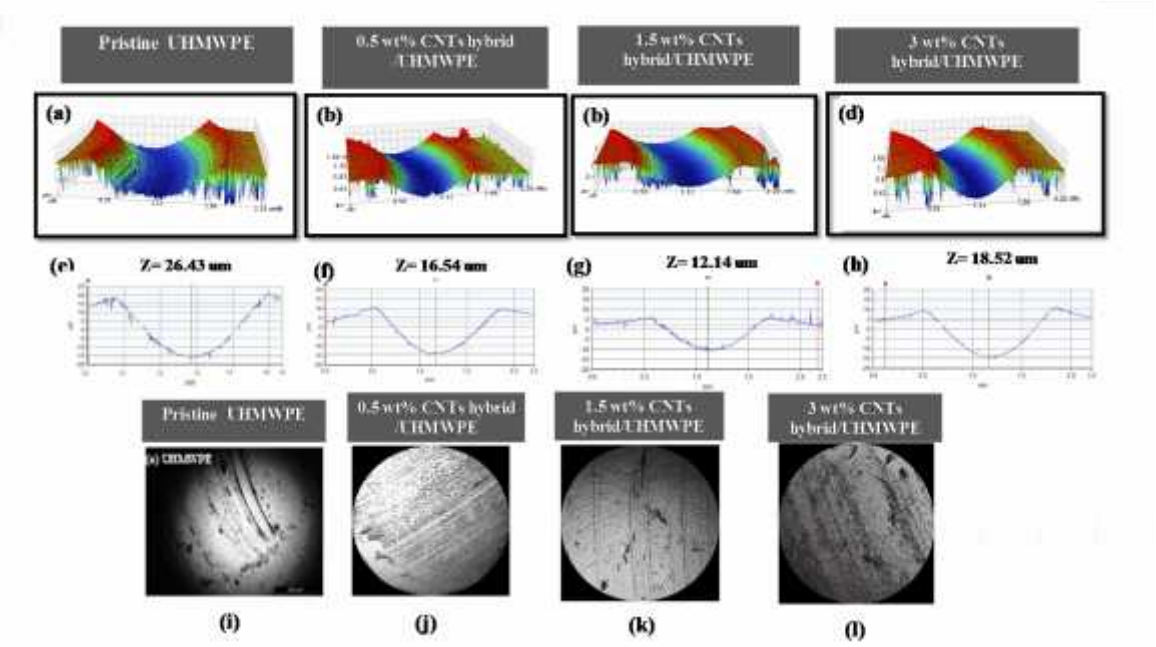

Figure 4.41 3D/2D Optical profile images of the wear tracks along with counterface for UHMWPE and its hybrid CNT composites

The graph of specific wear rate for optimized nanofiller content for all three nanocomposite systems is shown in figure 4.42 and figure 4.43. 1.5wt% C15A/UHMWPE, 1.5wt% CNTs/UHMWPE and 1.5wt % CNTs hybrid UHMWPE are the optimized nanofiller content based on reduction in specific wear rate. As compared to pristine UHMWPE, the 1.5wt% CNTs hybrid nanocomposites shows almost 63% reduction in specific wear rate which is the greatest as compared to nanoclay and CNTs reinforced composites. The least reduction of 41% was seen with 1.5wt% C15A/UHMWPE whereas 1.5wt% CNTs/UHMWPE showed almost 55% reduction in specific wear rate. Moreover, it was

also noticed that hybrid nanocomposites has the maximum increased load bearing ability more as compared to C15A/UHMWPE and CNTs/UHMWPE.

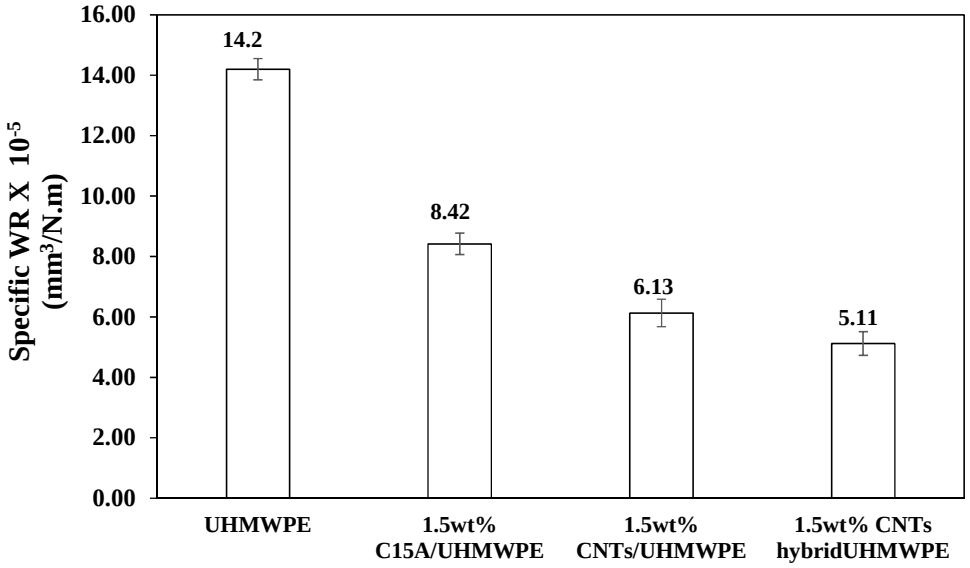

Figure 4.42 Specific wear rate for pristine UHMWPE and three different optimized UHMWPE nanocomposites

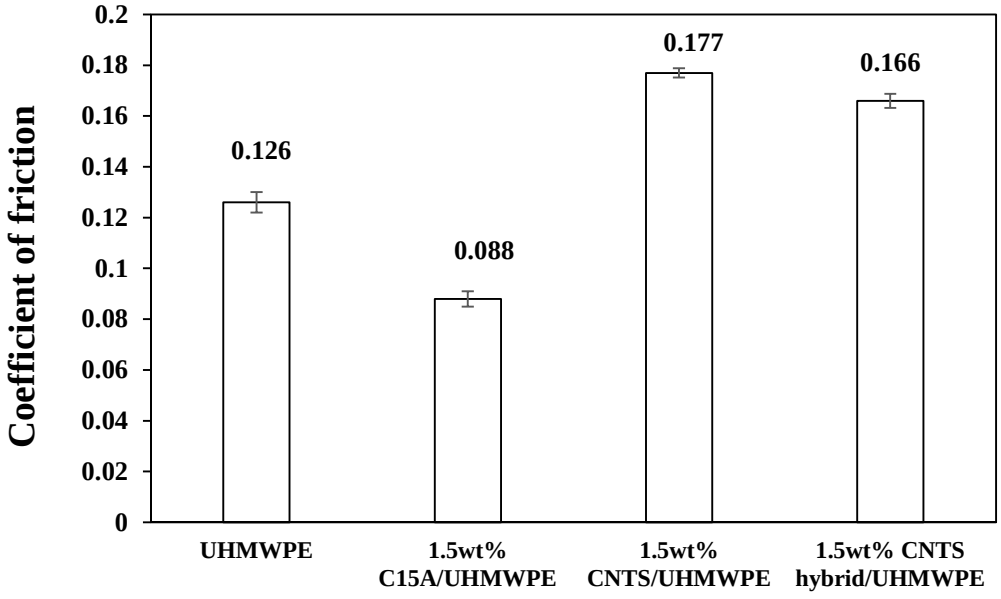

Figure 4.43 COF for pristine UHMWPE and three different optimized UHMWPE nanocomposites

From figures (4.28, 4.37, 4.41), the least depth of wear track is 16.64 µm for 1.5wt% C15A/UHMWPE, 14.11 µm for 1.5wt% CNTs/UHMWPE and 12.14 µm for 1.5wt% hybrid nanocomposites. However, COF shows different trend with reduced values for clay composites. The highest COF is observed for 1.5wt% CNTs/UHMWPE of about 0.177 while 1.5wt% CNTs hybrid nanocomposite showed a slightly reduced value of 0.166 possibly due to presence of nanoclay, as discussed earlier in section 4.6.1. The 1.5wt% C15A/UHMWPE shows the lowest COF value, due to presence of transfer film as seen from figure 4.19. CNTs reinforced UHMWPE do not show any transfer film on the counterface (figure 4.37) and slightly increased value of COF is seen for CNTs/UHMWPE.

4.7 Tribological testing for UHMWPE nanocomposites under water lubricated sliding condition

Tribological testing under dry sliding was done for all three nanocomposites systems under the same set of experimental parameters. Dry sliding testing under these conditions served as a filter to screen the best UHMWPE nanocomposite composition among each of the following categories: UHMWPE/C15A nanocomposites, UHMWPE/CNTs composites an hybrid UHMWPE nanocomposites. Figure 4.44 depicts the selected UHMWPE nanocomposites from dry sliding tests which were tested under water lubricated sliding conditions and same tested parameters given in figure 3.3

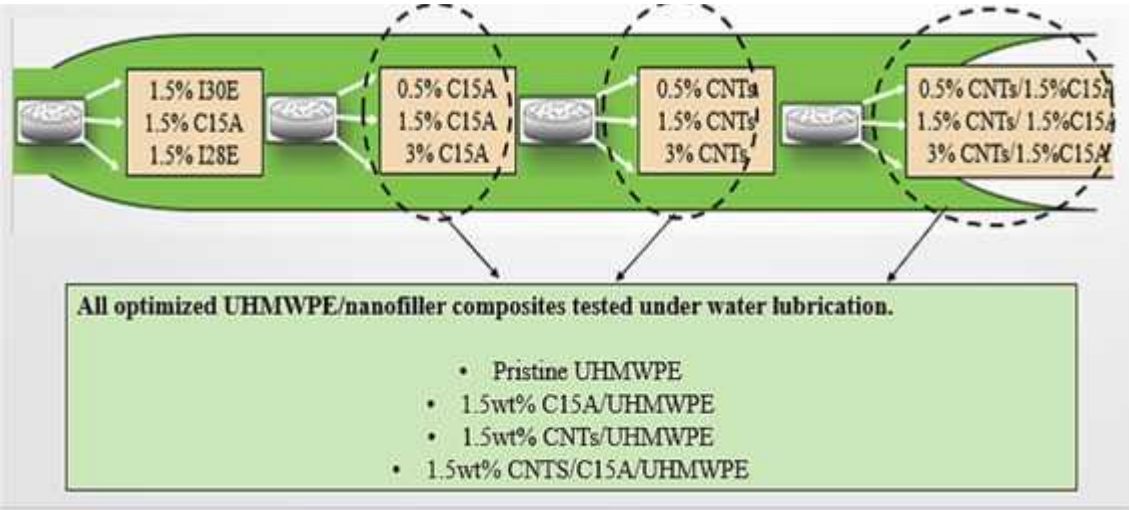

Figure 4.44 Schematic description of optimized UHMWPE nanocomposites for water lubricated sliding testing

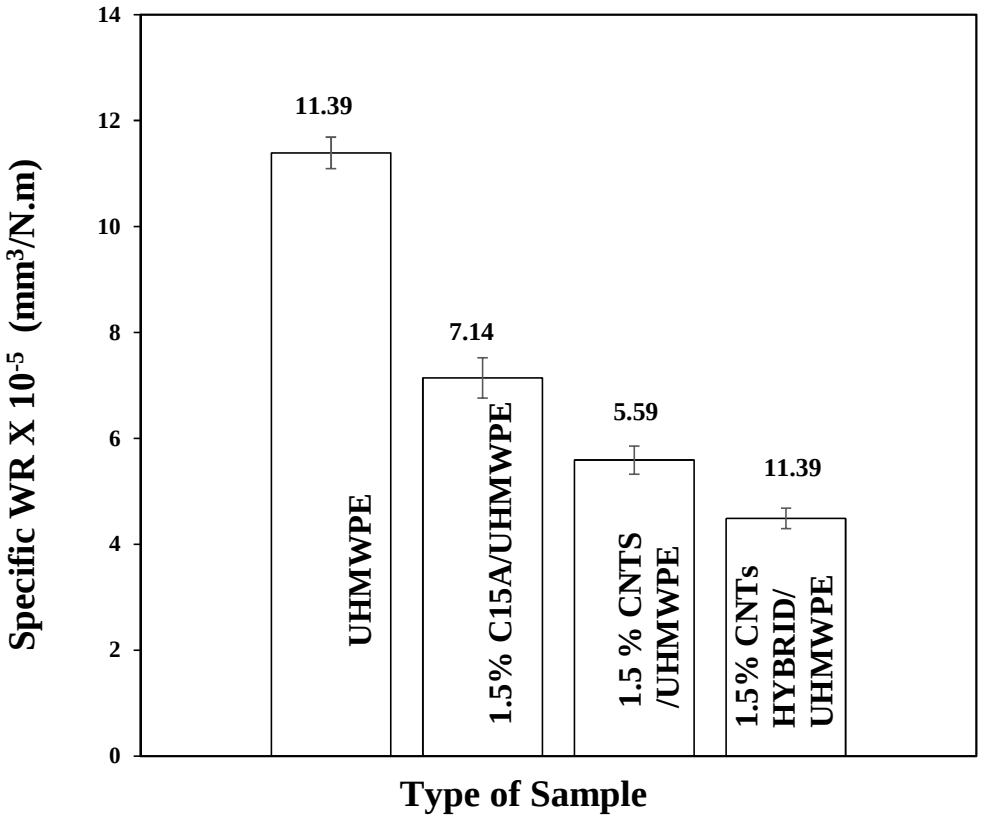

Figure 4.45 Effect of nanofiller on specific WR of pristine UHMWPE and three different optimized UHMWPE nanocomposites under water lubricated conditions

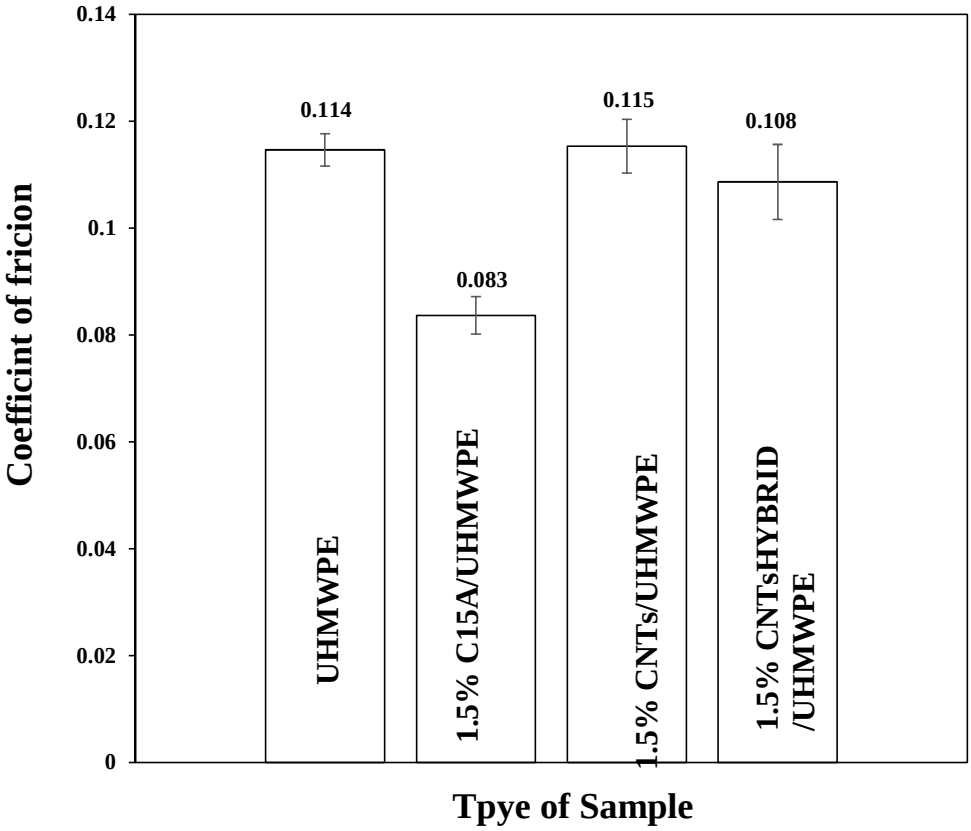

Figure 4.46 Effect of nanofiller on COF for pristine UHMWPE and three different optimized UHMWPE nanocomposites under water lubricated conditions

Figure 4.45 and figure 4.46 show the specific WR and COF for optimized UHMWPE nanocomposites and pristine UHMWPE. It is evident that all the optimized composites resulted in reduction of WR with an improvement of about 60% for the hybrid nanocomposites. Similar results were obtained for the case of dry sliding testing of these samples (figure 4.42) where almost 63% reduction of WR was observed as compared to pristine UHMWPE. Uniform dispersion of CNTs with Clay/UHMWPE has resulted in increased load bearing capacity as seen from FE-SEM and Raman spectroscopy results OF Figure 4.1 and 4.9.

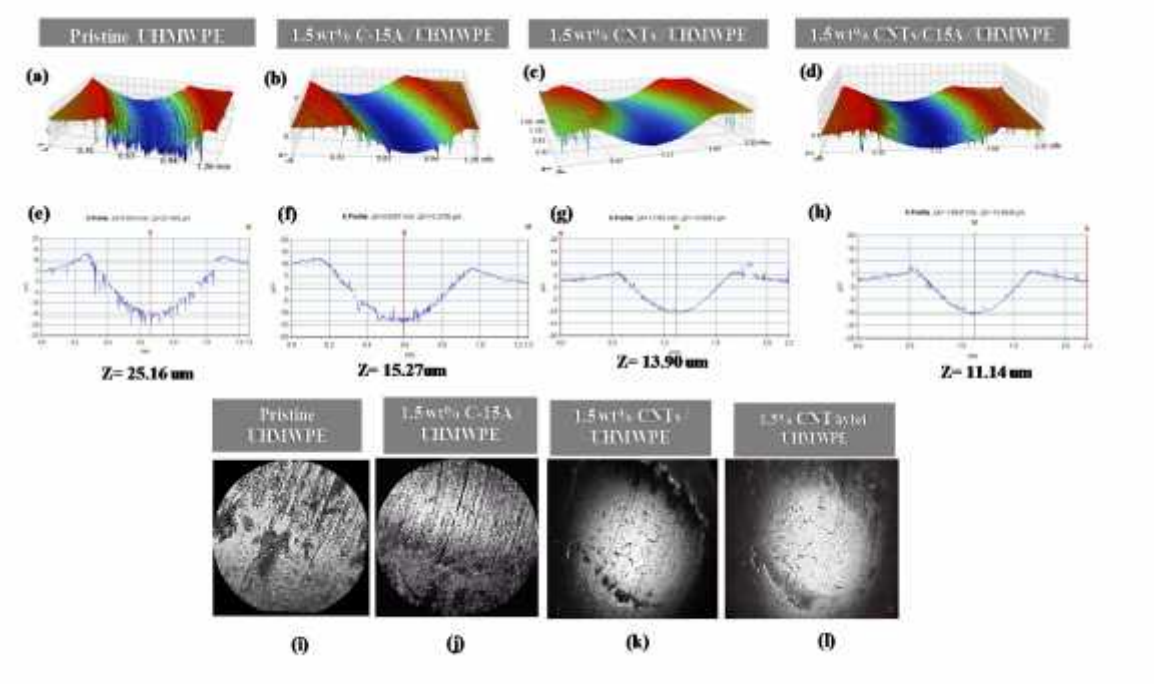

Figure 4.47 (a)-(h) 3D/ 2D profiler images for and counterface optical images (i-l) UHWMPE and its optimized nanocomposites under water lubricated sliding

The 3D profiler images of figure 4.47 show much smoother worn surfaces for nanocomposites with no signs of grooves and abrasive marks indicating minute material pull out, which is supported by reduced specific wear rate. From 2D profiles, it is clear that the maximum depth of wear track is least for hybrid UHMWPE nanocomposites with 11.14 µm indicating much improved load bearing ability. Moreover, from shore D hardness results figure (4.19), hybrid UMWPE showed improvement in hardness with 63.4 shore D for 1.5wt% CNTs hybrid nanocomposites, indicating improved tendency to support higher normal stresses. From figure 4.45, it can also be seen that under water lubrication all of the nanocomposites as well as pristine UHMWPE show slightly less WR compared to dry sliding testing figure (4.42). In comparison to dry sliding the wear rates results (section 4.5.3) have reduced for all the samples, mainly due to presence of lubricant media decreasing the COF and effective heat loss generated during sliding. Optical images of counterface for UHMWPE/CNTs and hybrid nanocomposites shown in figure 4.43 showed

no transfer film signs as compared to C15A reinforced UHMWPE composite similar to what has been observed under dry sliding.

It was observed during the dry sliding tests, that nanocomposite reinforced with CNTs showed increased COF value. Similar finding have been reported earlier also [34], where CNTs resulted in increased COF. Carbon fiber reinforced UHMWPE also showed higher values for COF under dry sliding as compared to distilled water sliding as reported [9]. In current study as well, the dry sliding values (1.5 wt% CNTs/UHMWPE = 0.177, 1.5wt% CNTs/hybrid UHMWPE = 0.166), showed higher values as compared to water lubricated sliding (1.5 wt% CNTS = 0.126, 1.5wt% CNTs hybrid/UHMWPE = 0.118). However among the three composites system under given set of loads and conditions, 1.5 w% CNTs hybrid/UHMWPE nanocomposites showed least specific wear rate even under water lubrication as seen for dry sliding as well (figure 4.42). COF is nearly same for UHMWPE and 1.5 % CNTs hybrid nanocomposites with no transfer film.

4.8 Accelerated life testing (ALT) for Hybrid UHMWPE Nanocomposites

Hybrid UHMWPE nanocomposites have shown resulted in improved tribological performance in terms of reduced specific WR as compared to pristine UHMWPE and other all types of UHMWPE nanocomposite systems under same set of load and conditions as mentioned in table 3.3. However to test it under accelerated life testing conditions, higher loads and speeds were used with increased number of cycles. Hybrid UHMWPE nanocomposites [1.5 wt% nanoclay + 1.5 wt% CNTs] and pristine UHMWPE are tested under 50N load with a sliding speed of 0.5 m/s for duration of 25,000 cycles.

The ALT results showed that hybrid nanocomposites performed better with 41% reduction in WR from (4 x 10^{-5} to 2.4 x 10^{-3} mm^3/N.m) than pristine UHMWPE. COF showed increase in almost 61% for nanocomposites, showing higher value (0.131) than pristine UHMWPE (0.078) as it was observed for CNTs reinforced UHMWPE for dry and water lubricated sliding conditions (section 4.7 and 4.8). The reduced specific wear rate for hybrid nanocomposites is attributed to presence of nanoclay and CNTs in UHMWPE improving the load bearing ability of UHMWPE. The increased hardness value from 58.9 to 65 shore D depicts improved ability to bear normal stresses. 3D and 2D optical images (figure 4.49) maximum depth of wear track has also increased. For pristine UHMWPE the maximum depth of wear track is approx. 57um while for hybrid nanocomposites the depth of wear track is reduced with approx. 36 µm.

Wear morphology images shows highly deformed surface for UHMWPE. From figure 4.48, plastic deformation is evident in the form of grooves and extensive ploughing by the hard counterface. Along with the deep furrows, higher amount of polymer displaced in the form of fragments and debris can be seen. The soft polymer surface is unable to resist the deformation and ploughing has resulted in cutting and fragmentation of the surface layers. Hybrid nanocomposite surface on the other hand seems fairly smooth with much reduced plastic deformation. There are negligible signs of fragmented segments of material on surface. The width of wear track shows increased value of 1.202 um for pristine UHMWPE while hybrid nanocomposites shows 1.165 um.

Moreover it is also observed that, the UHMWPE wear surface also shows ball upped places in on the surface, this can be possibly attributed to higher water absorption by UHMWPE. Frictional heat generated due to higher speeds has softened the polymer surface, this

softening has resulted in more plasticization of surface by enhanced water absorption. COF for UHMWPE shows reduced value, mainly due to this factor. It has been concluded in studies before that frictional behavior of UHMWPE is very much dependent on its water absorption state [46]. The frictional heating during sliding accompanied by plasticization of surface by water absorption reduces the shear strength of surface layers. This reduction in shear strength leads to easy removal of material from the surface, which is supported by the counterface images Figure 4.50 of UHMWPE showing transfer layer on the counterface ball.

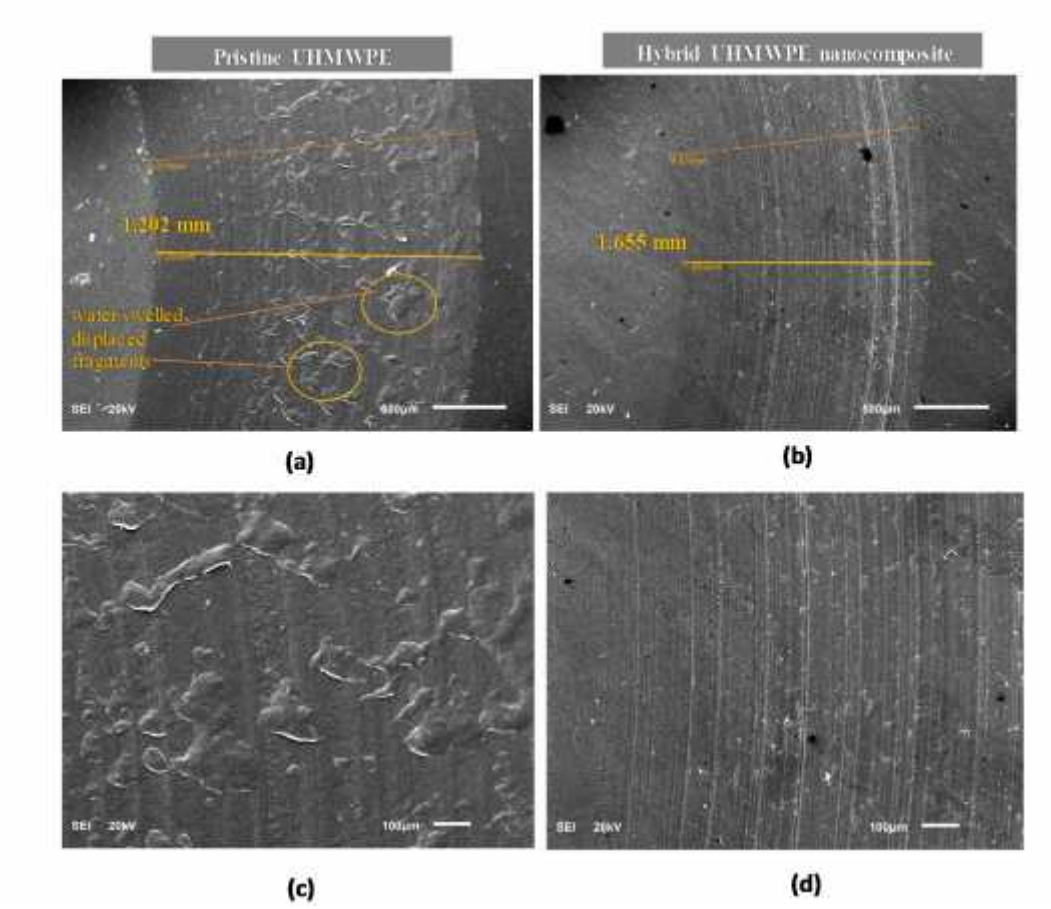

Figure 4.48 SEM wear morphology of Wear tracks for UHMPWE and hybrid UHMWPE nanocomposites for water lubricated ALT sliding conditions.

Contrary to this the, counterface running against hybrid nanocomposite showed no transfer. The presence of CNTs and nanoclays have effectively reduced the material removal along with the nanoclay. Along with that, as it has been concluded before section 4.3 that nanoclay reduces the water uptake, hence lesser plasticization of UHMWPE surface has taken place. The wear morphology surface Figure 4.48 doesn't show swelled layer parts as it can be seen for pristine UHMWPE. Hence the nanoclay has played its dual role in reducing the water uptake leading to less plasticization of surface and effectively holding the polymer chains along with CNTs, eventually leading to much reduced wear rate and maintaining higher load bearing ability as well.

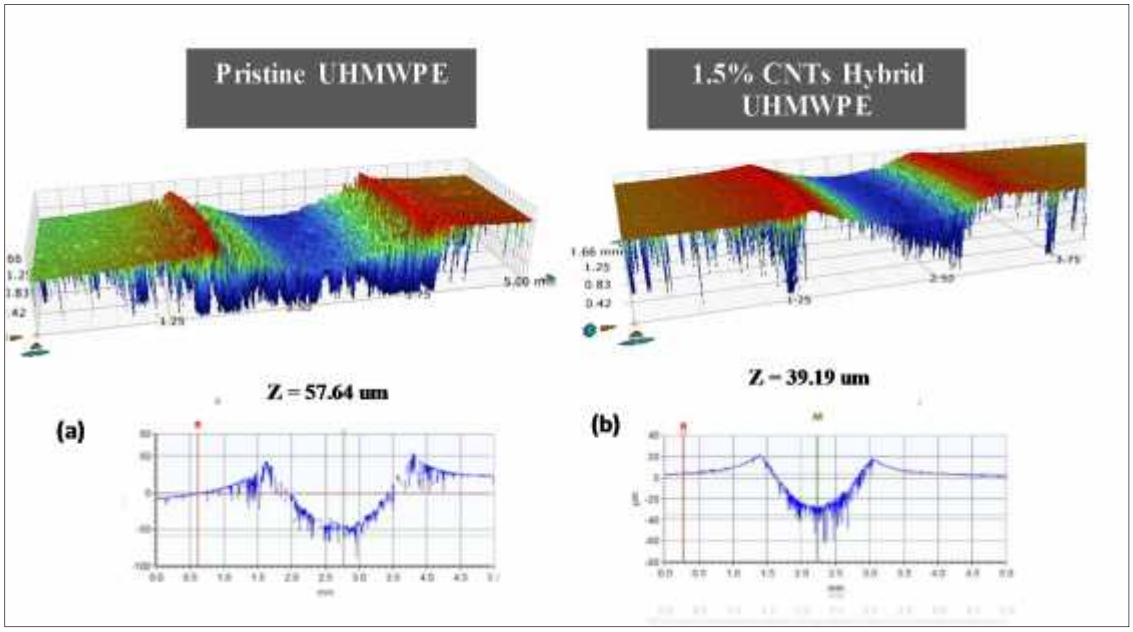

Figure 4.49 3D/ 2D optical profiler images for UHWMPE and Hybrid nanocomposites under ALT water lubricated sliding conditions.

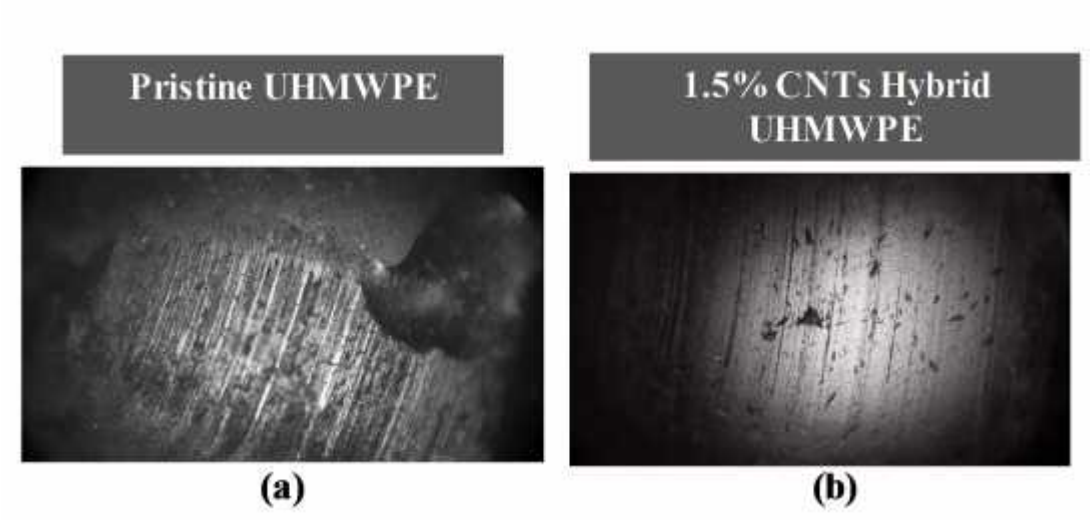

Figure 4.50 Optical images of counterface ball under water lubricated sliding ALT conditions

CHAPTER 5

Conclusions and Recommendations

5.1 Conclusions

The focus of the study was to develop UHMWPE nanocomposites for bearing applications under water lubricated conditions such as pumps and motor housings under water. The novelty in the current study was based on developing UHMWPE hybrid nanocomposites with improved tribological properties. The unique idea was to use two different nanofillers namely CNTs and nanoclays not only to improve the tribological properties but also to reduce the water absorption by polymer in water lubricated conditions. Therefore, the work was based on three different nanocomposites systems, (1) UHMWPE-nanoclay composites (2) UHMWPE-CNTs composites (3) UHMWPE hybrid (nanoclay + CNTs) nanocomposites. Optimization of the nanofiller type and content was done under dry sliding conditions for all three nanocomposite systems and then tribological performance of optimized nanocomposites were evaluated under water lubricated sliding conditions.

1.5 wt% of three different modified clays were employed as reinforcements namely: C15A, I.30E and I.28E. To select the best nanoclay among these, nanocomposites were developed and characterized for structural and tribological properties. Results reveled that a reduction of about 41 % in WR for C15A clay composites as compared to pristine UHMWPE this is due to its better dispersion resulting in possible exfoliated morphology as observed by XRD. Moreover, reduction of 38% in COF was observed for almost all UHMWPE clay composites due to formation of continuous and adhered transfer film that avoided the direct contact of hard counterface asperities with the soft composites surface. To optimize the

C15A content in UHMWPE, 0.5 wt% and 3 wt% C15A composites were developed and characterized leading to conclusion that 1.5wt% was the optimum C15A content. All of the C15A/UHMPWE nanocomposites reduced the wear rate and COF, however 0.5 wt% C15A/UHMWPE nanocomposites due to lower clay content was ineffective to reduce the wear rate as 1.5wt% C15A/UHMWPE. Moreover, results for 3wt% indicated higher wear rate as compared to 1.5wt% C15A/UHMWPE (18% increase in wear rate from 1.5wt% C15A) which was attributed to increased agglomeration of clay platelets unable to bridge the polymer chains during plastic deformation as also observed from the SEM of worn surfaces.

Water absorption testing was done at room temperature and at 70 °C to analyze the effect of clay content on water uptake. All three clay loadings (0.5 wt%, 1.5 wt% and 3wt %) along with pristine UHMWPE were tested. Higher temperature results concluded the reduction in water absorption for all the clay nanocomposites with 1.5wt% and 3wt% of C15A resulting in maximum of 23 % reduction in water uptake in comparison to UHMWPE. Similarly the water uptake results conducted at room temperature also showed reduced values for clay composites with 1.5 and 3wt% with the minimum value with 12 % reduction in water absorption. Water uptake percentage of ~ 0.01 % for 24hrs for UHMWPE was in agreement with literature.

For the second nanocomposite system CNTs/UHMWPE, similar filler content loadings (0.5 wt%, 1.5 and 3wt%) were used and nanocomposites were developed. FESEM and Raman spectroscopy were employed to characterize the dispersion and entanglement of CNTs network in UHMWPE polymer. Raman spectroscopy results showed shifting of characteristic G band of CNTs to higher waver numbers. The highest shift was detected for

1.5wt% CNTs/UHMWPE nanocomposite samples with ~ 18 cm^{-1} of shift to higher wavenumber. This shift is indicative of efficient mixing of CNTs in UHMWPE and disentanglements of CNTs bundles. FESEM images indicated uniform dispersion of CNTs in UHMWPE, while 3wt% showed some regions of agglomeration along with some uniform dispersed regions. Shore D hardness results concluded of maximum 5% increase in hardness for 3wt% CNTs/UHMWPE with other percentages resulting in slight increase in shore D value as well. The results for tribological characterization showed reduction in WR by 55 % for 1.5wt% CNTs/UHMWPE. The SEM worn morphology images for CNTs/UHMWPE composites revealed smoother and much less plastically deformed surface. It was also observed from the 2D optical profiles of the wear track that maximum reduced value of 14.11 µm for 1.5wt% CNTs/UHMWPE) as compared to 28.43 µm for pristine UHMWPE. However, for 3wt%, a slight increase in WR was observed due to agglomeration of CNTs at higher content as observed from FE-SEM images too. Unlike UHMWPE/nanoclay composites, COF showed slight increase in COF values for CNTs composites. This is attributed to the absence of transfer film on the counterface and higher mechanical properties of CNTs..

UHMWPE hybrid nanocomposites were developed by fixing the C15A content to 1.5 wt% while CNTs content was varied with same percentages as mentioned above. For UHMWPE hybrid nanocomposite systems, the Raman spectroscopy also showed shifting of characteristic G band to higher wave numbers for all the three different nanocomposites. FESEM results showed higher degree of dispersion with individual CNTs visible on UHMWPE particle while here as well 3 wt% CNTs hybrid UHMWPE nanocomposites showed agglomerated regions. Shore D hardness showed increased value with increased

amount of CNTs in UHMWPE, and the highest average shore D value of 64.00 was observed for 3wt% CNTs hybrid UHMWPE nanocomposites. Tribological testing results showed least specific wear rate for 1.5wt% hybrid UHMWPE nanocomposites with about 64 % reduction in specific wear rate as compared to pristine polymer. The reduced material removal was attributed to the presence of nanoclays and carbon nanotubes both effectively acting as anchors. Wear track maximum depth also showed lower value of 12.11 μm. COF results concluded higher values for nanocomposites compared to pristine UHMWPE due to presence of CNTs as observed for CNTs/UHMWPE nanocomposite system.

Water lubricated testing was performed for the optimized nanocomposites. Same conditions were used to conduct testing under water lubrication. The results reveal that the maximum reduction in wear rate was observed for Hybrid UHMWPE nanocomposites of about 60%. The worn morphology indicated smoother lighter plastically deformed surface for hybrid nanocomposite. Moreover, the optical profilometry indicated shallower depth of wear track for hybrid nanocomposites of 12.14 um as compared to other nanocomposites and pristine UHMWPE (25.16 um). Hence even under water lubricated sliding conditions the wear rate was much reduced for hybrid nanocomposite, however COF showed varied trend due to phenomena of smooth transfer film formation for C15A/UHMWPE nanocomposites. The transfer film observed under dry sliding conditions for C15A/UHMWPE was also observed under water lubricated conditions. Due to this transfer film the COF for C15A/UHMWPE show reduced values. On the other hand, no transfer film was formed for CNTs/UHMWPE and hybrid UHMWPE nanocomposites. For the case of 1.5 wt% hybrid nanocomposite, though the nanoclay is there present as reinforcement and the weight percentage is same as for CNTs (1.5wt% of both), no transfer film was seen

so it hints to the fact that CNTs is the dominating nanofillers. C15A nanoclay presence in UHMWPE leads to increased adhesion of transfer film as seen however for hybrid nanocomposites, clay has failed to support the adhesion of initial removed material in the form of transfer film. Finally tribological testing of hybrid nanocomposites was done under accelerated life testing conditions using 50N load, 5 m/s speed and 25,000 cycles. Results showed that even under extreme conditions under water lubrication, the hybrid nanocomposites showed higher resistance to wear. The specific wear rate was reduced to 33% as compared to pristine UHMWPE. SEM images showed highly ploughed surface for UHMWPE with highly deformed surface. Moreover, due to plasticization of surface balled up areas were seen. However hybrid nanocomposites showed comparatively much less deformed surface.

To summarize, UHMWPE nanocomposites were developed and characterized for improved tribological properties. After screening all three composite systems under dry sliding conditions, optimized nanocomposites were tested under water lubricated conditions. UHMWPE hybrid nanocomposite demonstrated best in reducing the specific wear rate under water lubrication. It was effective in doing so due to use of two different nanofillers CNTs and clays, playing role in reducing plasticization (reduced water absorption) and increasing load bearing capacity of pristine UHMWPE.

5.2 Recommendation for future Work

Although effort is being made to put some advancement in the polymer nanocomposites for bearing applications under water lubrication. Hybrid nanocomposites was novelty in a sense to utilize the potential of both nanoclay and carbon nanotube. However, there are some points can be comprehensively studied which are as follow:

1- Hybrid nanocomposite can be tested under different lubricated conditions such as base oil synovial fluid etc.
2- Including temperature as a factor and observe its effect on the tribological properties of hybrid UHMWPE nanocomposites.
3- Developing and tribological characterization of UHMWPE nanocomposites coatings using the same experimental matrix.

REFERENCES

[1] B. Briscoe, S. Sinha, Tribology of polymeric solids and their composites, Wear–Mechanisms, Materials and Practice, (2005) 223-268.

[2] K. Friedrich, A.K. Schlarb, Tribology of polymeric nanocomposites: friction and wear of bulk materials and coatings, Elsevier, 2011.

[3] M. Bermúdez, F. Carrión, C. Espejo, J. Sanes, G. Ojados, Tribology of Bulk Polymer Nanocomposites and Nanocomposite Coatings, Tribology of Nanocomposites, Springer, 2013, pp. 1-18.

[4] J.A. Njuguna, K. Pielichowski, S. Desai, Nanofiller Fibre-Reinforced Polymer Nanocomposites, (2008).

[5] D. Paul, L. Robeson, Polymer nanotechnology: nanocomposites, Polymer, 49 (2008) 3187-3204.

[6] J.N. Coleman, U. Khan, W.J. Blau, Y.K. Gun'ko, Small but strong: a review of the mechanical properties of carbon nanotube–polymer composites, Carbon, 44 (2006) 1624-1652.

[7] Z. Spitalsky, D. Tasis, K. Papagelis, C. Galiotis, Carbon nanotube–polymer composites: chemistry, processing, mechanical and electrical properties, Progress in polymer science, 35 (2010) 357-401.

[8] D.L. Burris, B. Boesl, G.R. Bourne, W.G. Sawyer, Polymeric nanocomposites for tribological applications, Macromolecular materials and engineering, 292 (2007) 387-402.

[9] M. Galetz, T. Blaβ, H. Ruckdäschel, J. Sandler, V. Altstädt, U. Glatzel, Carbon nanofibre-reinforced ultrahigh molecular weight polyethylene for tribological applications, Journal of applied polymer science, 104 (2007) 4173-4181.

[10] S.K. Sinha, B.J. Briscoe, Polymer tribology, World Scientific, 2009.

[11] B. Suresha, B.R. Kumar, M. Venkataramareddy, T. Jayaraju, Role of micro/nano fillers on mechanical and tribological properties of polyamide66/polypropylene composites, Materials & Design, 31 (2010) 1993-200

[12] N. Dayma, B.K. Satapathy, A. Patnaik, Structural correlations to sliding wear performance of PA-6/PP-g-MA/nanoclay ternary nanocomposites, Wear, 271 (2011) 827-836.

[13] A. Arora, G. Padua, Review: nanocomposites in food packaging, Journal of Food Science, 75 (2010) R43-R49.

[14] M. Al-Qadhi, N. Merah, Z. Gasem, Mechanical properties and water uptake of epoxy–clay nanocomposites containing different clay loadings, Journal of Materials Science, 48 (2013) 3798-3804.

[15] O. Becker, R.J. Varley, G.P. Simon, Thermal stability and water uptake of high performance epoxy layered silicate nanocomposites, European polymer journal, 40 (2004) 187-195.

[16] D. Dowson, History of tribology, 1979, Longman Group Limited, London.

[17] M.R. Piggott, Load bearing fibre composites, Springer Science & Business Media, 2002.

[18] W. Brostow, V. Kovačevic, D. Vrsaljko, J. Whitworth, Tribology of polymers and polymer-based composites, Journal of Materials Education, 32 (2010) 273.

[19] L.S. Schadler, Polymer-Based and Polymer-Filled Nanocomposites, Wiley Online Library, 2003.

[20] K. Friedrich, Z. Lu, A. Hager, Recent advances in polymer composites' tribology, Wear, 190 (1995) 139-144.

[21] K. Friedrich, Advances in composite tribology, Elsevier, 2012.

[22] M. Conte, A. Igartua, Study of PTFE composites tribological behavior, Wear, 296 (2012) 568-574.

[23] S. Lampman, Characterization and failure analysis of plastics, ASM International, 2003.

[24] P. Harvey, L. Stein, Ultra High Molecular Weight Polyethylene (UHMWPE), Ticona LLC, ASM International, (1999).

[25] B. Aldousiri, A. Shalwan, C. Chin, A review on tribological behaviour of polymeric composites and future reinforcements, Advances in Materials Science and Engineering, 2013 (2013).

[26] Z. Pan, S. Xie, B. Chang, C. Wang, L. Lu, W. Liu, W. Zhou, W. Li, L. Qian, Very long carbon nanotubes, Nature, 394 (1998) 631-632.

[27] R.H. Baughman, A.A. Zakhidov, W.A. de Heer, Carbon nanotubes--the route toward applications, Science, 297 (2002) 787-792.

[28] M.A. Samad, S.K. Sinha, Mechanical, thermal and tribological characterization of a UHMWPE film reinforced with carbon nanotubes coated on steel, Tribology International, 44 (2011) 1932-1941.

[29] M.A. Samad, S.K. Sinha, Dry sliding and boundary lubrication performance of a UHMWPE/CNTs nanocomposite coating on steel substrates at elevated temperatures, Wear, 270 (2011) 395-402.

[30] B. Panjwani, N. Satyanarayana, S.K. Sinha, Tribological characterization of a biocompatible thin film of UHMWPE on Ti6Al4V and the effects of PFPE as top lubricating layer, Journal of the mechanical behavior of biomedical materials, 4 (2011) 953-96

[31] M.A. Samad, N. Satyanarayana, S.K. Sinha, Tribology of UHMWPE film on air-plasma treated tool steel and the effect of PFPE overcoat, Surface and Coatings Technology, 204 (2010) 1330-1338.

[32] P. Ajayan, O. Stephan, C. Colliex, D. Trauth, Aligned carbon nanotube arrays formed by cutting a polymer resin—nanotube composite, Science, 265 (1994) 1212-1214.

[33] S. Bal, S. Samal, Carbon nanotube reinforced polymer composites—a state of the art, Bulletin of Materials Science, 30 (2007) 379-386.

[34] Y.-S. Zoo, J.-W. An, D.-P. Lim, D.-S. Lim, Effect of carbon nanotube addition on tribological behavior of UHMWPE, Tribology Letters, 16 (2004) 305-309.

[35] S. Ruan, P. Gao, X. Yang, T. Yu, Toughening high performance ultrahigh molecular weight polyethylene using multiwalled carbon nanotubes, Polymer, 44 (2003) 5643-5654.

[36] Y. Xue, W. Wu, O. Jacobs, B. Schädel, Tribological behaviour of UHMWPE/HDPE blends reinforced with multi-wall carbon nanotubes, Polymer Testing, 25 (2006) 221-229.

[37] B.B. Johnson, M.H. Santare, J.E. Novotny, S.G. Advani, Wear behavior of carbon nanotube/high density polyethylene composites, Mechanics of Materials, 41 (2009) 1108-1115.

[38] M. Ivanković, LA Utracki: Clay-Containing Polymeric Nanocomposites, Polimeri: časopis za plastiku i gumu, 25 (2005) 106-106.

[39] V. Mittal, Polymer layered silicate nanocomposites: a review, Materials, 2 (2009) 992-1057.

[40] A. Olad, Polymer/clay nanocomposites, Advances in diverse industrial applications of nanocomposites, (2011) 113-138.

[41] S. Kaloshkin, K. Ergin, V. Tcherdyntsev, A. Maksimkin, M. Petrzhik, E. Antipov, V. Gerasin, Structure and propertties of ball milled utrahigh-molecular weight Polyethylene-clay composite, (2011).

[42] Q.-Y. Peng, P.-H. Cong, X.-J. Liu, T.-X. Liu, S. Huang, T.-S. Li, The preparation of PVDF/clay nanocomposites and the investigation of their tribological properties, Wear, 266 (2009) 713-72

[43] K. Kanny, P. Jawahar, V. Moodley, Mechanical and tribological behavior of clay–polypropylene nanocomposites, Journal of materials science, 43 (2008) 7230-7238.

[44] Y. An, Z. Tai, Y. Qi, X. Yan, B. Liu, Q. Xue, J. Pei, Friction and wear properties of graphene oxide/ultrahigh-molecular-weight polyethylene composites under the lubrication of deionized water and normal saline solution, Journal of Applied Polymer Science, 131 (2014).

[45] X. Dangsheng, Friction and wear properties of UHMWPE composites reinforced with carbon fiber, Materials letters, 59 (2005) 175-179.

[46] D. Xiong, S. Ge, Friction and wear properties of UHMWPE/Al 2 O 3 ceramic under different lubricating conditions, Wear, 250 (2001) 242-245.

[47] C. Liu, J. Wu, J. Li, L. Ren, J. Tong, A. Arnell, Tribological behaviours of PA/UHMWPE blend under dry and lubricating condition, Wear, 260 (2006) 109-115.

[48] J. Wen, P. Yin, M. Zhen, Friction and wear properties of UHMWPE/nano-MMT composites under oilfield sewage condition, Materials Letters, 62 (2008) 4161-4163.

[49] S. Nath, S. Bodhak, B. Basu, Tribological investigation of novel HDPE-HAp-Al2O3 hybrid biocomposites against steel under dry and simulated body fluid condition, Journal of Biomedical Materials Research Part A, 83 (2007) 191-208.

[50] A. Fonseca, S. Kanagaraj, M.S. Oliveira, J.A. Simões, Enhanced UHMWPE reinforced with MWCNT through mechanical ball-milling, Defect and Diffusion Forum, Trans Tech Publ, 2011, pp. 1238-1243.

[51] Y. Leng, Materials characterization: introduction to microscopic and spectroscopic methods, John Wiley & Sons, 2009.

[52] L. Bokobza, J. Zhang, Raman spectroscopic characterization of multiwall carbon nanotubes and of composites, Express Polym. Lett, 6 (2012) 601-608.

[53] ASTM D2240-15, Standard Test Method for Rubber Property—Durometer Hardness, ASTM International, West Conshohocken, PA, 2015, www.astm.org

[54] B. Bhushan, Introduction to tribology, John Wiley & Sons, 2013.

[55] A. Maksimkin, S. Kaloshkin, V. Tcherdyntsev, D. Chukov, I. Shchetinin, Effect of high-energy ball milling on the structure and mechanical properties of ultra-high

molecular weight polyethylene, Journal of Applied Polymer Science, 130 (2013) 2971-2977.

[56] A. Yasmin, J.L. Abot, I.M. Daniel, Processing of clay/epoxy nanocomposites by shear mixing, Scripta Materialia, 49 (2003) 81-86.

[57] K. Nagesha, M. Rajanish, D. Shivappa, A Review On Mechanical Alloying, Change, 3 (2013).

[58] R. Andrews, D. Jacques, D. Qian, T. Rantell, Multiwall carbon nanotubes:synthesis and application, Accounts of Chemical Research, 35 (2002) 1008-1017.

[59] M. Endo, K. Takeuchi, T. Hiraoka, T. Furuta, T. Kasai, X. Sun, C.-H. Kiang, M. Dresselhaus, Stacking nature of graphene layers in carbon nanotubes and nanofibres, Journal of Physics and Chemistry of Solids, 58 (1997) 1707-1712.

[60] B.J. Kip, M.C. Van Eijk, R.J. Meier, Molecular deformation of high-modulus polyethylene fibers studied by micro-raman spectroscopy, Journal of Polymer Science Part B: Polymer Physics, 29 (1991) 99-108.

[61] C.C. Naylor, R.J. Meier, B.J. Kip, K.P. Williams, S.M. Mason, N. Conroy, D.L. Gerrard, Raman spectroscopy employed for the determination of the intermediate phase in polyethylene, Macromolecules, 28 (1995) 2969-2978.

[62] D.T. Grubb, Z.-F. Li, Molecular stress distribution and creep of high-modulus polyethylene fibres, Polymer, 33 (1992) 2587-2597.

[63] S.L. Wunder, S.D. Merajver, Ultrahigh-molecular-weight polyethylene: Raman spectroscopic study of melt anisotropy, Journal of Polymer Science Part B: Polymer Physics, 24 (1986) 99-11

[64] R. Nemanich, S. Solin, First-and second-order Raman scattering from finite-size crystals of graphite, Physical Review B, 20 (1979) 392.

[65] R. Saito, G. Dresselhaus, M.S. Dresselhaus, Physical properties of carbon nanotubes, World Scientific, 1998.

[66] T. McNally, P. Pötschke, P. Halley, M. Murphy, D. Martin, S.E. Bell, G.P. Brennan, D. Bein, P. Lemoine, J.P. Quinn, Polyethylene multiwalled carbon nanotube composites, Polymer, 46 (2005) 8222-8232.

[67] L. Valentini, J. Biagiotti, J. Kenny, S. Santucci, Morphological characterization of single-walled carbon nanotubes-PP composites, Composites Science and Technology, 63 (2003) 1149-1153.

[68] A. Prabowo, Structure and Physical Properties of Organoclay/Epoxy Nanocomposite, (2012).

[69] N. Colthup, Introduction to infrared and Raman spectroscopy, Elsevier, 2012.

[70] S.M. Kurtz, The UHMWPE handbook: ultra-high molecular weight polyethylene in total joint replacement, Academic Press, 2004.

[71] M.A. Samad, S.K. Sinha, Nanocomposite UHMWPE–CNT polymer coatings for boundary lubrication on Aluminium substrates, Tribology letters, 38 (2010) 301-311.

[72] M. Tortora, G. Gorrasi, V. Vittoria, G. Galli, S. Ritrovati, E. Chiellini, Structural characterization and transport properties of organically modified montmorillonite/polyurethane nanocomposites, Polymer, 43 (2002) 6147-6157.

[73] E.P. Giannelis, Polymer layered silicate nanocomposites, Advanced materials, 8 (1996) 29-35.

[74] Y. Zhang, Q. Liu, Q. Zhang, Y. Lu, Gas barrier properties of natural rubber/kaolin composites prepared by melt blending, Applied Clay Science, 50 (2010) 255-259.

[75] M. Al-Qadhi, N. Merah, Z. Gasem, N. Abu-Dheir, B. Aleem, Effect of water and crude oil on mechanical and thermal properties of epoxy-clay nanocomposites, Polymer Composites, 35 (2014) 318-326.

[76] H. Dhakal, Z. Zhang, M. Richardson, Effect of water absorption on the mechanical properties of hemp fibre reinforced unsaturated polyester composites, Composites Science and Technology, 67 (2007) 1674-1683.

[77] G. Baschek, G. Hartwig, F. Zahradnik, Effect of water absorption in polymers at low and high temperatures, Polymer, 40 (1999) 3433-3441.

[78] B.K. Kim, J.W. Seo, H.M. Jeong, Morphology and properties of waterborne polyurethane/clay nanocomposites, European Polymer Journal, 39 (2003) 85-91.

[79] S.K. Sinha, T. Song, X. Wan, Y. Tong, Scratch and normal hardness characteristics of polyamide 6/nano-clay composite, Wear, 266 (2009) 814-821.

[80] J.-P. Salvetat, J.-M. Bonard, N. Thomson, A. Kulik, L. Forro, W. Benoit, L. Zuppiroli, Mechanical properties of carbon nanotubes, Applied Physics A, 69 (1999) 255-26

[81] P. Jawahar, R. Gnanamoorthy, M. Balasubramanian, Tribological behaviour of clay–thermoset polyester nanocomposites, Wear, 261 (2006) 835-84

[82] G. Srinath, R. Gnanamoorthy, Effect of nanoclay reinforcement on tensile and tribo behaviour of Nylon 6, Journal of materials science, 40 (2005) 2897-2901.

[83] B. Briscoe, S. Sinha, Wear of polymers, Proceedings of the Institution of Mechanical Engineers, Part J: Journal of Engineering Tribology, 216 (2002) 401-413.

[84] S. Bahadur, The development of transfer layers and their role in polymer tribology, Wear, 245 (2000) 92-99.

[85] T. Mohan, K. Kanny, Water barrier properties of nanoclay filled sisal fibre reinforced epoxy composites, Composites Part A: Applied Science and Manufacturing, 42 (2011) 385-393.

[86] S. Kanagaraj, F.R. Varanda, T.V. Zhil'tsova, M.S. Oliveira, J.A. Simões, Mechanical properties of high density polyethylene/carbon nanotube composites, Composites Science and Technology, 67 (2007) 3071-3077.

VITAE

EDUCATION

Master of Science, Materials Science and Engineering

College of Sciences, King Fahd University of Petroleum & Minerals (KFUPM), KSA
CGPA: 3.62/4.00
Thesis: *Development and Characterization of Hybrid UHMWPE Nanocomposites for Bearing Applications under water lubricated conditions*
Supervisor-: Neçar Merah

Bachelor of Engineering, Materials Engineering

School of Chemical and Materials Engineering (SCME), National University of Science and Technology (NUST), Pakistan
CGPA: 3.62/4.00
Thesis*: Physical and Mechanical Properties of Acrylonitrile Butadiene Styrene (ABS) polymer reinforced nano clay composites*
Supervisor*:* Ahmad Nawaz Khan

Publications (All Journal Publications)

1. Samad MA, Ali AB, "Investigating the effect of water absorption on the tribological properties of UHMWPE reinforced organoclay composites". (**Tribology letters: DOI: 10.1007/s11249-016-0652-4).**

2. "Evaluation of Tribological properties of Organo-clay reinforced UHMWPE Nanocomposites" **(Journal of Tribology: ASME, doi:10.1115/1.4033188).**

3. Ali AB, Samad MA, Merah N, Tribological Performance of UHMWPE Nanocompoistes under Water lubricated Sliding conditions, **(Wear: under Peer review).**

4. Ali AB and Samad MA," Tribological Investigations of UHMWPE Nanocomposites Reinforced with Three Different Organo-Modified Clays", **(Polymer Composites:**

Peer review)

5. Samad MA, Ali AB, Merah N, "Hybrid UHMWPE nanocomposites with improved tribological properties under water lubricated sliding conditions" **(Pipe line)**

Accomplishments

- Participated in 3rd Saudi International Nanotechnology conference 2014 (3SINC).
- Participated in Vacuum and Surface Science Conference of Australia and Asia (**VASSCA-6**) 2012.
- Pursued master`s degree at KFUPM on fully funded scholarship.
- Participation at National workshop on vacuum and Thin Film technology, (NWVTFT) at NCP Islamabad.
- Member (PVS), Pakistan Vacuum Society, fellow member IUVSTA.

REFERENCES

- **Dr. Neçar Merah,**
  Professor, Mechanical Engineering
  Director: Center of Excellence for Scientific Collaboration with MIT
  King Fahd University of Petroleum & Minerals
  E-mail**:** **nesar@kfupm.edu.sa; nesarmerah@gmail.com**
  Webpage: http://www.kfupm.edu.sa/me/faculty/merah.htm;
  http://ccwce.mit.edu/People/Administration

- **Dr. Abdul Samad, Mohammed (PhD, MS, PMP)**
  Assistant professor
  Director of tribology lab, Mechanical engineering department
  King Fahd University of Petroleum & Minerals
  Email: samad@kfupm.edu.sa
  Webpage: http://www2.kfupm.edu.sa/me/samad.htm